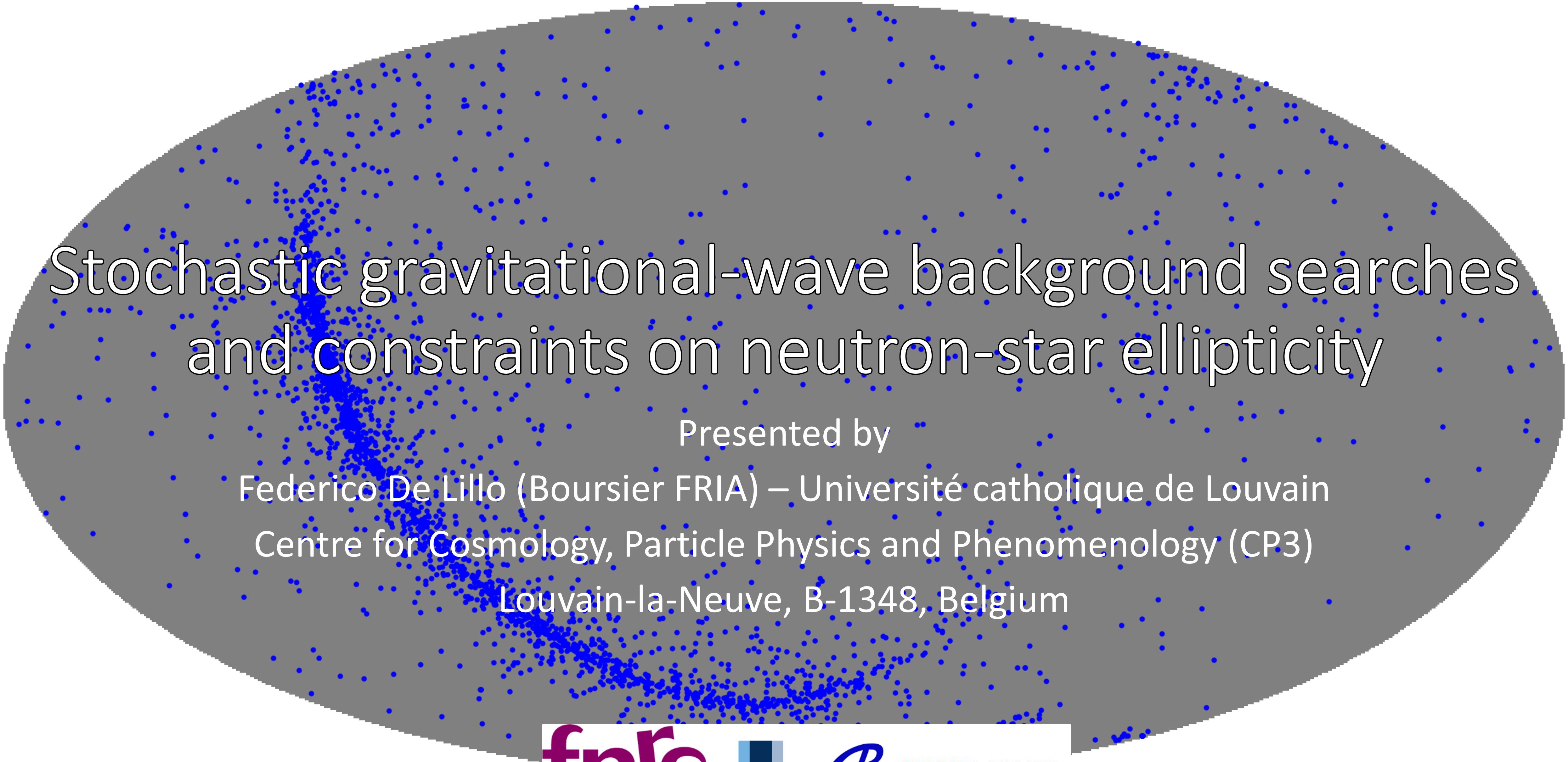

Stochastic gravitational-wave background searches and constraints on neutron-star ellipticity

Presented by

Federico De Lillo (Boursier FRIA) – Université catholique de Louvain

Centre for Cosmology, Particle Physics and Phenomenology (CP3)

Louvain-la-Neuve, B-1348, Belgium

fnrs LA LIBERTÉ DE CHERCHER UCLouvain VIRGO

Institut d'Astrophysique de Paris (IAP)

Paris, 16th June 2022

Outline

Gravitational Waves (GWs) and LIGO-Virgo-KAGRA (LVK) collaboration

- Quick recap about GWs
- Introduction to LVK: detector network and main analyses
- Milestones in GW astronomy and future observing runs

Stochastic Gravitational-Wave Background: Introduction and LVK searches

- SGWB: definition and sources
- LVK searches: cross-correlation method

Stochastic gravitational-wave background searches and constraints on neutron-star ellipticity

- Motivations and signal model
- Search for isotropic SGWB from Galactic NSs and implication for NS ellipticity

If time will allow (backup slides)

- Directional searches, SGWB from extragalactic NSs ‘‘hotspots’’

Gravitational Waves and LIGO-Virgo-KAGRA collaboration

What are Gravitational Waves?

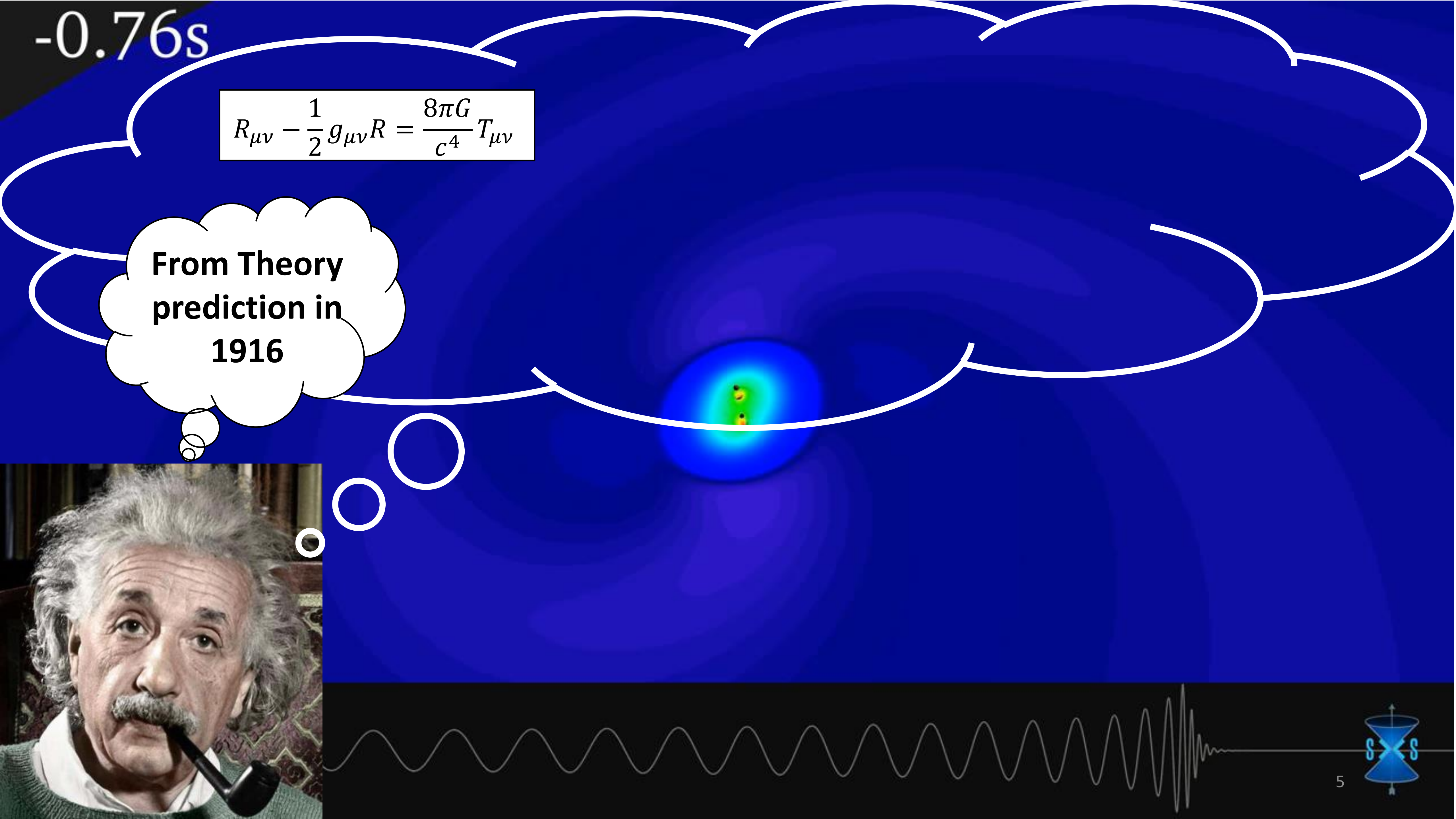
-0.76s
$R_{\mu\nu} - \frac{1}{2} g_{\mu\nu} R = \frac{8\pi G}{c^4} T_{\mu\nu}$
From Theory prediction in 1916

-0.76s

$$R_{\mu\nu} - \frac{1}{2} g_{\mu\nu} R = \frac{8\pi G}{c^4} T_{\mu\nu}$$

Linearisation

$g_{\mu\nu} = \eta_{\mu\nu} + h_{\mu\nu}$

$|h_{\mu\nu}| \ll 1$

$$\Box \bar{h}_{\mu\nu} = -\frac{16\,\pi G}{c^4} T_{\mu\nu}$$

$$\bar{h}_{\mu\nu} \equiv h_{\mu\nu} - \frac{1}{2}\eta_{\mu\nu} h_{\lambda}^{\lambda}$$

$$\partial^{\nu} \bar{h}_{\mu\nu} = 0$$

Wave equation!
What is oscillating?

$g_{\mu\nu} \leftrightarrow$ spacetime

GWs as spacetime ripples that propagate at the speed of light

From Theory prediction in 1916

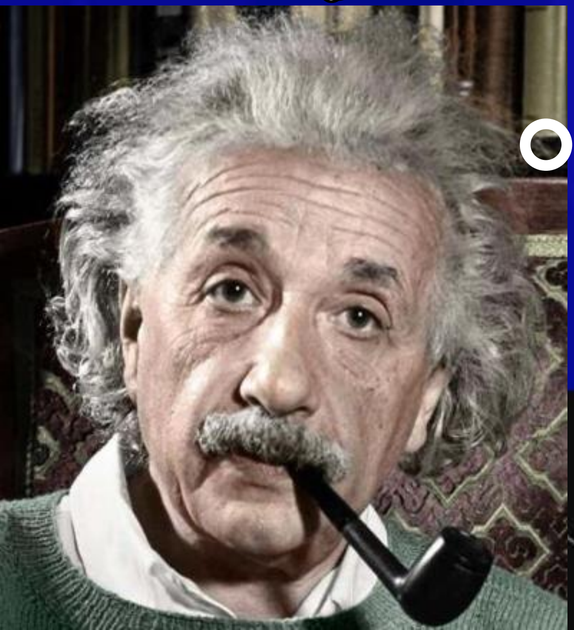

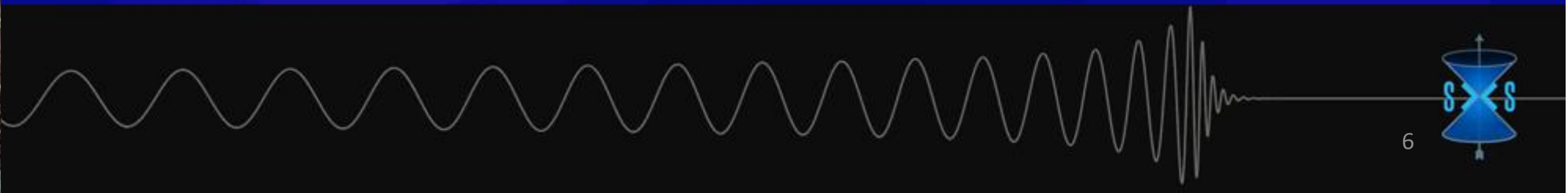

-0.76s

$$R_{\mu\nu} - \frac{1}{2} g_{\mu\nu} R = \frac{8\pi G}{c^4} T_{\mu\nu}$$

Linearisation

$$g_{\mu\nu} = \eta_{\mu\nu} + h_{\mu\nu}$$

$$|h_{\mu\nu}| \ll 1$$

$$\Box \bar{h}_{\mu\nu} = -\frac{16\,\pi G}{c^4} T_{\mu\nu}$$

$$\bar{h}_{\mu\nu} \equiv h_{\mu\nu} - \frac{1}{2} \eta_{\mu\nu} h^{\lambda}_{\lambda}$$

$$\partial^{\nu} \bar{h}_{\mu\nu} = 0$$

Wave equation!
What is oscillating?

$g_{\mu\nu} \leftrightarrow$ spacetime

GWs as spacetime ripples that propagate at the speed of light

From Theory prediction in 1916

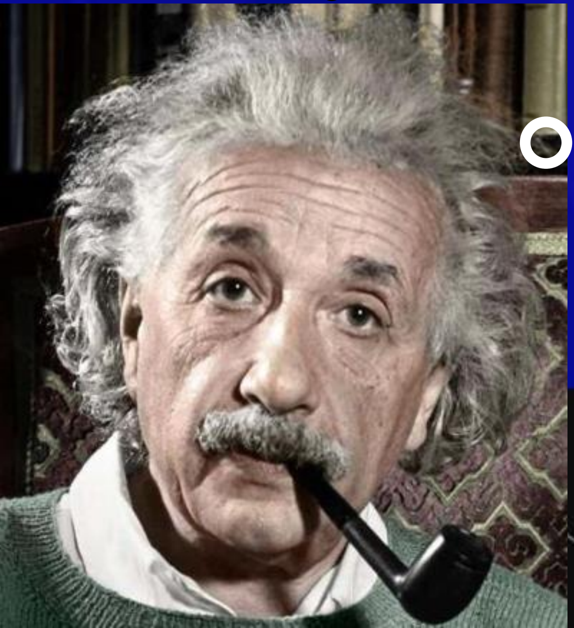

GW150914

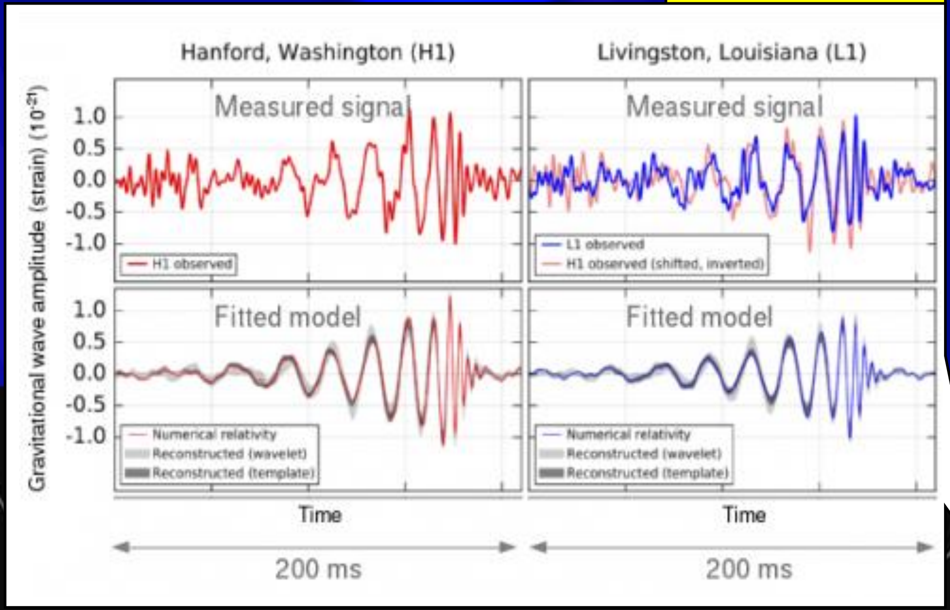

To Discovery announcement in 2016

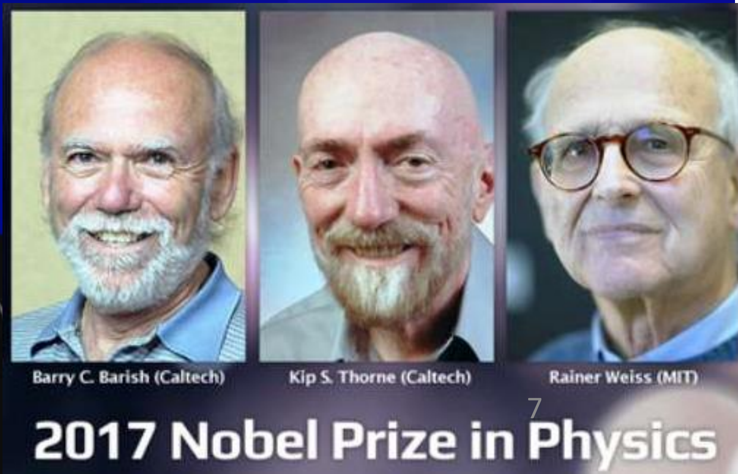

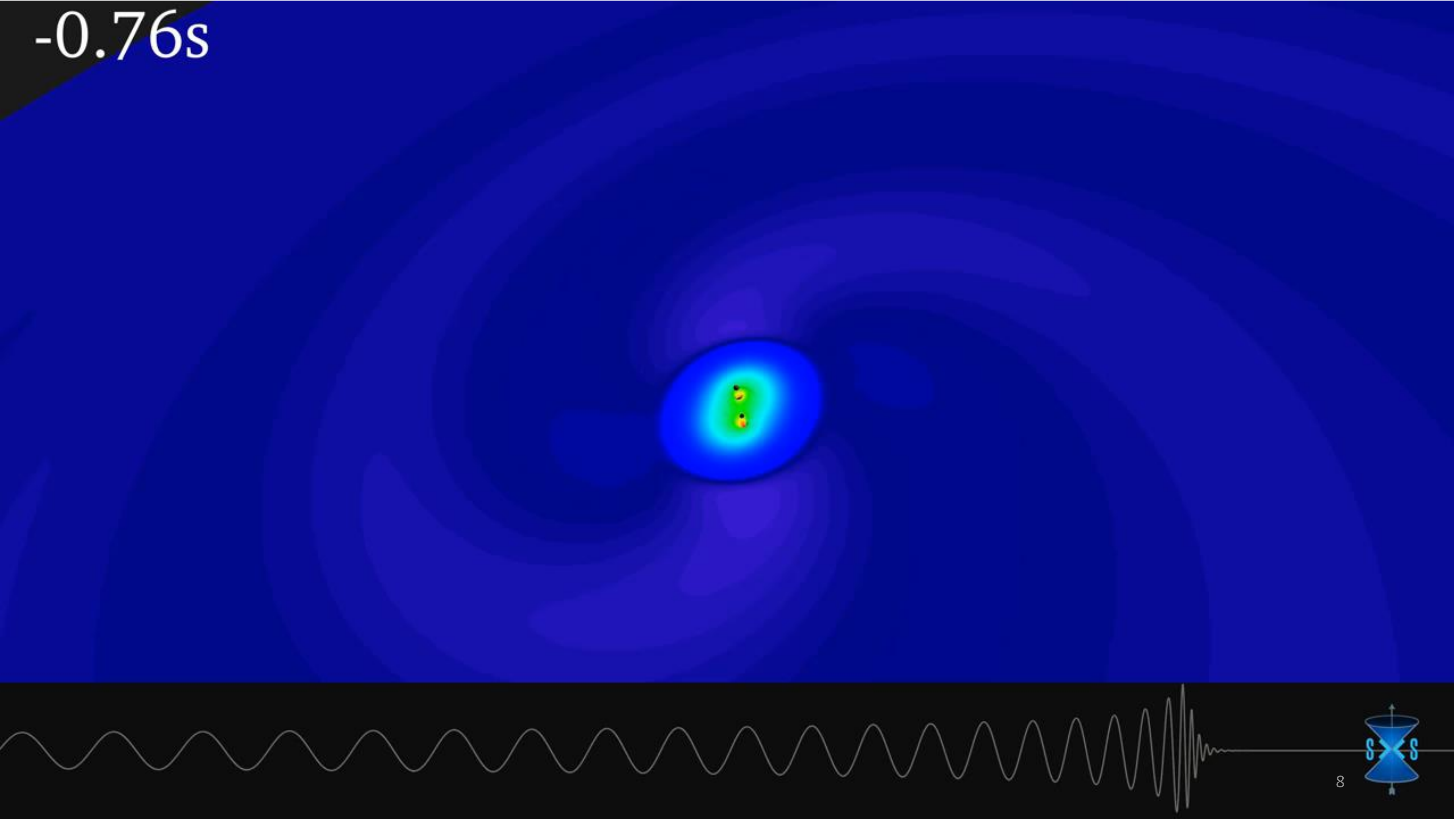
-0.76s

How are GWs detected?

THE GRAVITATIONAL WAVE SPECTRUM

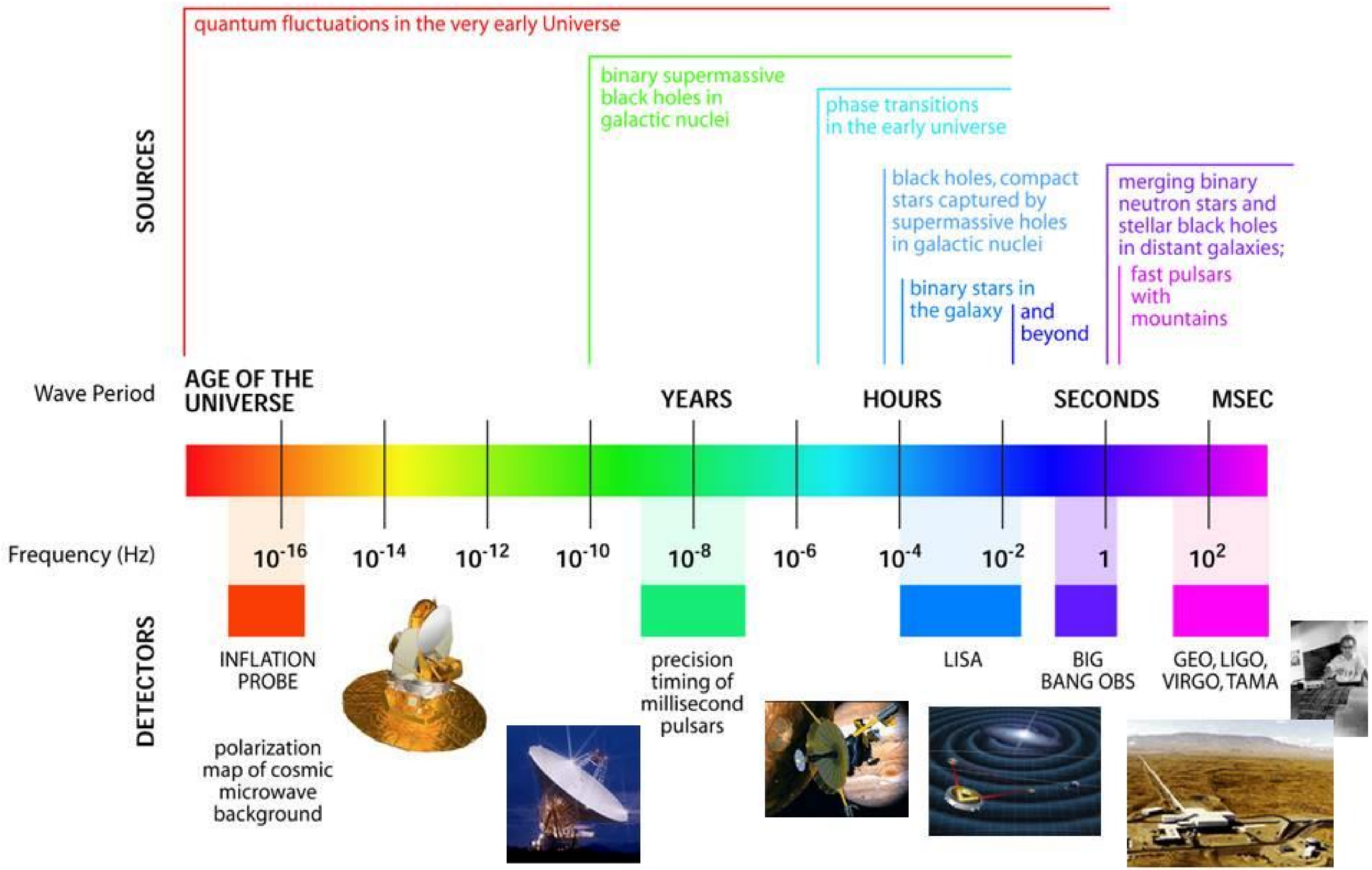

http://www.thespectrumofriemannium.com/2019/10/19/log237-gw-music/

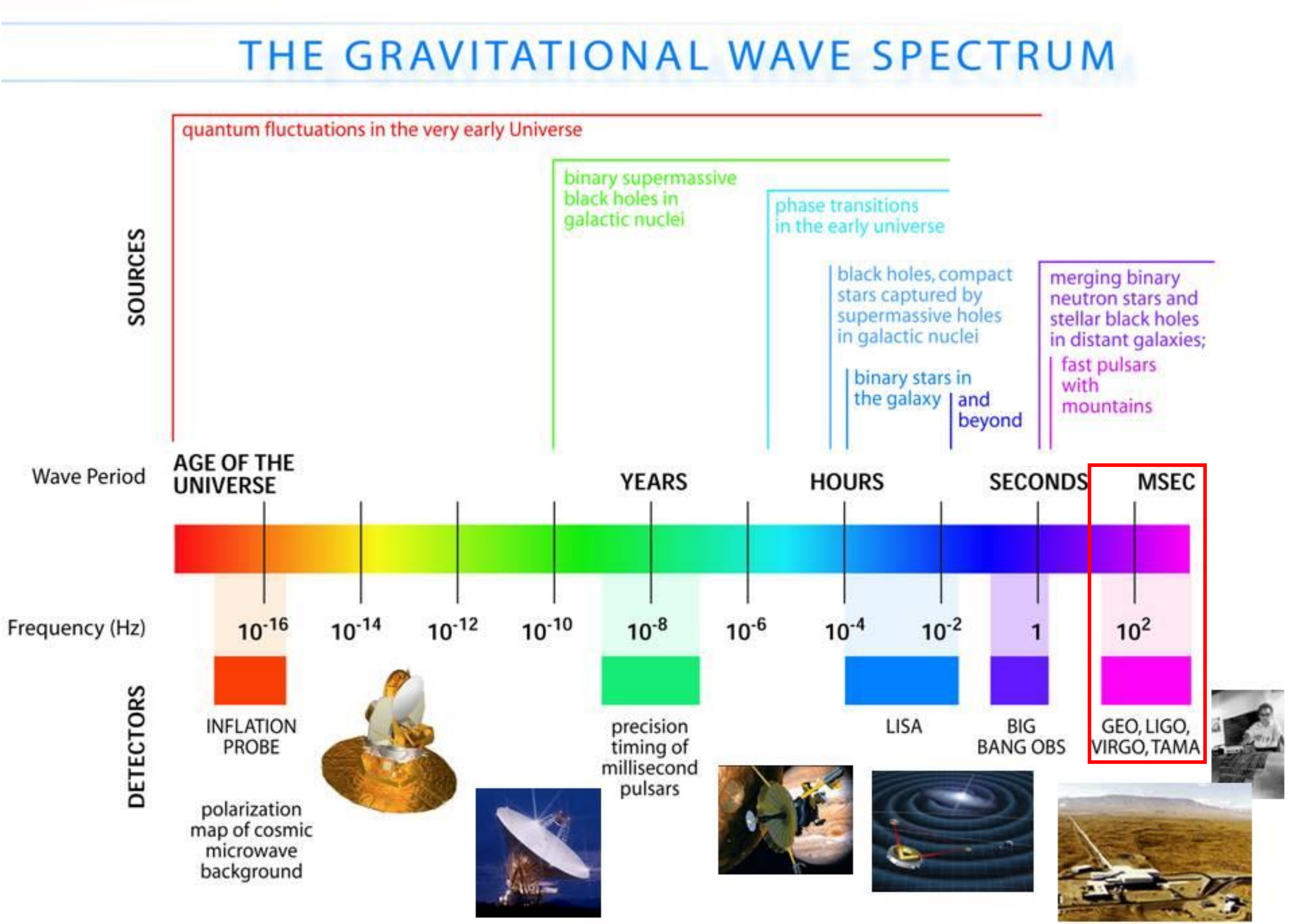

http://www.thespectrumofriemannium.com/2019/10/19/log237-gw-music/

2nd generation ground based detectors network

Credits: Readapted from Neil Cornish GWMess2021 presentation

LIGO-Hanford, Washington, USA(2015)

LIGO-Livingston, Louisiana, USA (2015)

VIRGO, Cascina (PI), Italy (2017)

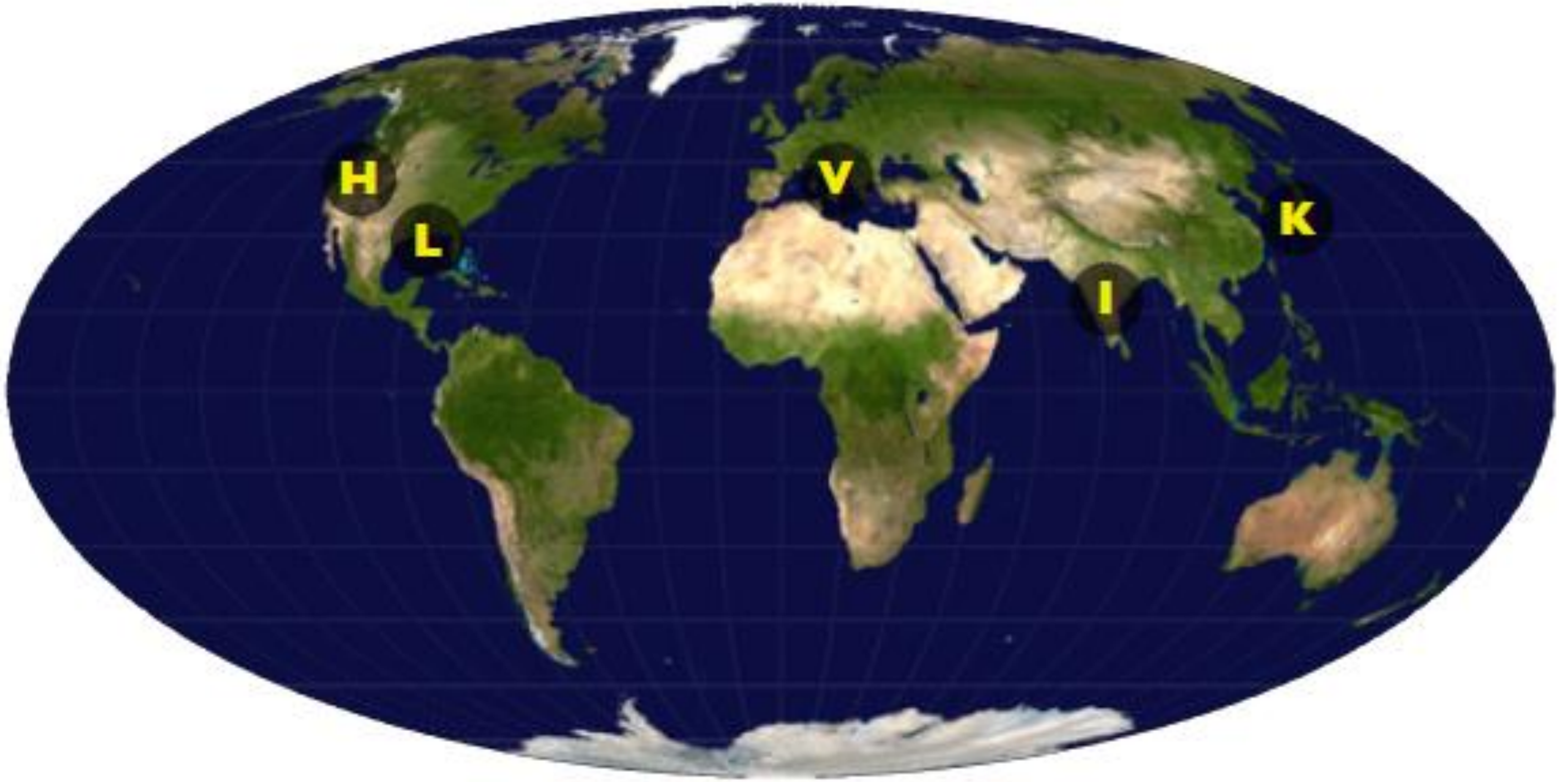

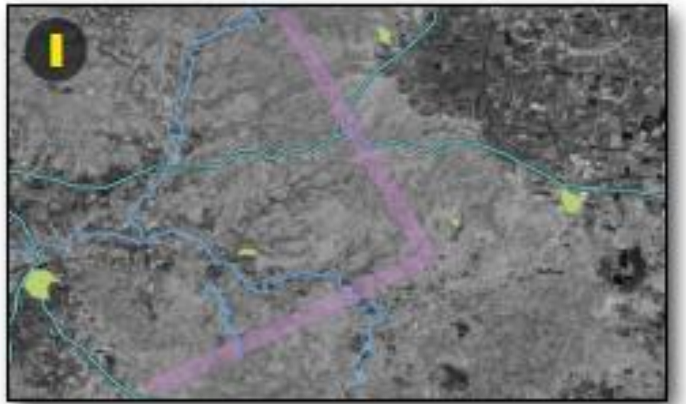

LIGO-India, Hingoli District, Maharashtra,India(202X)

KAGRA, Kamioka, Japan (2020)

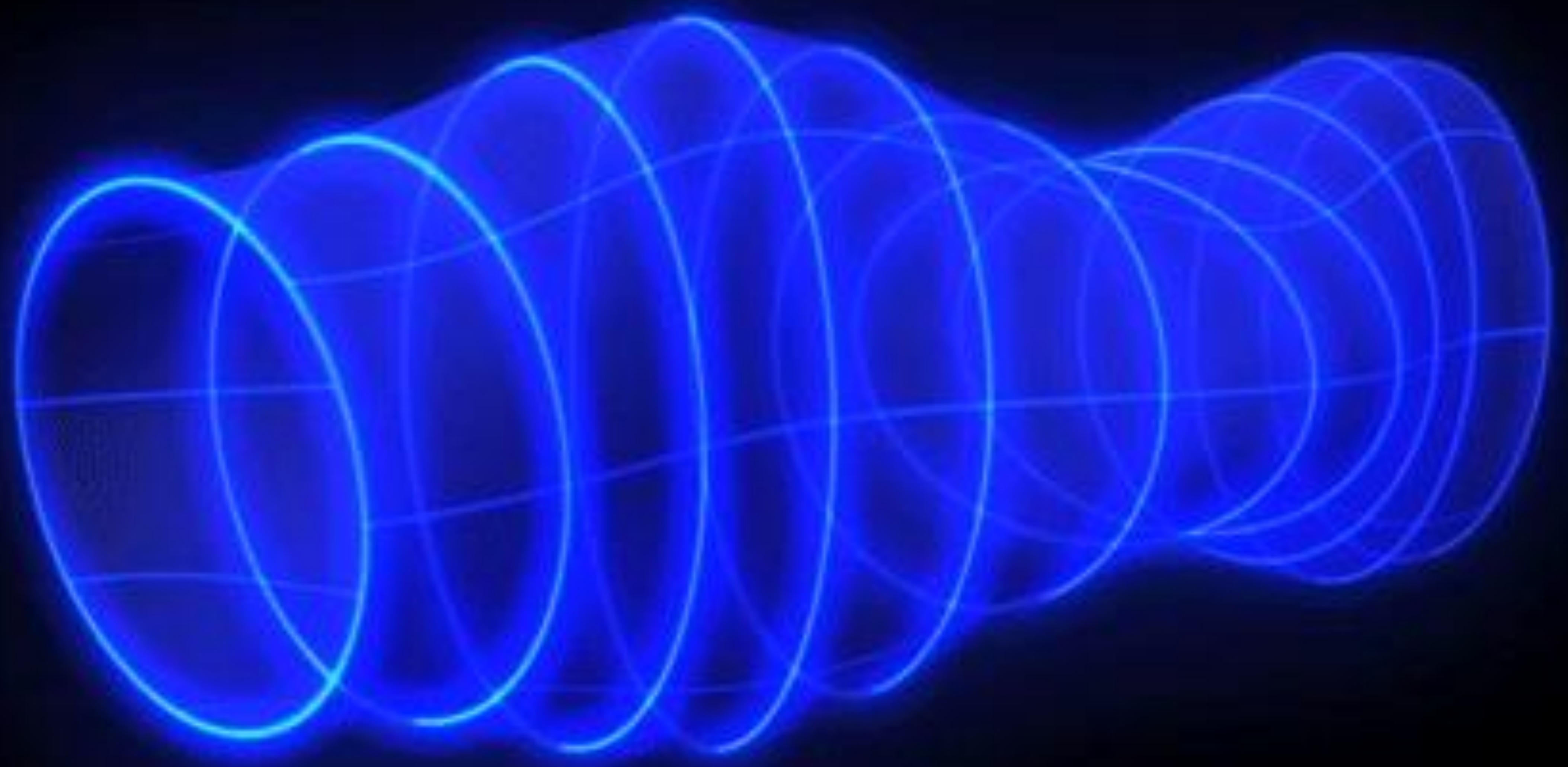

Credits: esa.int

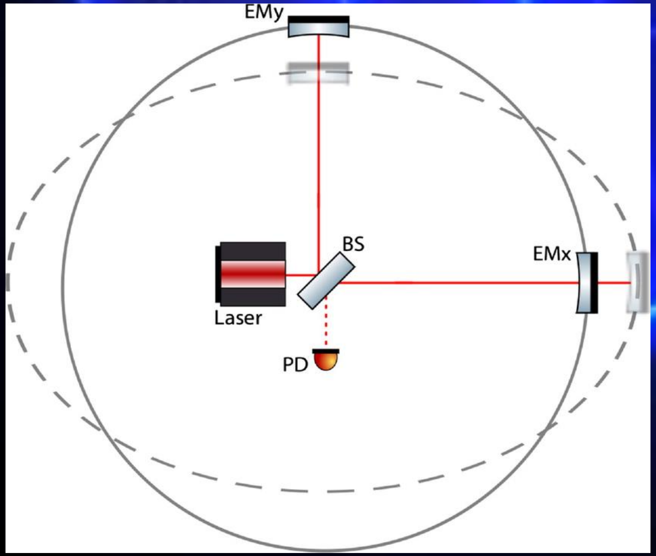

Detector response to GWs

$$h_{strain}(t) = \frac{\Delta L(t)}{L}$$

Simplified Michelson Inteferometer
acting as GWs detector.

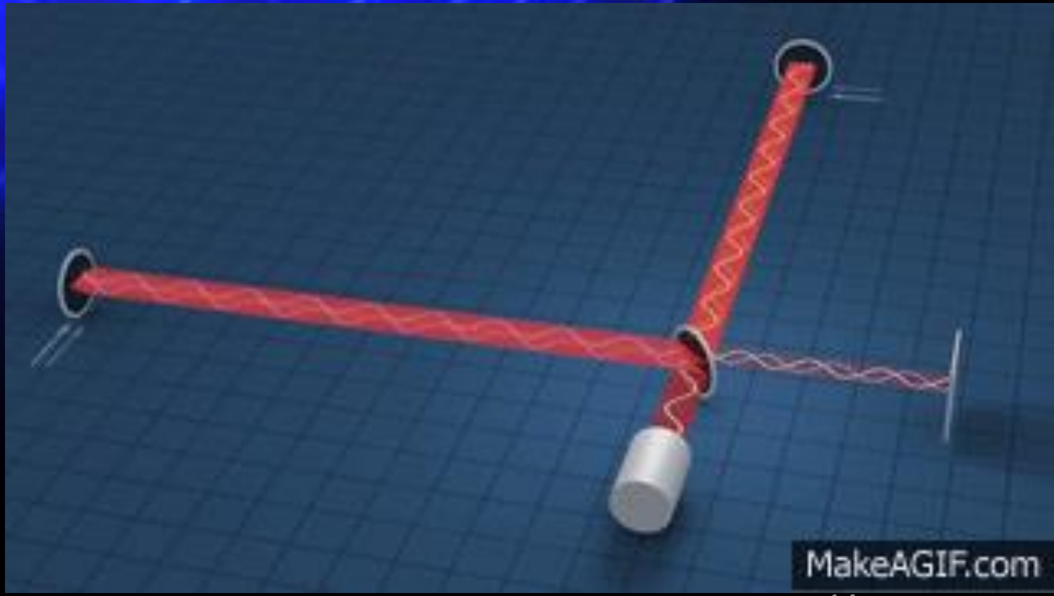

Credits: [esa.int](esa.int)

What kind of searches are performed?

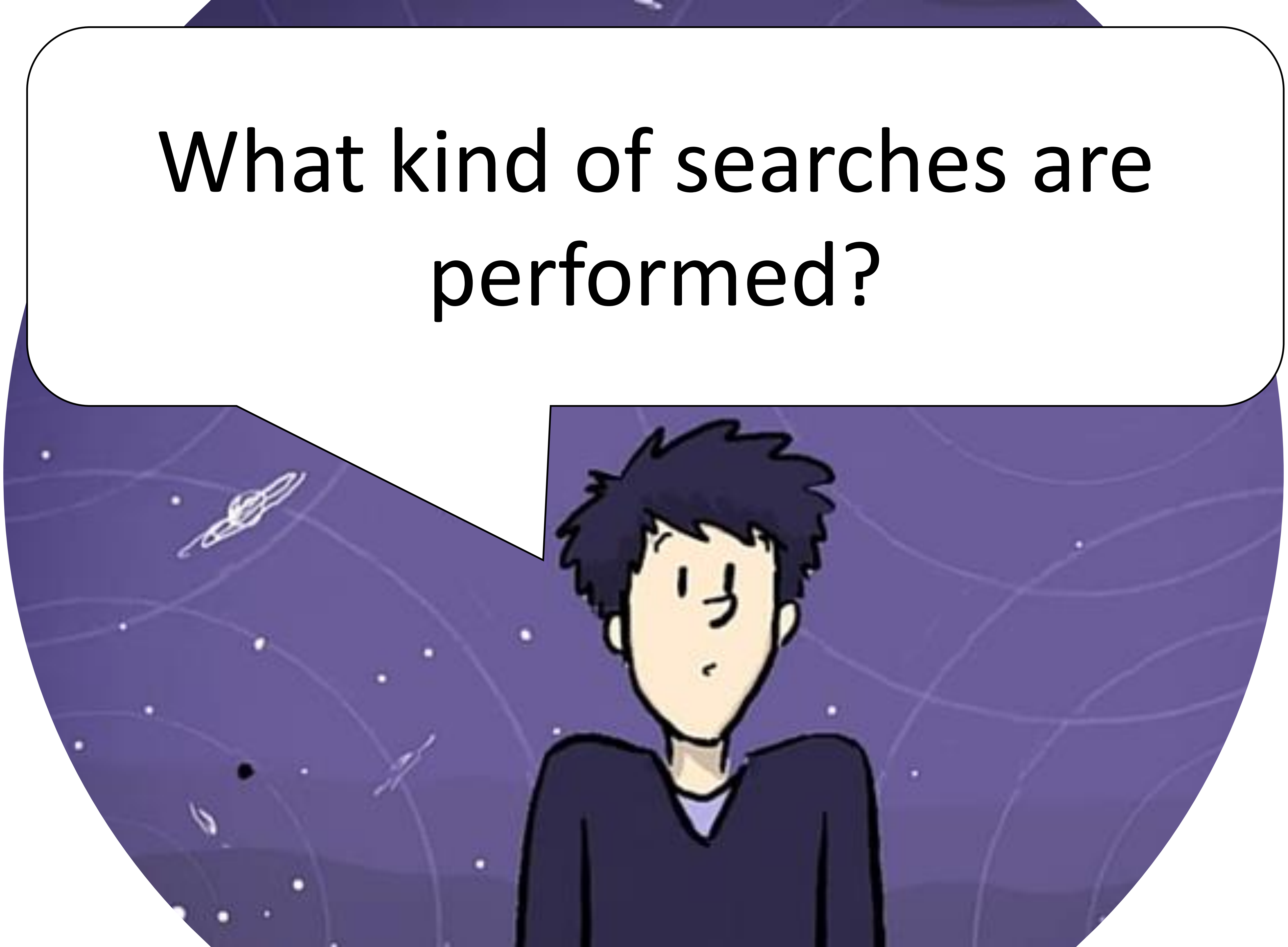

SHORT DURATION

LONG DURATION

MODELLED

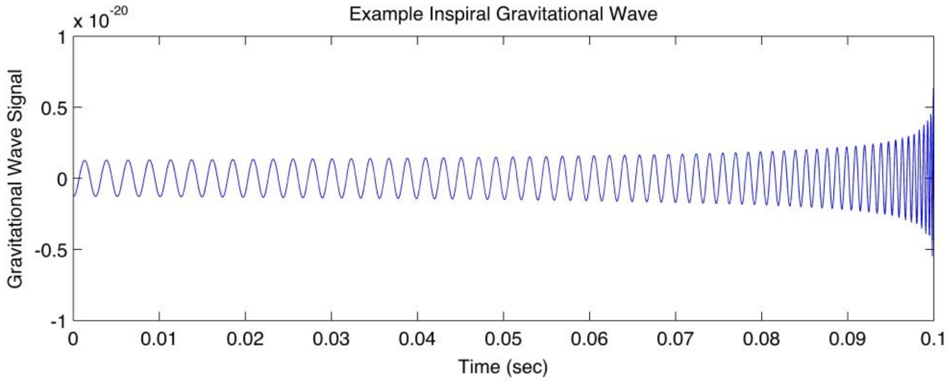

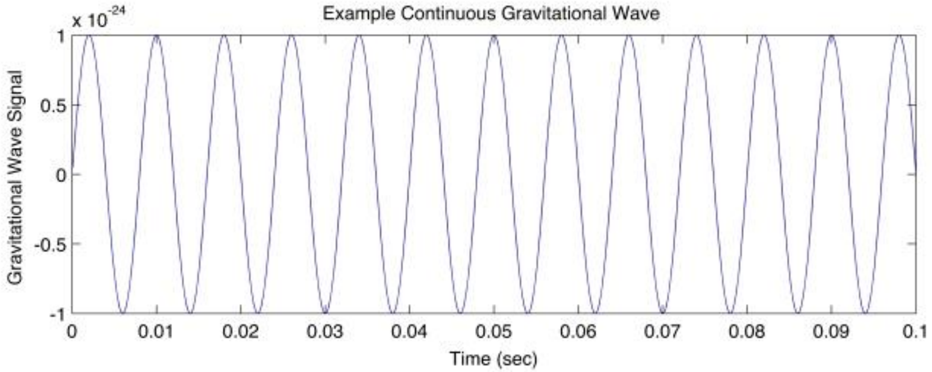

Compact binary coalescence

Continuous waves (CW)

GWs searches

Bursts

Stochastic

UNMODELLED

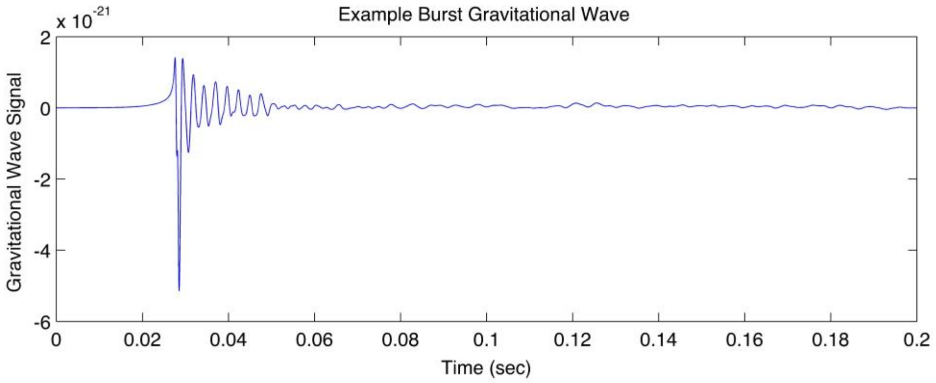

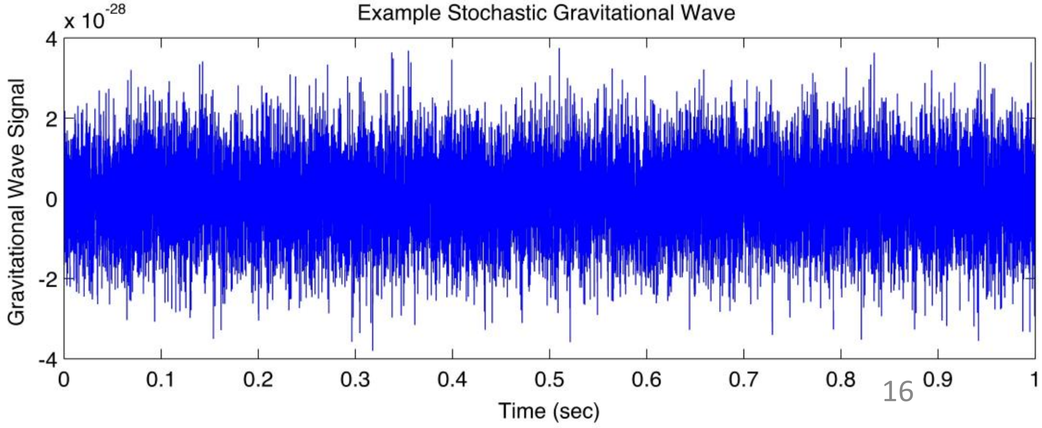

Timeline and future plans

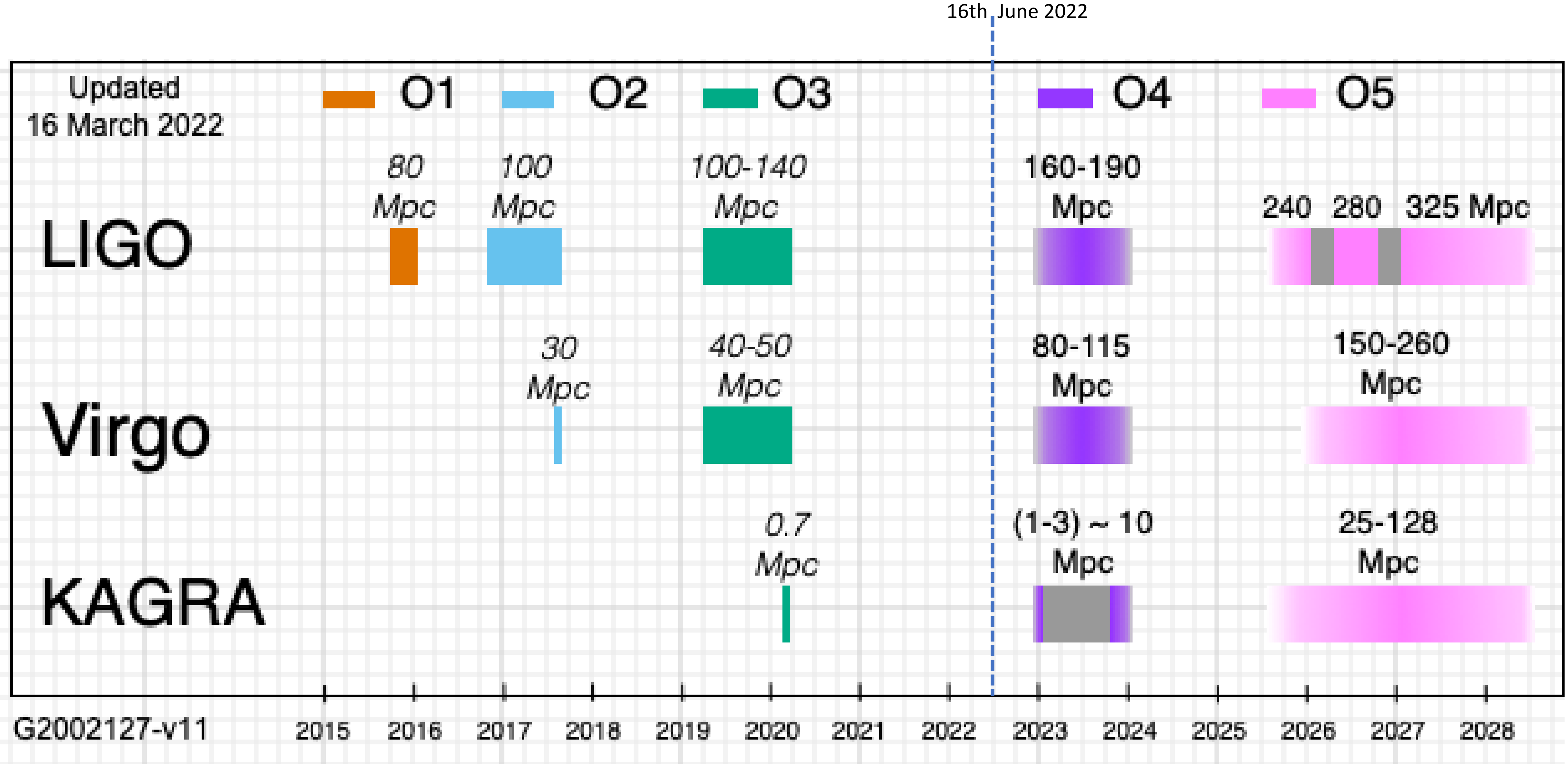

https://observing.docs.ligo.org/plan/


What happened during the first three observing runs?

GWTC: Gravitational Waves Transient Catalog - 3

arXiv
1811.12907
2108.01045
2111.03606

3 GW detection during O1
- First direct detection of GW
- From coalescing binary systems of black holes

8 GW detection during O2
- 1 coalescing binary system of neutron stars: electromagnetic counterpart detected

79 GW detection during O3
- 44 during O3a, including 1 confirmed binary system of neutron stars
- 35 during O3b, including 2 confirmed systems of neutron stars - black holes
- No electromagnetic counterpart

O4 to start end of 2022
- Duration: 1 year

90 GW detections reported

Coalescence of black holes and neutron stars

1 multimessenger event (GW + EM observation)

Mass range 1.2 → 107 $M_\odot$ (stellar)

Distance range 40 Mpc → 8 Gpc (z → 1.14)

Leïla Haegel for the LVK collaboration [2022] https://ligo.northwestern.edu/media/mass-plot/index.html

GWTC-3

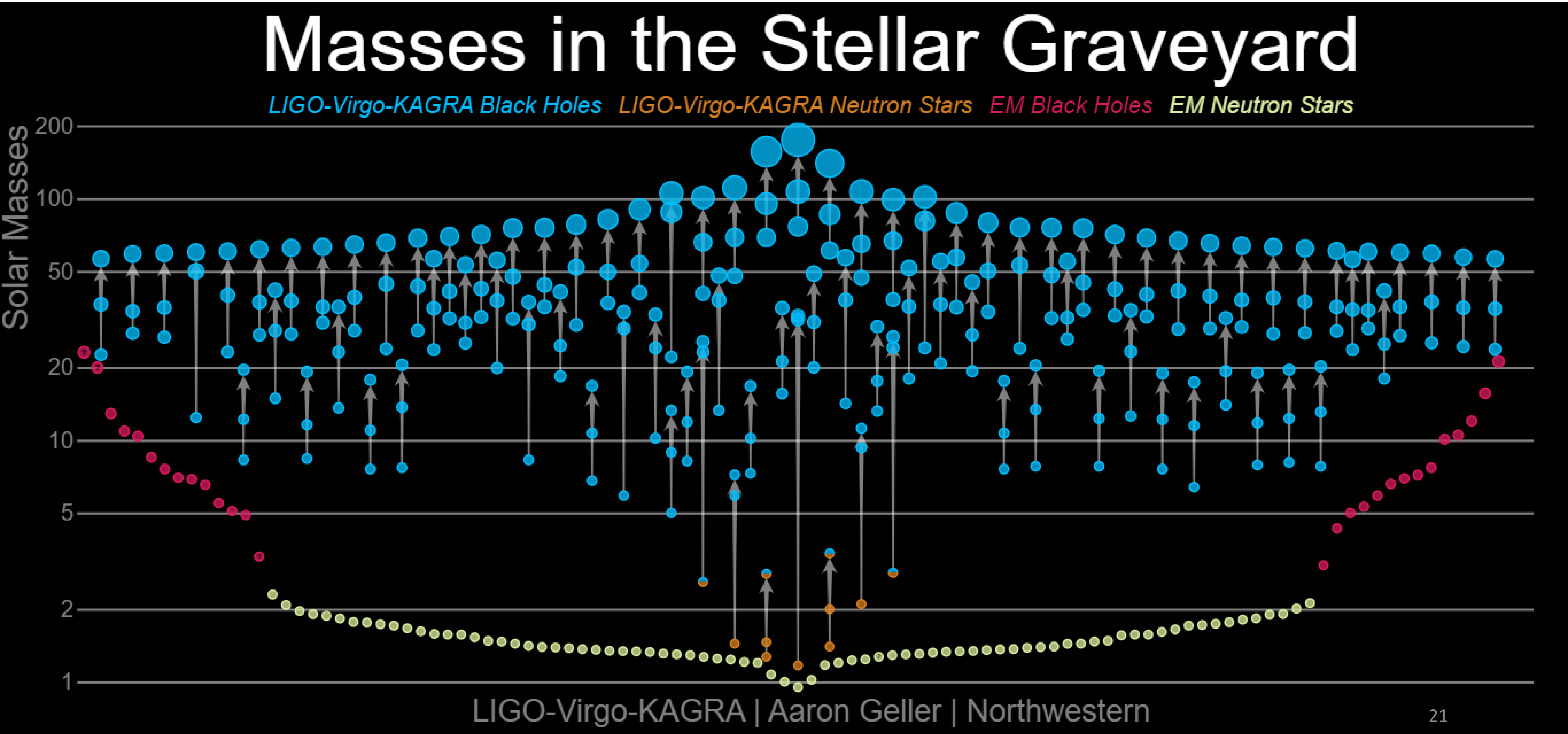

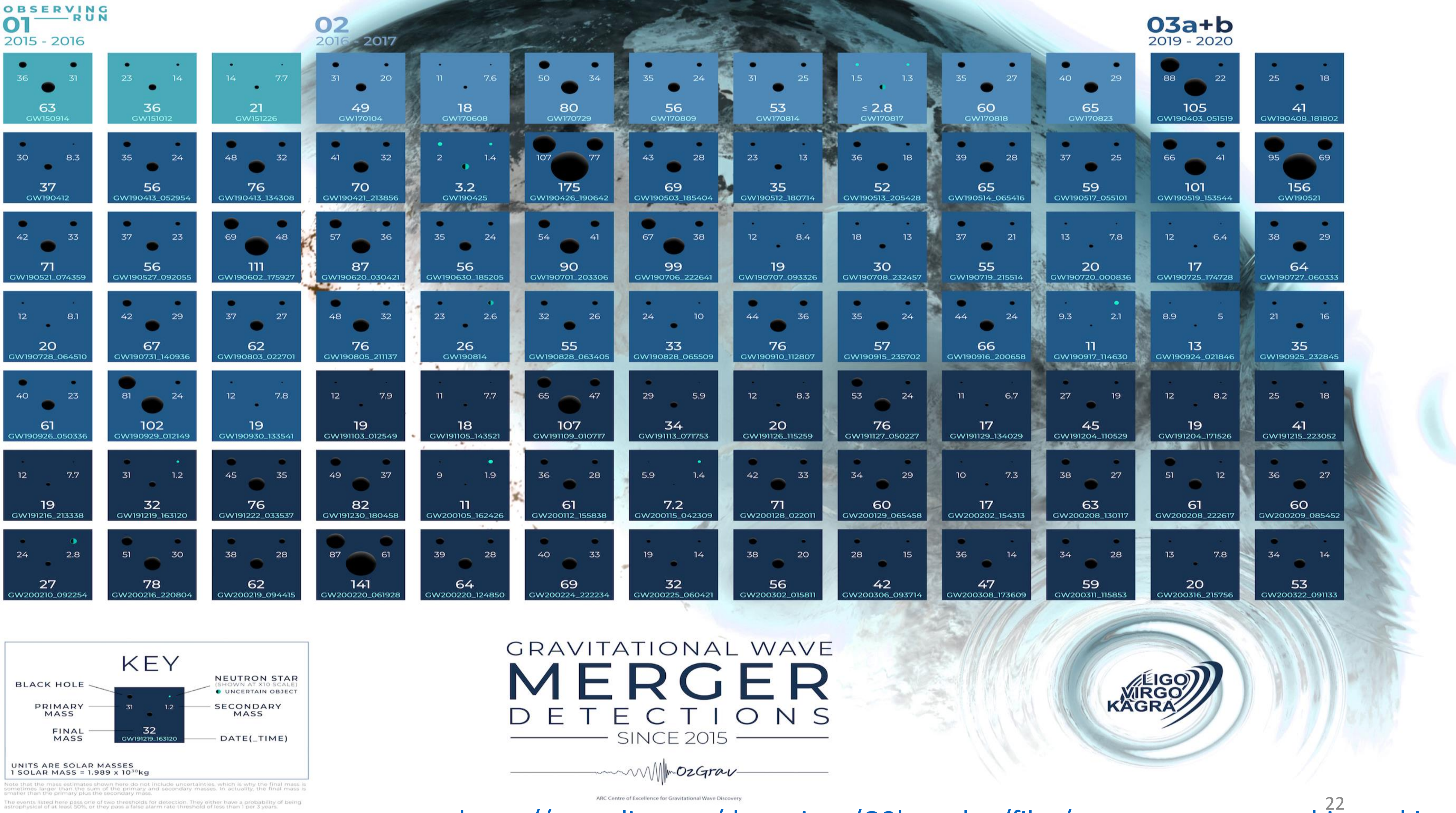

https://www.ligo.org/detections/O3bcatalog/files/gwmerger-poster-white-md.jpg

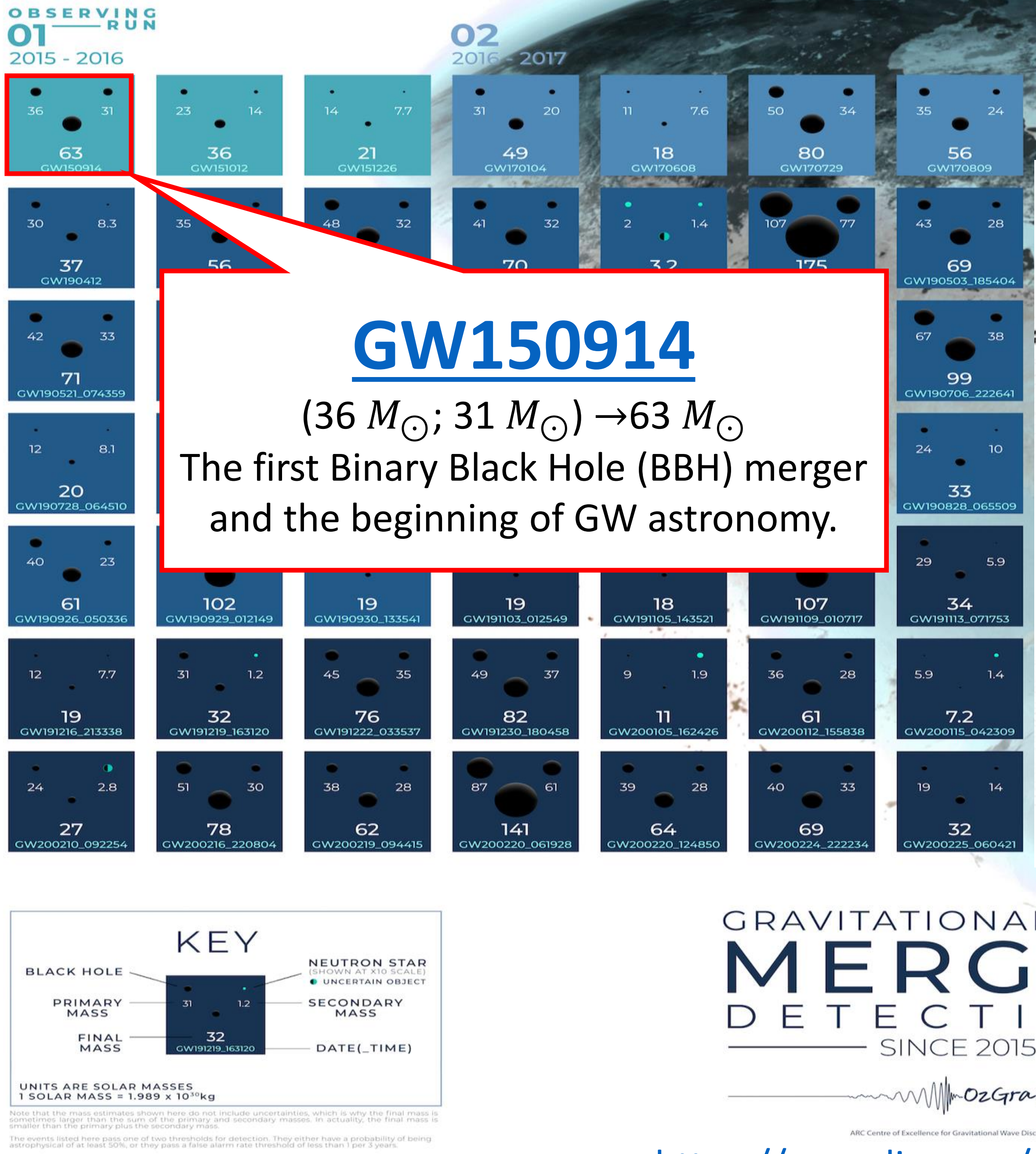

GW150914

($36\ M_\odot$; $31\ M_\odot$) →$63\ M_\odot$

The first Binary Black Hole (BBH) merger and the beginning of GW astronomy.

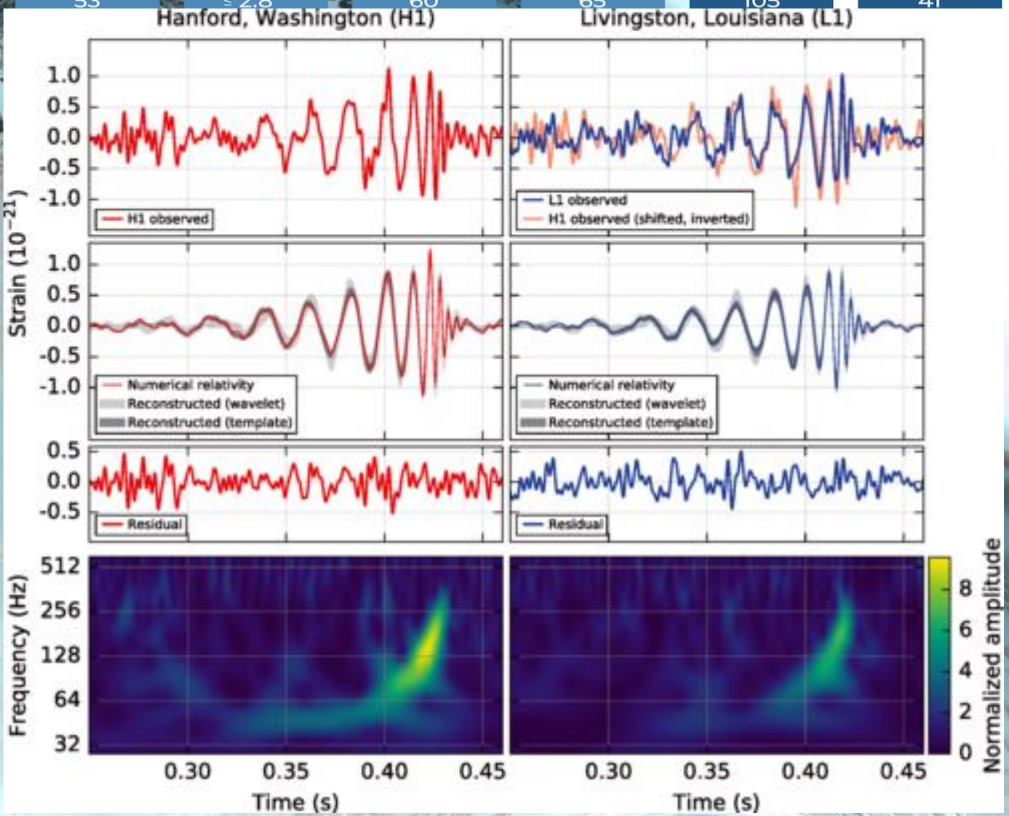

https://www.ligo.org/science/Publication-GW150914/

https://www.ligo.org/detections/O3bcatalog/files/gwmerger-poster-white-md.jpg

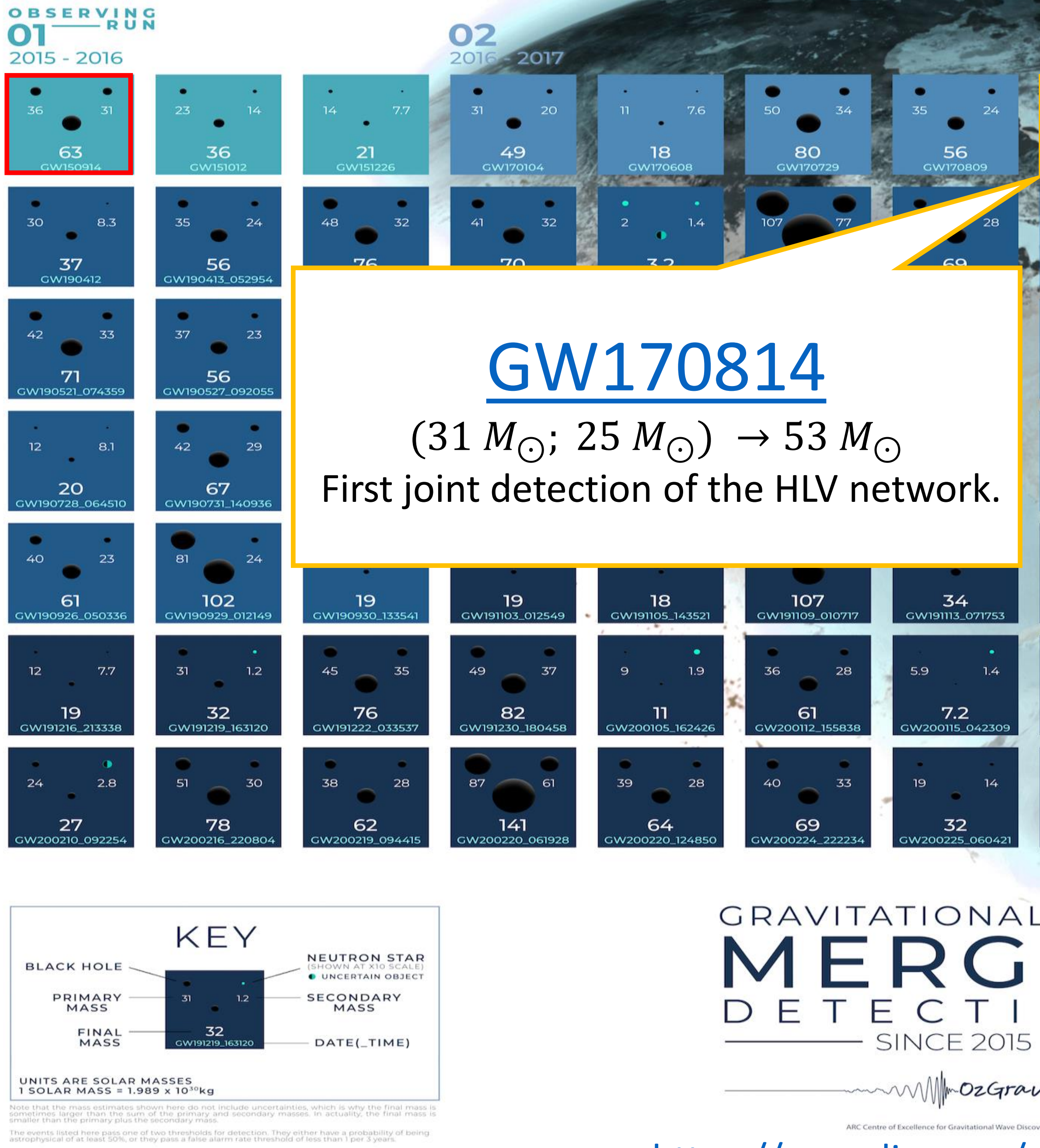

[GW170814](https://www.ligo.org/detections/GW170814.php)

$(31\ M_{\odot};\ 25\ M_{\odot})\ \rightarrow 53\ M_{\odot}$

First joint detection of the HLV network.

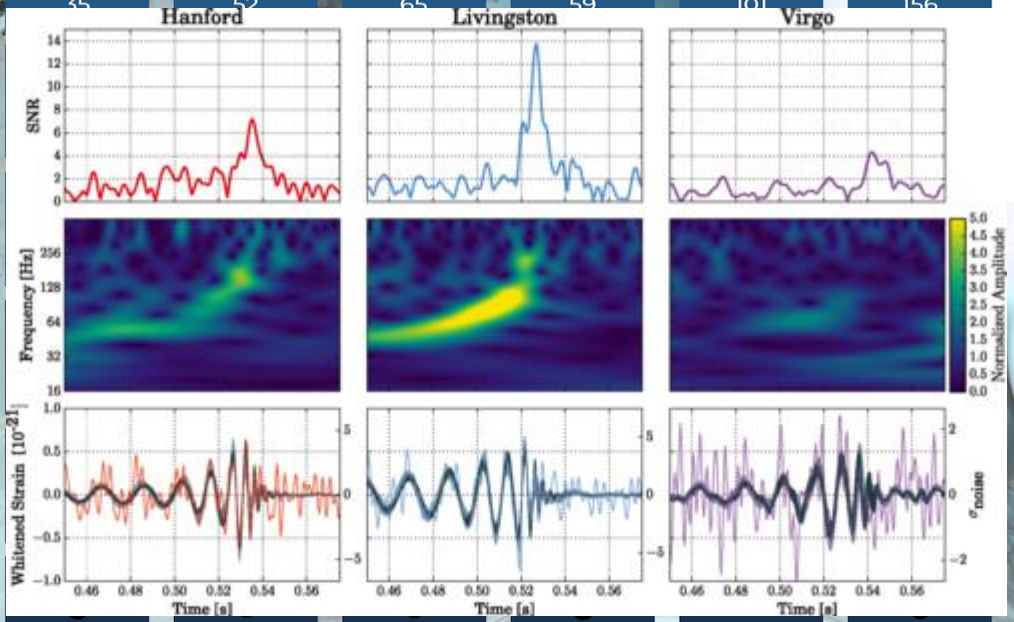

https://www.ligo.org/detections/GW170814.php

https://www.ligo.org/detections/O3bcatalog/files/gwmerger-poster-white-md.jpg

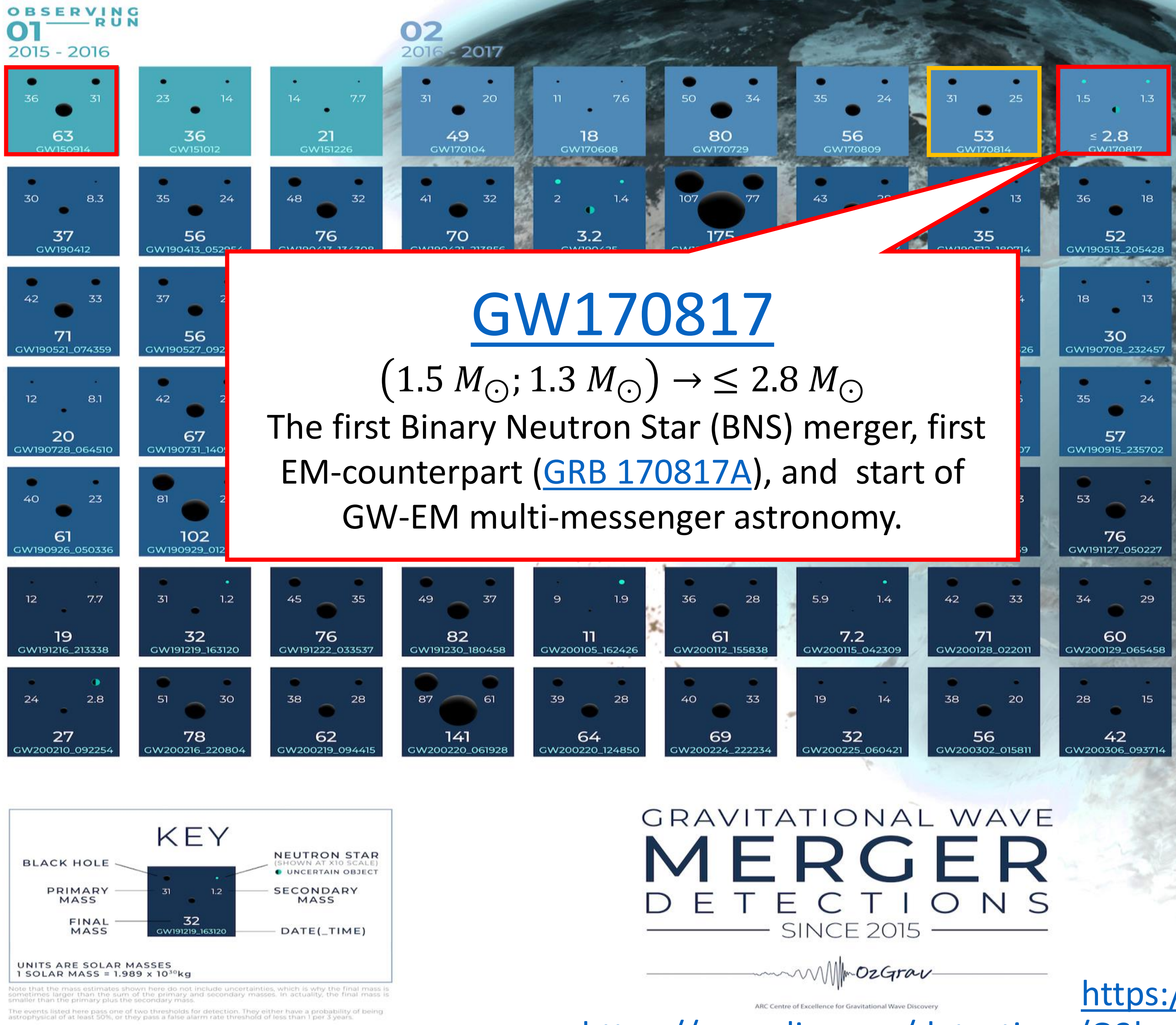

GW170817

$$(1.5\ M_{\odot}; 1.3\ M_{\odot}) \rightarrow \leq 2.8\ M_{\odot}$$

The first Binary Neutron Star (BNS) merger, first EM-counterpart (GRB 170817A), and start of GW-EM multi-messenger astronomy.

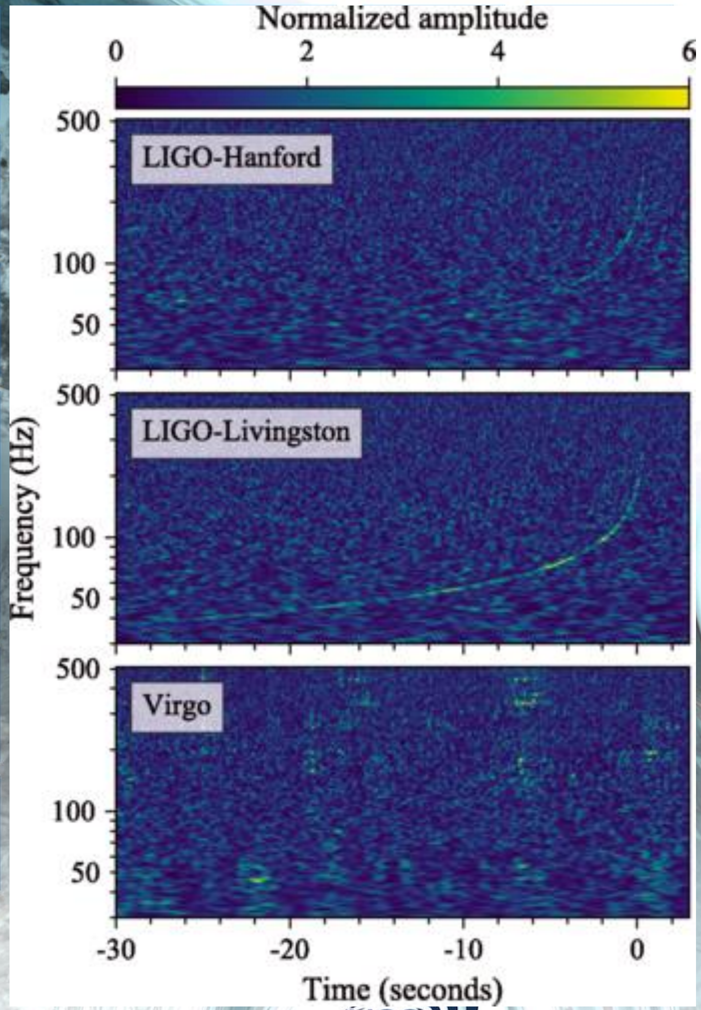

https://www.ligo.org/detections/GW170817.php

https://www.ligo.org/detections/O3bcatalog/files/gwmerger-poster-white-md.jpg

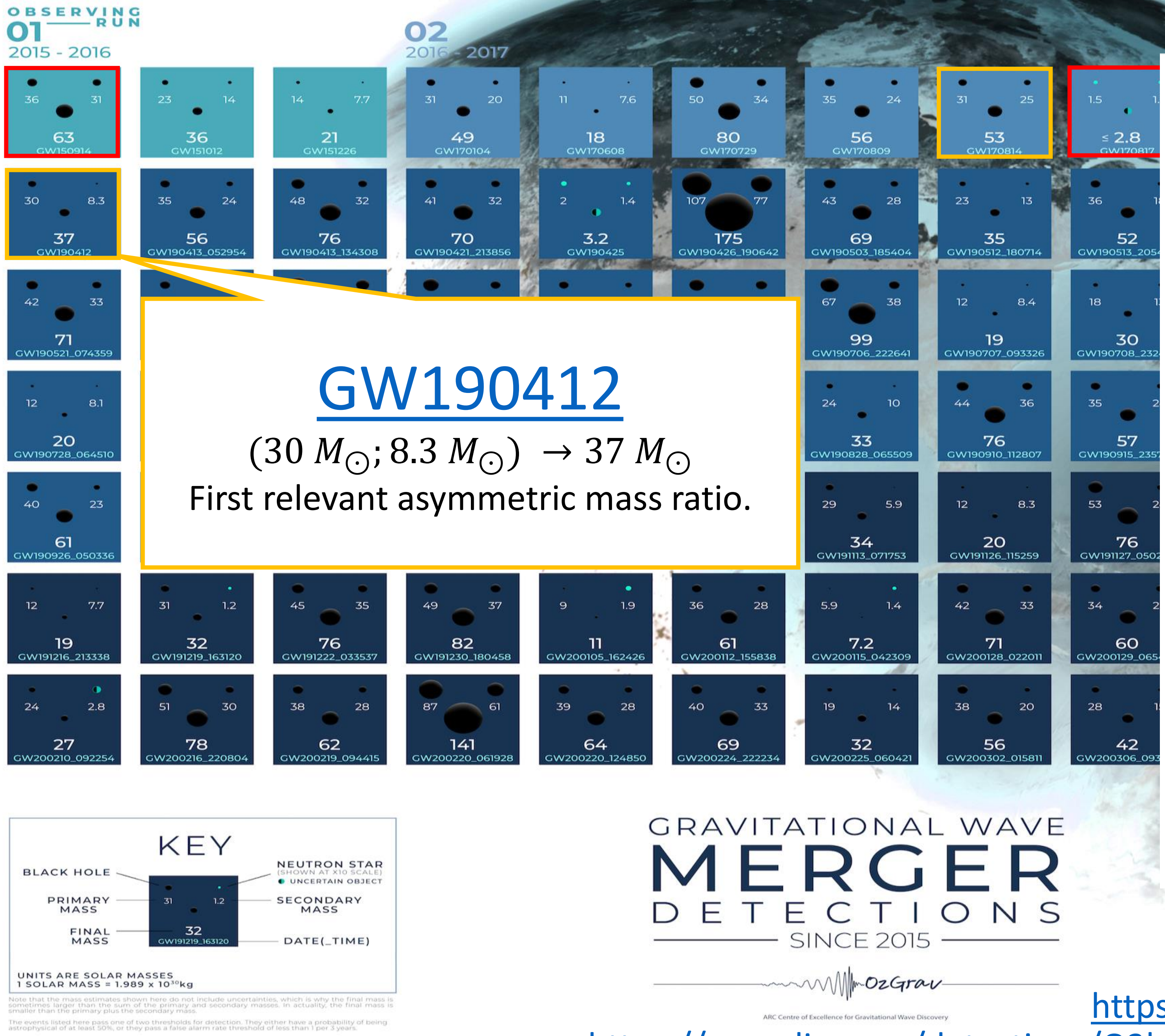

[GW190412](https://www.ligo.org/detections/GW190412.php)

$(30\ M_{\odot}; 8.3\ M_{\odot})\ \rightarrow 37\ M_{\odot}$

First relevant asymmetric mass ratio.

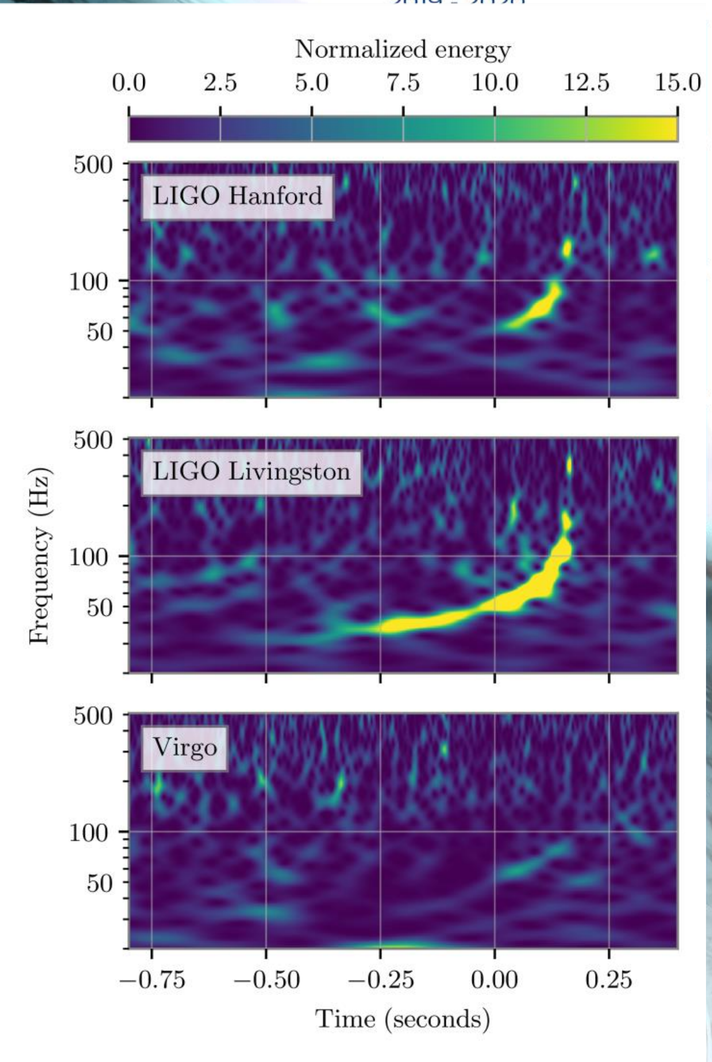

https://www.ligo.org/detections/GW190412.php

https://www.ligo.org/detections/O3bcatalog/files/gwmerger-poster-white-md.jpg

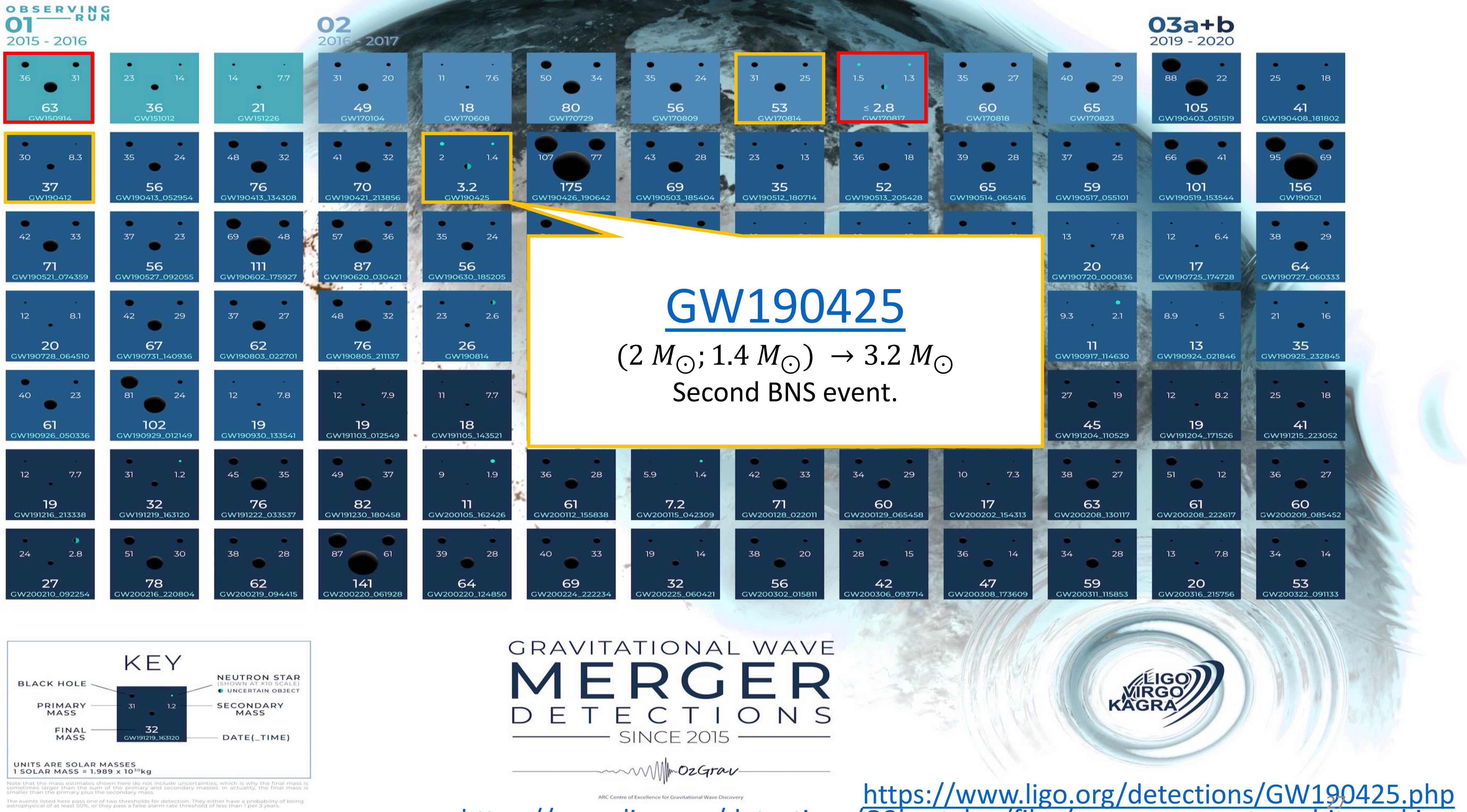

[GW190425](https://www.ligo.org/detections/GW190425.php)

$(2\ M_{\odot}; 1.4\ M_{\odot}) \rightarrow 3.2\ M_{\odot}$

Second BNS event.

https://www.ligo.org/detections/GW190425.php

https://www.ligo.org/detections/O3bcatalog/files/gwmerger-poster-white-md.jpg

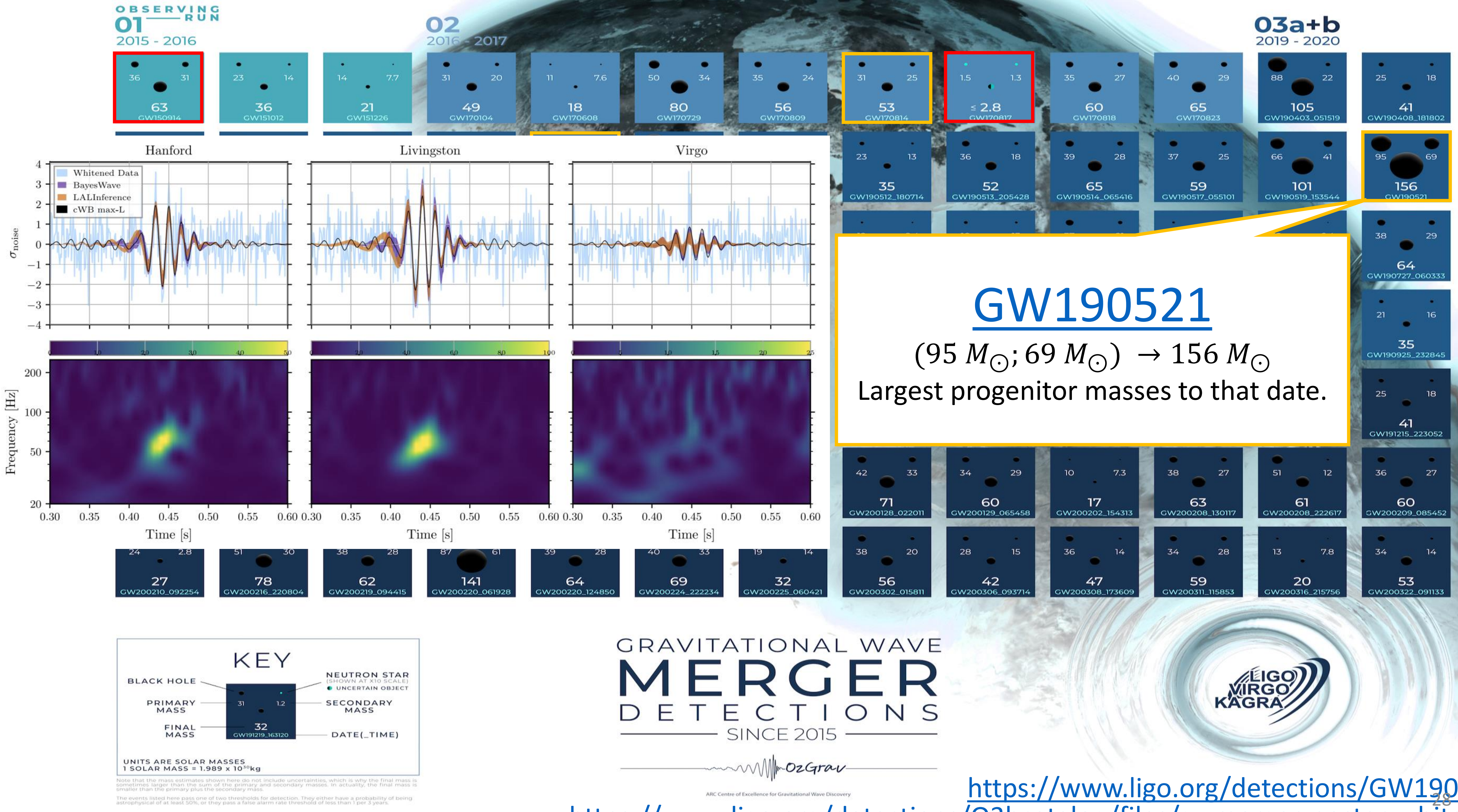

[GW190521](https://www.ligo.org/detections/GW190521.php)

$(95\ M_\odot; 69\ M_\odot) \ \rightarrow 156\ M_\odot$

Largest progenitor masses to that date.

https://www.ligo.org/detections/GW190521.php

https://www.ligo.org/detections/O3bcatalog/files/gwmerger-poster-white-md.jpg

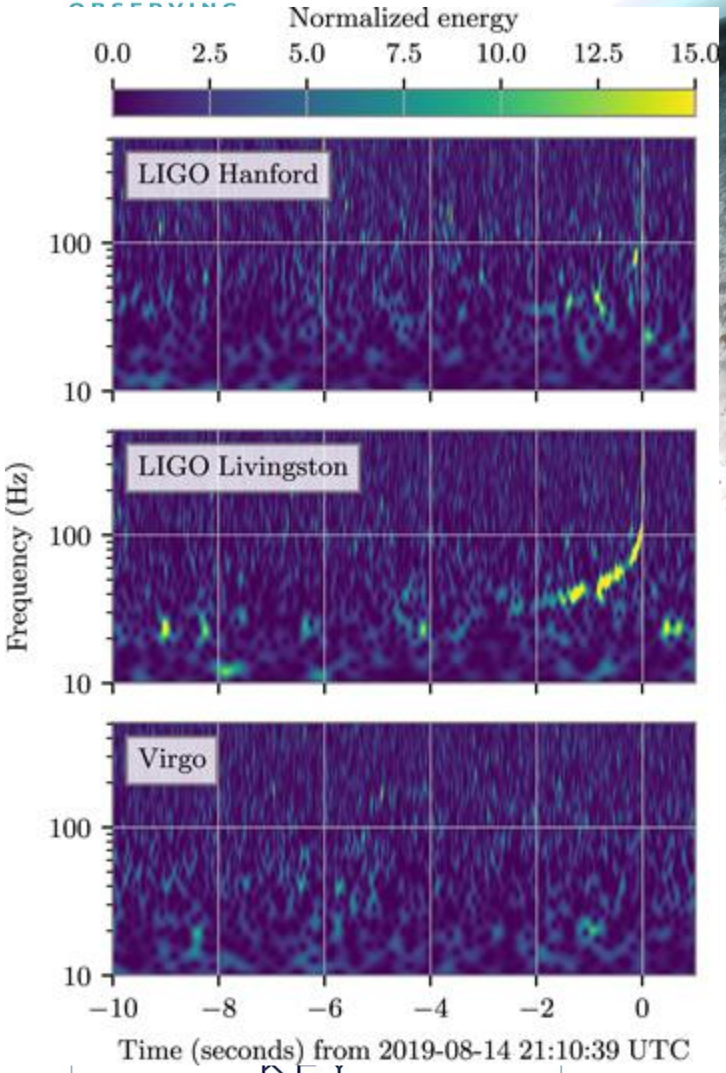

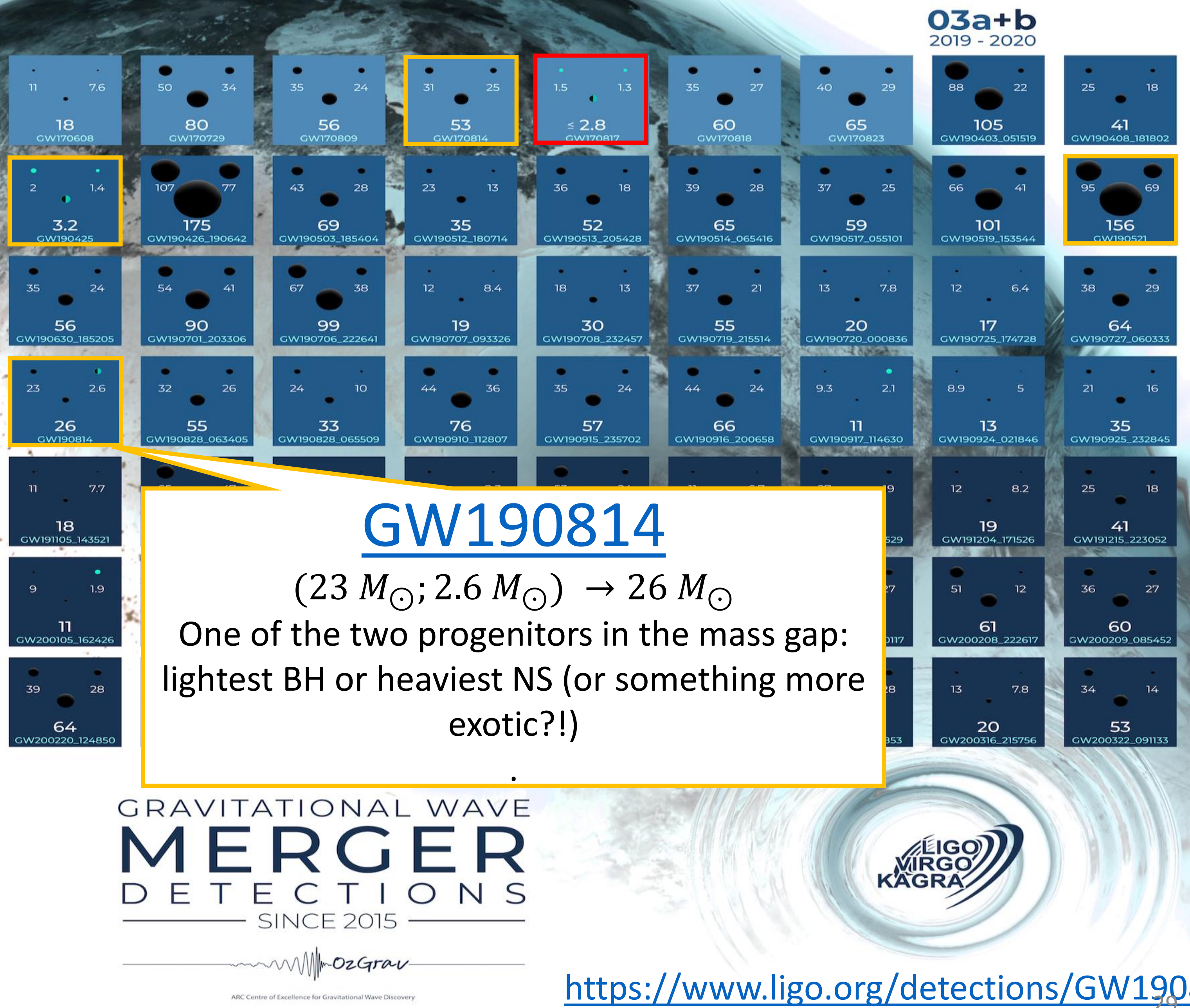

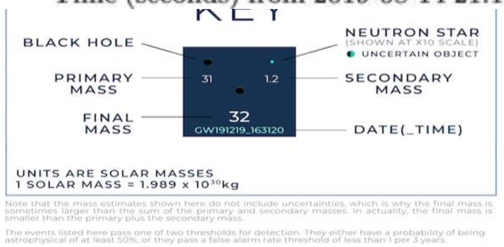

GW190814

$(23\ M_{\odot}; 2.6\ M_{\odot})\ \rightarrow 26\ M_{\odot}$

One of the two progenitors in the mass gap: lightest BH or heaviest NS (or something more exotic?!)

.

https://www.ligo.org/detections/GW190814.php

https://www.ligo.org/detections/O3bcatalog/files/gwmerger-poster-white-md.jpg

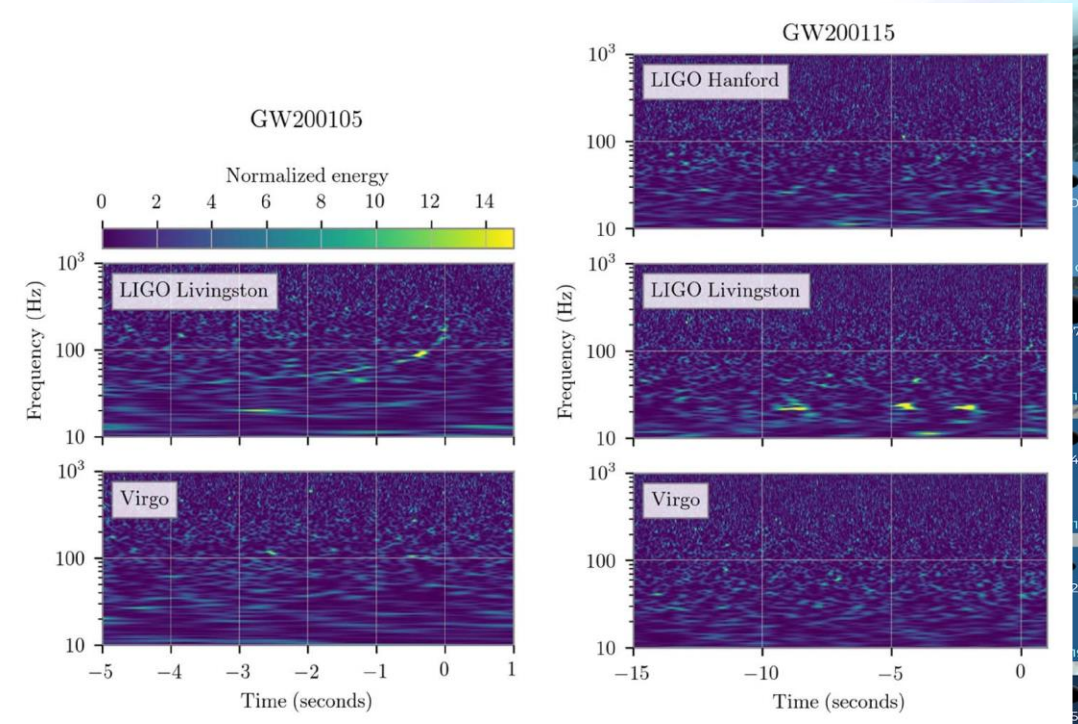

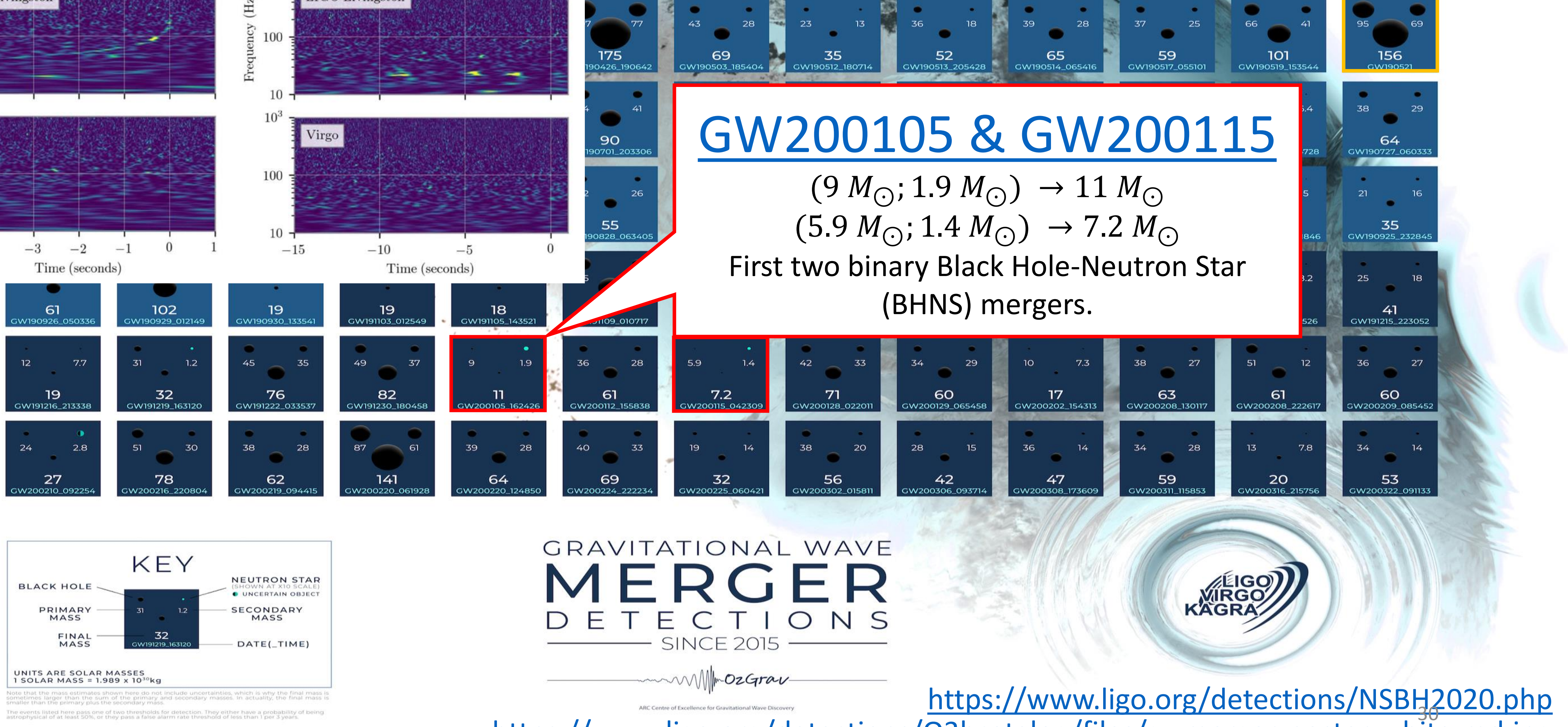

[GW200105 & GW200115](https://www.ligo.org/detections/NSBH2020.php)

$(9\ M_\odot; 1.9\ M_\odot) \rightarrow 11\ M_\odot$

$(5.9\ M_\odot; 1.4\ M_\odot) \rightarrow 7.2\ M_\odot$

First two binary Black Hole-Neutron Star (BHNS) mergers.

https://www.ligo.org/detections/NSBH2020.php

https://www.ligo.org/detections/O3bcatalog/files/gwmerger-poster-white-md.jpg

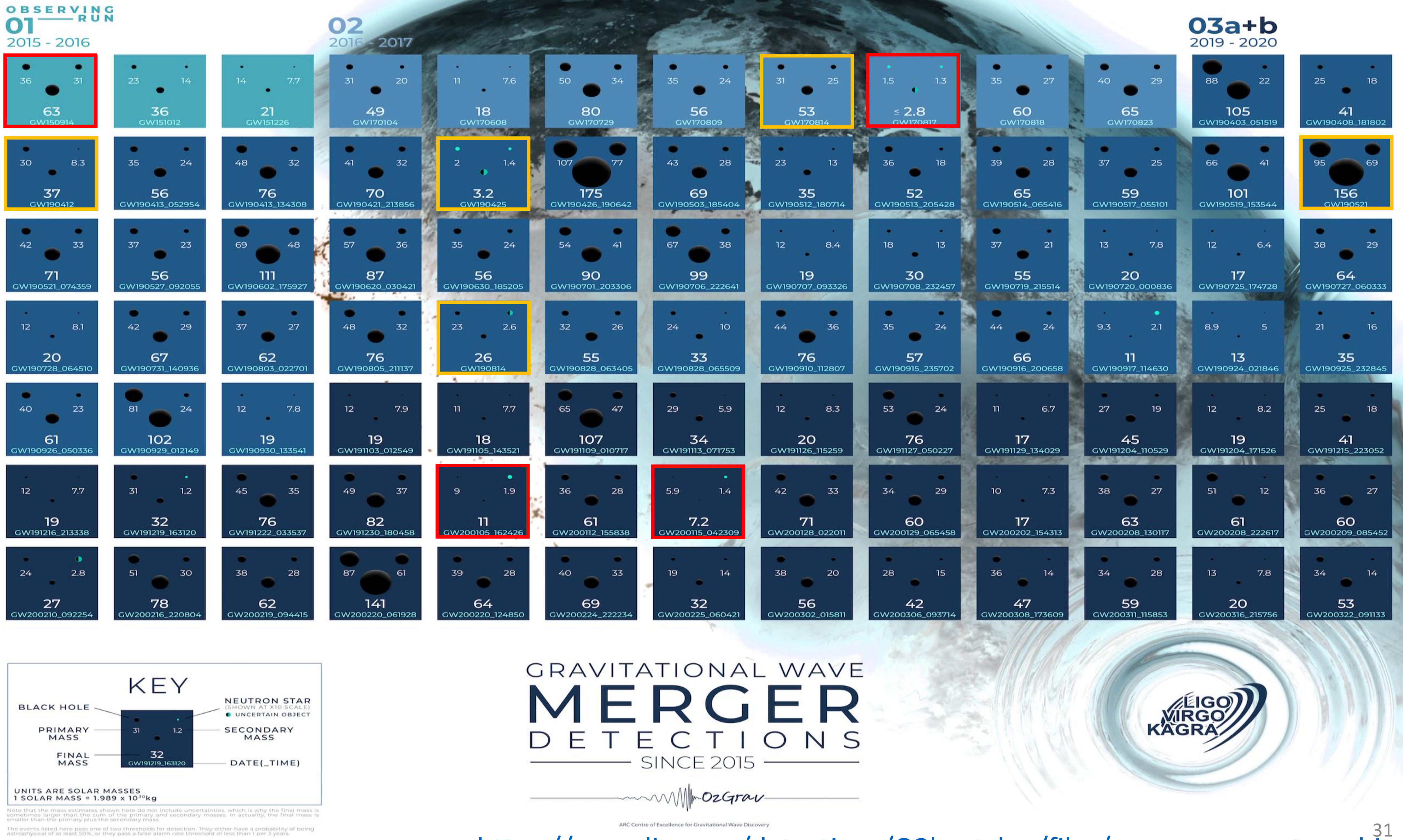

https://www.ligo.org/detections/O3bcatalog/files/gwmerger-poster-white-md.jpg

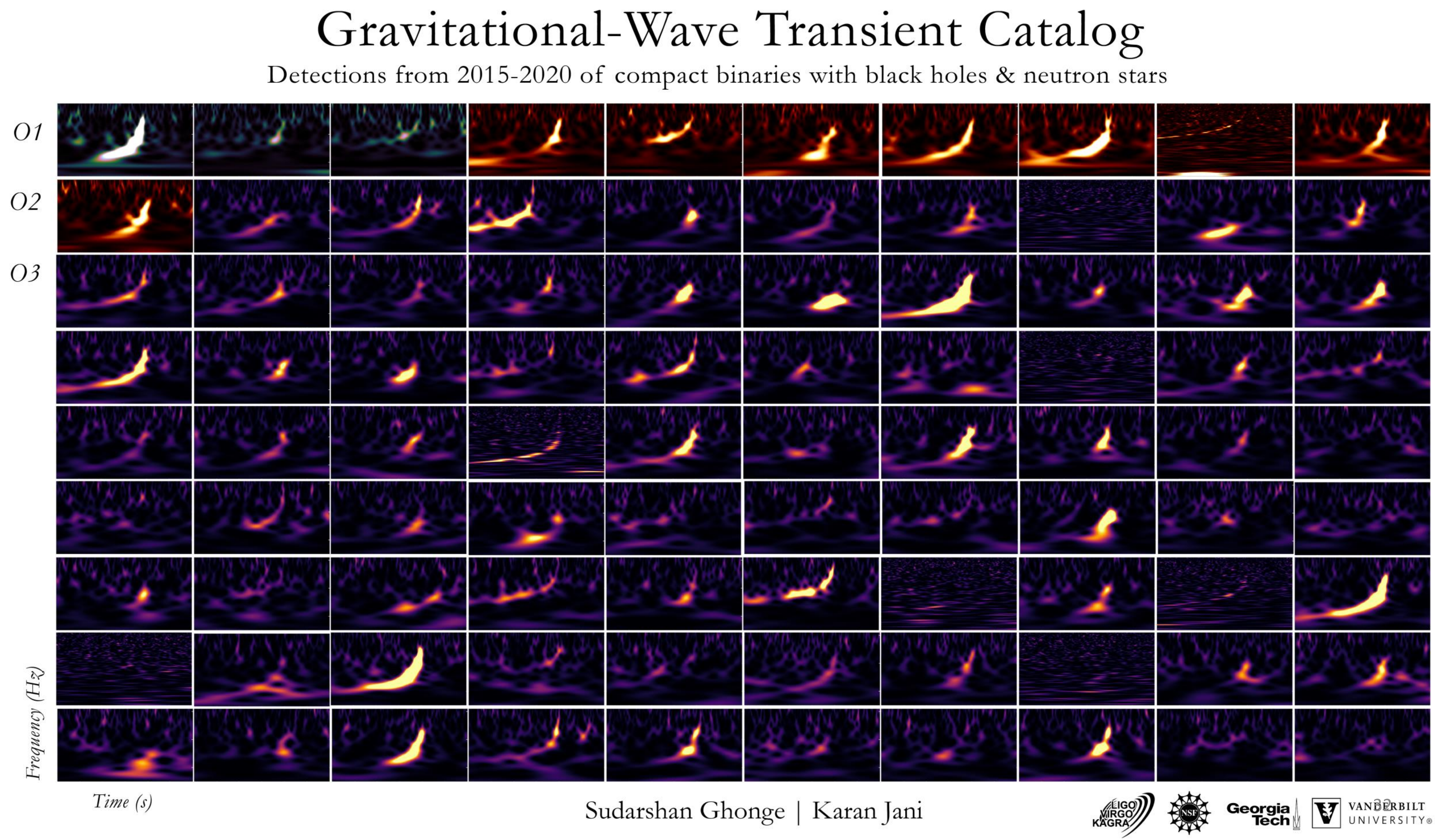

https://www.ligo.org/detections/O3bcatalog/files/GWTC-Poster-O123-Landscape-WhiteBkg.png

Cumulative detections during O1-O2-O3

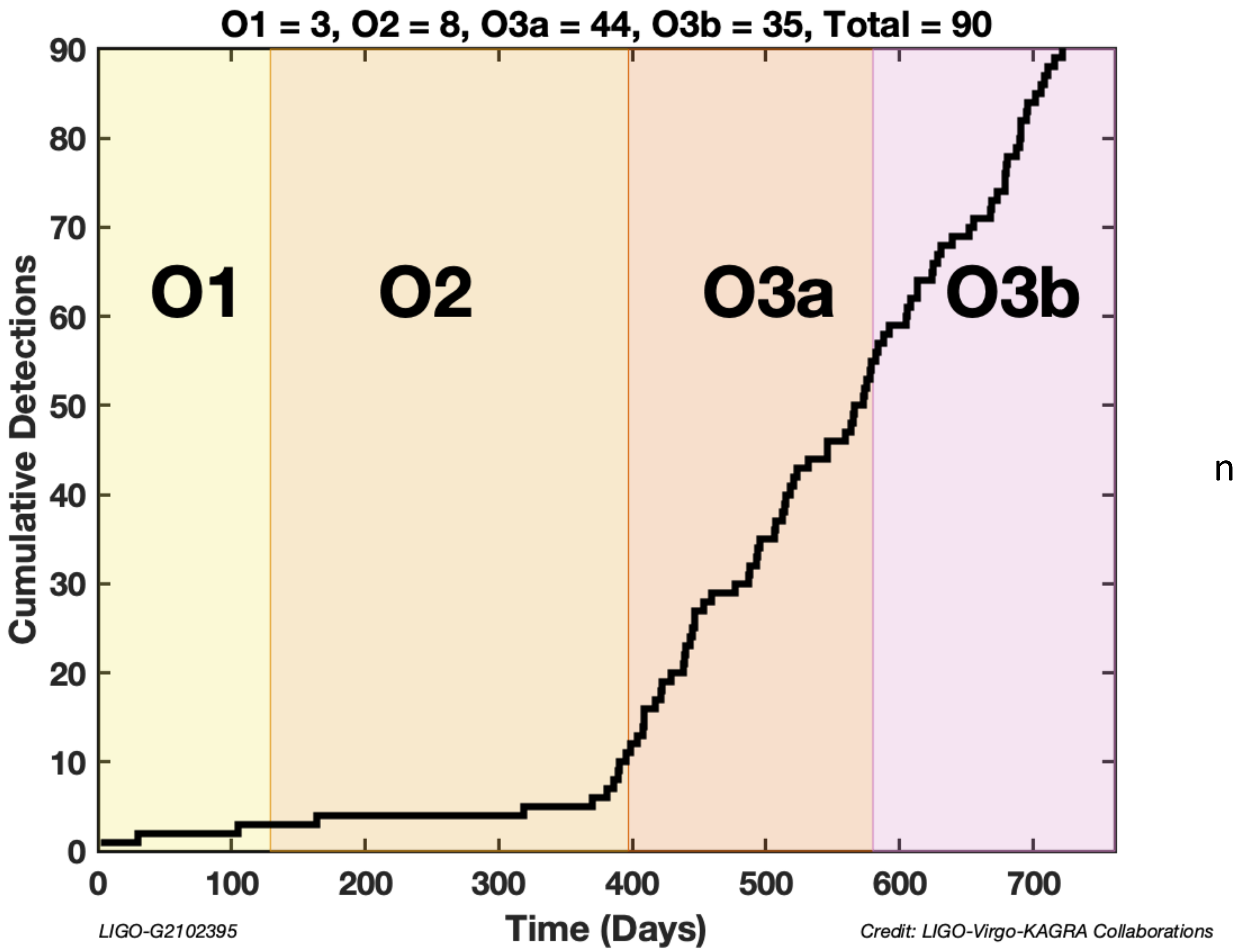

O4 projections: final number of detected events more than doubled!

https://dcc.ligo.org/public/0180/G2102395/001/cumulative_events_GWTC3colors200322.png

Stochastic Gravitational Wave Background (SGWB)

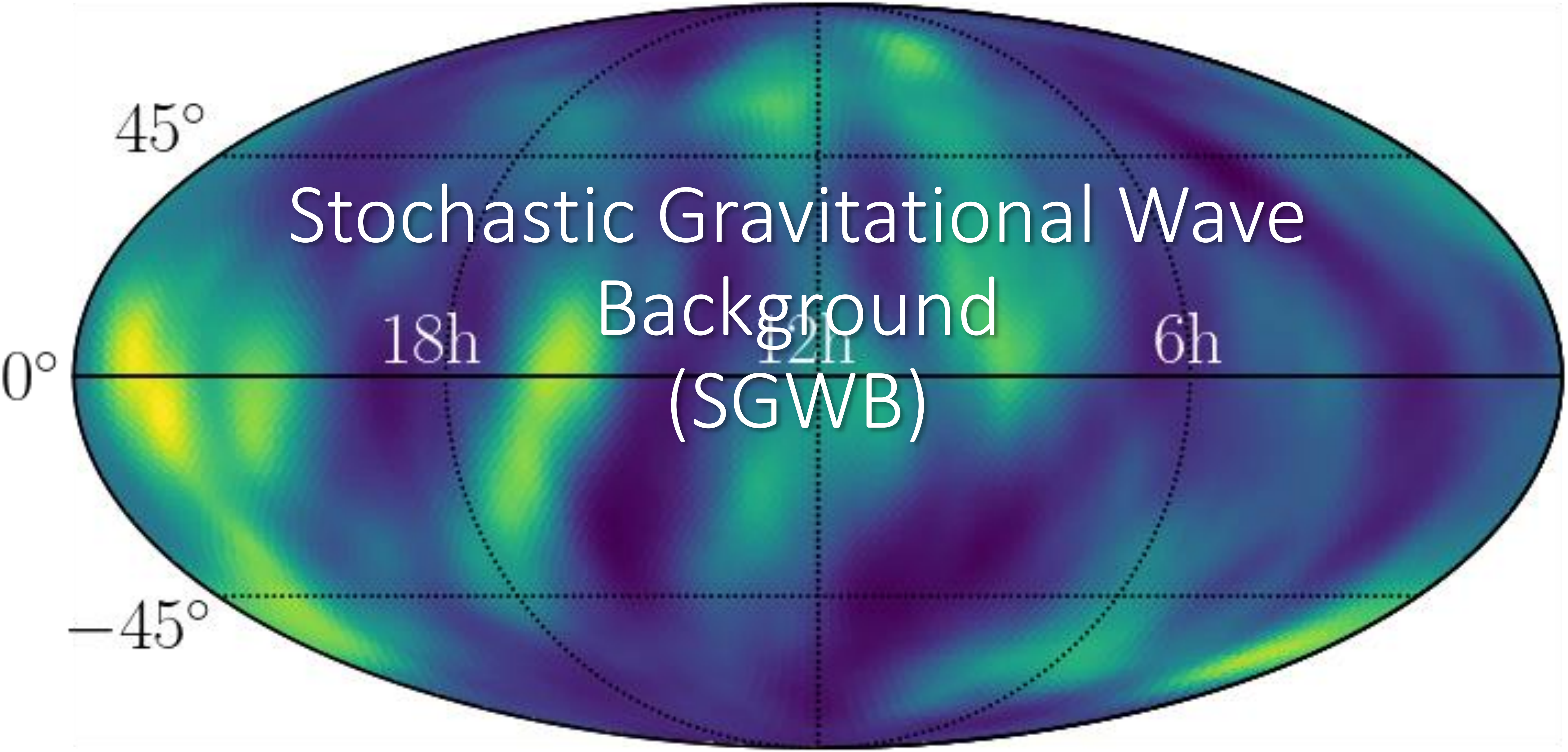

What is a stochastic gravitational-wave background?

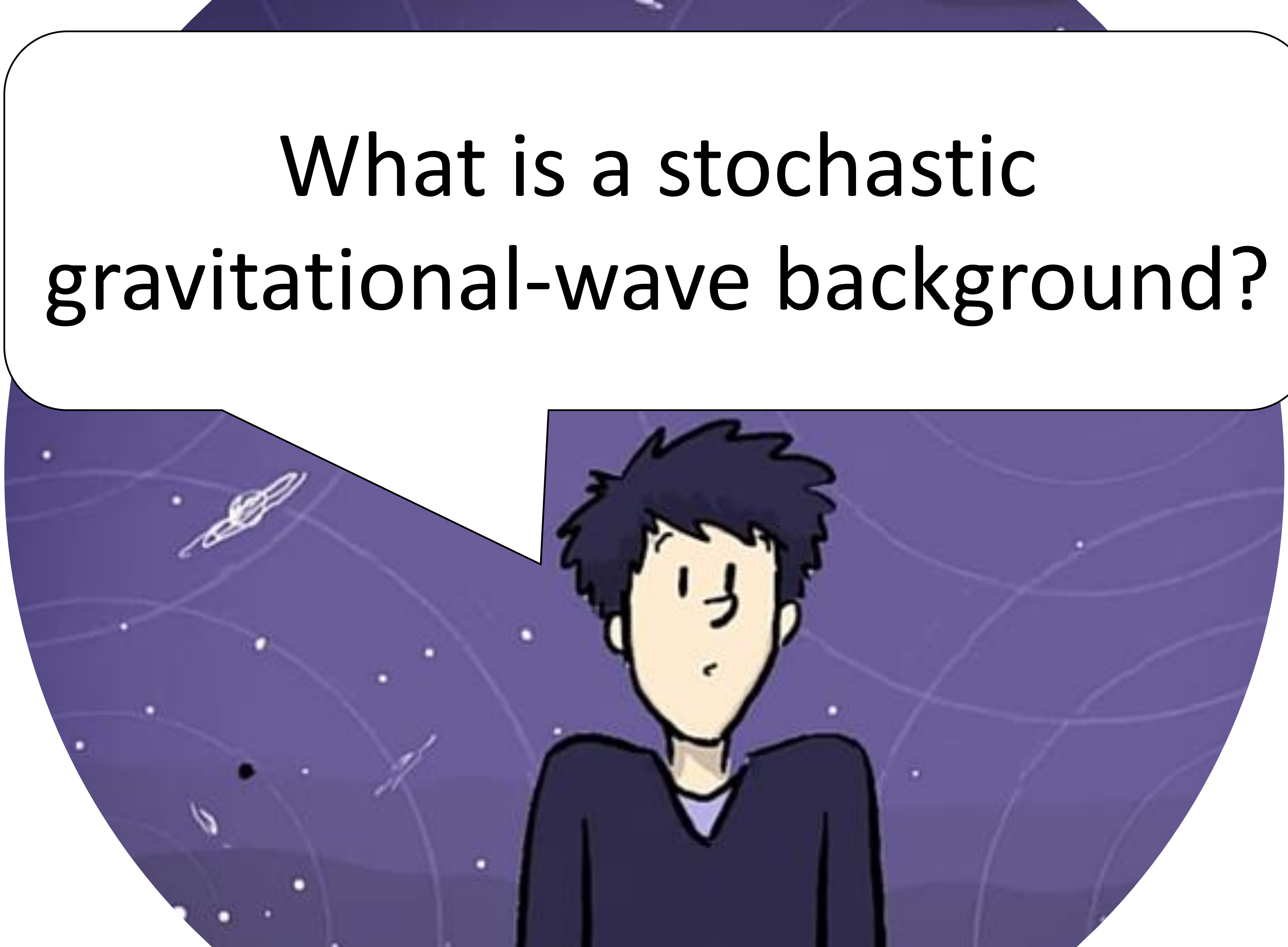

What is a SGWB?

Noise?!

What is a SGWB?

Noise?!

or rather

SYMPHONY OF THE UNIVERSE!

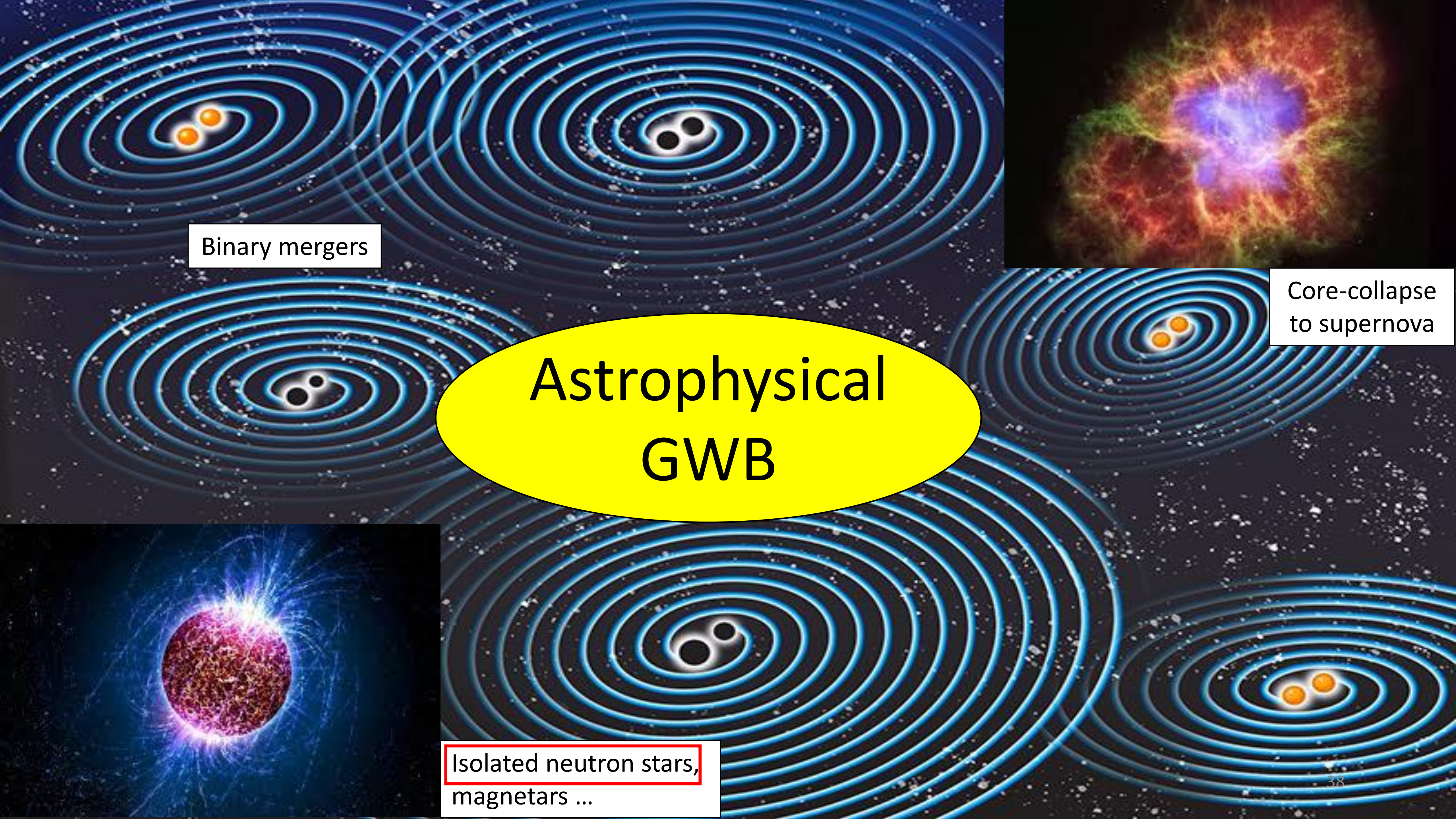
Binary mergers
Core-collapse to supernova
Astrophysical GWB
Isolated neutron stars, magnetars …

Cosmic GWB: Sources/mechanisms

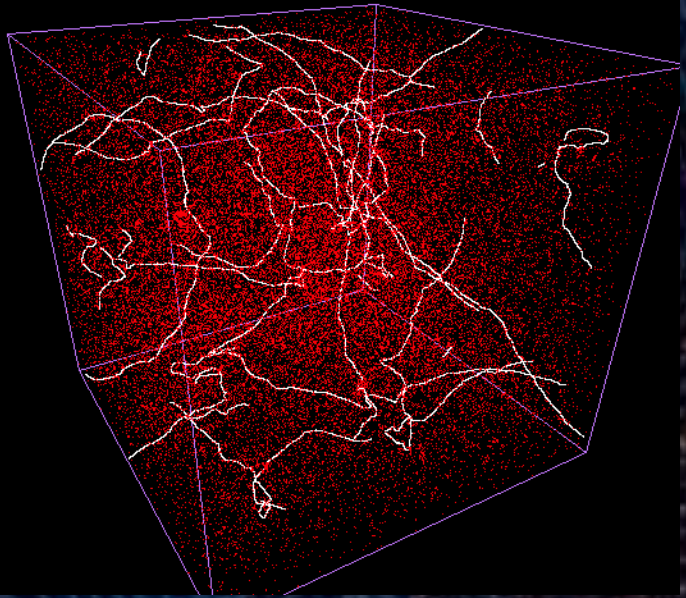

Cosmic Strings

Primordial Black Holes

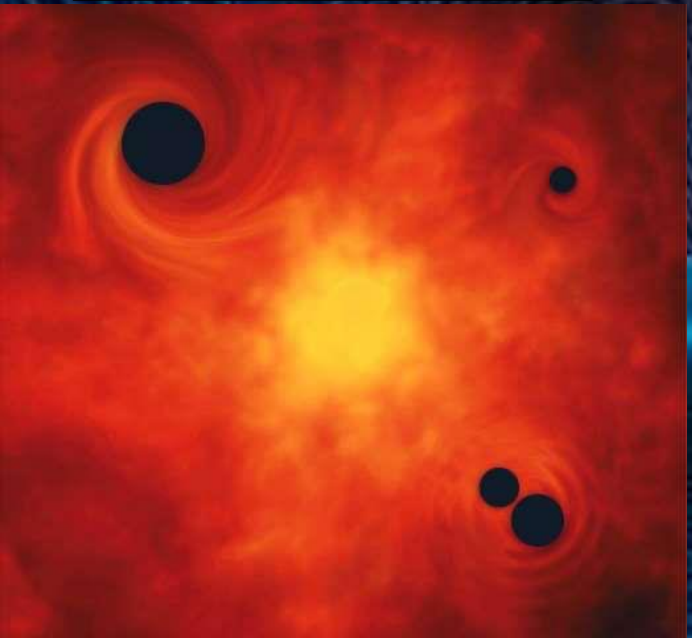

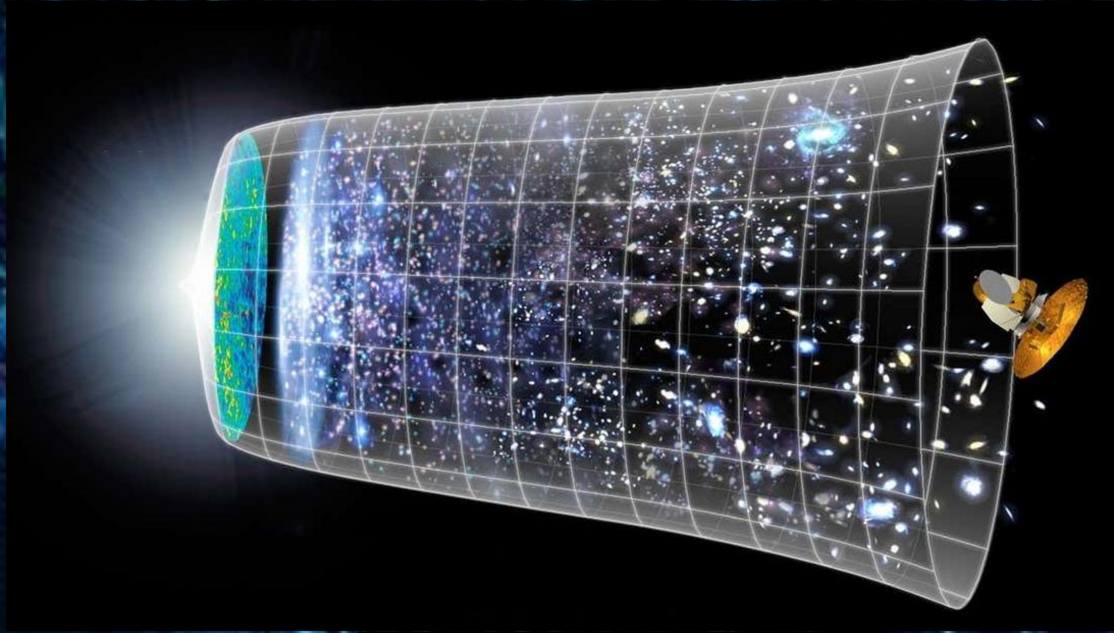

Slow-Roll Inflation

First Order Phase Transition

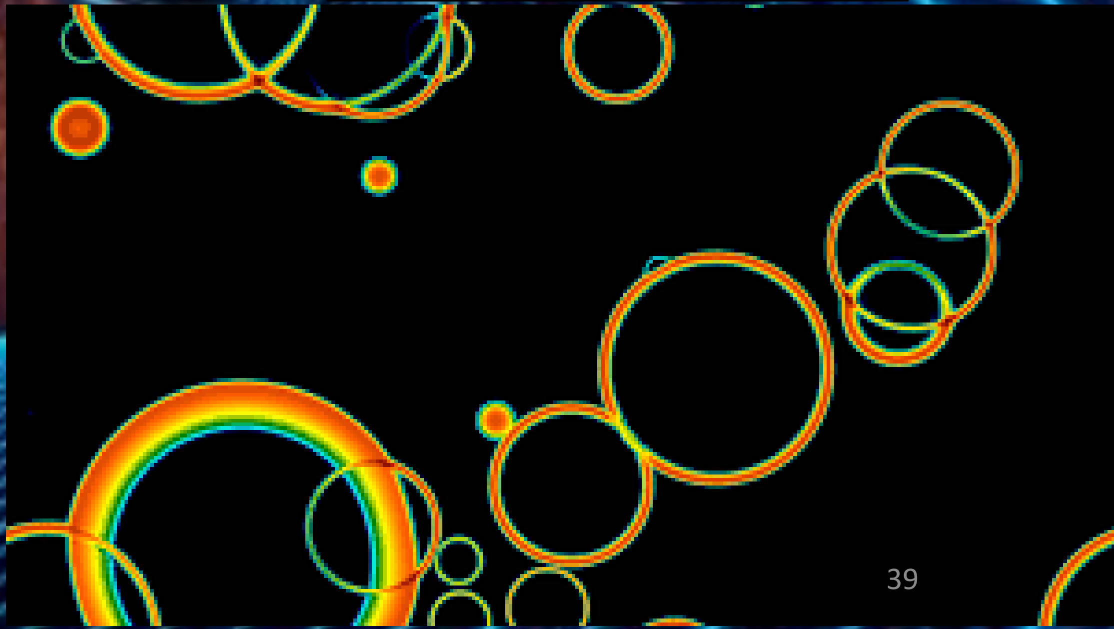

What is a SGWB? - Definition

“Textboook” definition

A random gravitational-wave signal produced by a large number of weak, independent and unresolved sources.

Characterizable only statistically

Depend on details of the observation

Not decomposable into separate and individually detectable sources

What is a SGWB? - Definition

"Textboook" definition

A random gravitational-wave signal produced by a large number of weak, independent and unresolved sources.

Characterizable only statistically

Depend on details of the observation

Not decomposable into separate and individually detectable sources

Plane wave expansion (TT gauge)

$$h_{ab}(t,\vec{\boldsymbol{x}}) = \int_{-\infty}^{\infty} df \int d^2\Omega_{\hat{\boldsymbol{n}}}\, h_{ab}(f,\hat{\boldsymbol{n}}) e^{2\pi i f(t+\hat{\boldsymbol{n}}\cdot\vec{\boldsymbol{x}}/c)} \qquad h_{ab}(f,\hat{\boldsymbol{n}}) = \sum_{A=+,\times} h_A(f,\hat{\boldsymbol{n}}) e^A_{ab}(\hat{\boldsymbol{n}})$$

RANDOM VARIABLES

Fully characterized by

Statistical momenta

$$\langle h_{ab}(t,\vec{\boldsymbol{x}})\rangle, \qquad \langle h_{ab}(t,\vec{\boldsymbol{x}}) h_{cd}(t',\vec{\boldsymbol{x}}')\rangle, \qquad \langle h_{ab}(t,\vec{\boldsymbol{x}}) h_{cd}(t,'\vec{\boldsymbol{x}}') h_{ef}(t'',\vec{\boldsymbol{x}}'')\rangle, \ldots$$

What is a SGWB? - Definition

"Textboook" definition

A random gravitational-wave signal produced by a large number of weak, independent and unresolved sources.

Characterizable only statistically

Depend on details of the observation

Not decomposable into separate and individually detectable sources

Plane wave expansion (TT gauge)

$$h_{ab}(t,\vec{\boldsymbol{x}}) = \int_{-\infty}^{\infty} df \int d^2\Omega_{\hat{\boldsymbol{n}}}\, h_{ab}(f,\hat{\boldsymbol{n}}) e^{2\pi i f(t+\hat{\boldsymbol{n}}\cdot\vec{\boldsymbol{x}}/c)} \qquad h_{ab}(f,\hat{\boldsymbol{n}}) = \sum_{A=+,\times} h_A(f,\hat{\boldsymbol{n}}) e^A_{ab}(\hat{\boldsymbol{n}})$$

RANDOM VARIABLES

Fully characterized by

Statistical momenta

$$\langle h_{ab}(t,\vec{\boldsymbol{x}})\rangle, \qquad \langle h_{ab}(t,\vec{\boldsymbol{x}}) h_{cd}(t',\vec{\boldsymbol{x}}')\rangle, \qquad \langle h_{ab}(t,\vec{\boldsymbol{x}}) h_{cd}(t,'\vec{\boldsymbol{x}}') h_{ef}(t'',\vec{\boldsymbol{x}}'')\rangle, \ldots$$

Standard hypothesis

$\langle h_{ab}(t,\vec{\boldsymbol{x}})\rangle = 0 \Leftrightarrow \langle h_A(f,\hat{\boldsymbol{n}})\rangle = 0$ + **Gaussianity**

Fully characterized by the 2-points correlator!

What is a SGWB? – Quantities of interest

Energy density ratio for GW

$$\boxed{\Omega_{GW} = \int_{f=0}^{f_{max}} \Omega_{gw}(f)\, df}$$

What is a SGWB? – Quantities of interest

Energy density ratio for GW

$$\Omega_{GW} = \int_{f=0}^{f_{max}} \Omega_{gw}(f)\, df$$

GW Energy density

$$\Omega_{gw}(f) = \frac{f}{\rho_c}\frac{d\rho_{gw}}{df}(f), \qquad \rho_c = \frac{3H_0^2}{8\pi G}$$

Critical density

$$\rho_{GW} = \frac{\langle \dot{h}_{ij}(t,\vec{\boldsymbol{x}})\, \dot{h}_{ij}(t,\vec{\boldsymbol{x}})\rangle}{32\pi G} = \int_{f=0}^{f_{max}} f\,\frac{d\rho_{gw}}{df}\, df$$

Related to

Characteristic strain amplitude

$$\Omega_{gw}(f) = \frac{2\pi^2}{3H_0^2} f^2 h_c^2(f), \qquad h_c(f) \equiv \sqrt{f S_h(f)}$$

What is a SGWB? – Quantities of interest

Energy density ratio for GW

$$\Omega_{GW} = \int_{f=0}^{f_{max}} \Omega_{gw}(f)\, df$$

GW Energy density

$$\Omega_{gw}(f) = \frac{f}{\rho_c}\frac{d\rho_{gw}}{df}(f), \qquad \rho_c = \frac{3H_0^2}{8\pi G}$$ Critical density

$$\rho_{GW} = \frac{\langle \dot{h}_{ij}(t,\vec{x})\, \dot{h}_{ij}(t,\vec{x})\rangle}{32\pi G} = \int_{f=0}^{f_{max}} f\frac{d\rho_{gw}}{df}\, df$$

Related to

Characteristic strain amplitude

$$\Omega_{gw}(f) = \frac{2\pi^2}{3H_0^2} f^2 h_c^2(f), \qquad h_c(f) \equiv \sqrt{f S_h(f)}$$

Gaussian, stationary, unpolarized, isotropic background

Spacial homogeneity and isotropy

Stationarity

$$\langle h_A^*(f,\hat{\boldsymbol{n}}) h_A(f',\hat{\boldsymbol{n}}')\rangle = \frac{1}{16\pi} S_h(f)\, \delta(f-f')\, \delta_{AA'}\, \delta^2(\hat{\boldsymbol{n}},\hat{\boldsymbol{n}}')$$

Unpolarized

Related to quantities closer to the detector

$$S_h(f) = \frac{3H_0^2}{2\pi^2}\frac{\Omega_{gw}(f)}{f^3}$$

One-sided GW strain power spectral density

(summed over polarizations and integrated over the sky)

Astrophysical SGWB

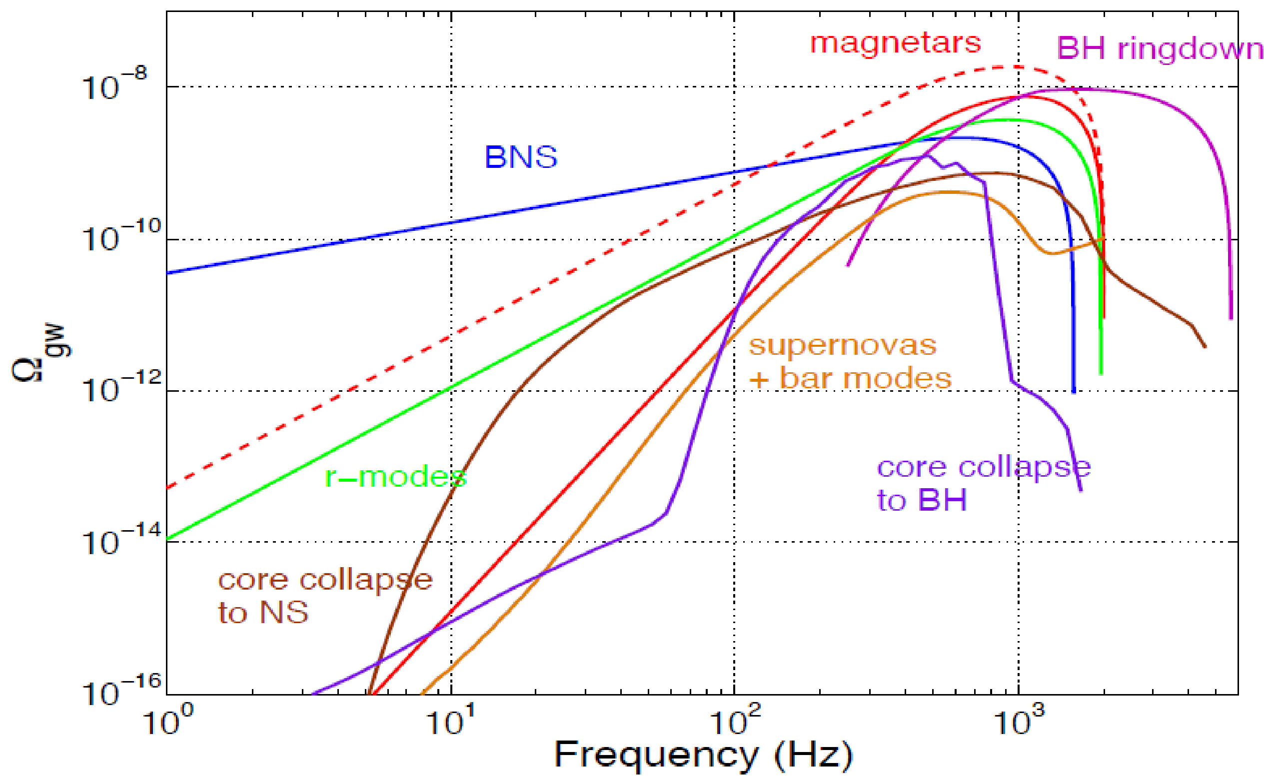

Regimbau T., 2011

Cosmological SGWB
and sensitivities of the experiments

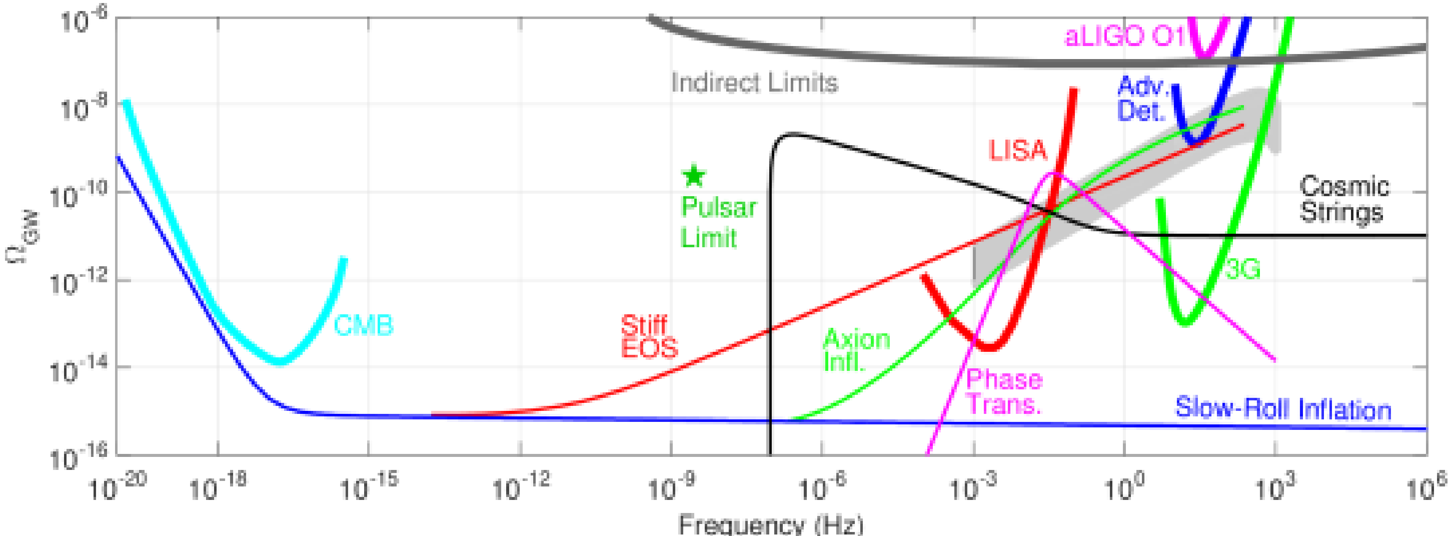

Sathyaprakash B.S. et al., 2019


How to search for a SGWB with ground-based detectors?

Basic idea of the cross-correlation search

Answer to the question:
''How to deal with the fact that SGWB is indistinguishable from unidentified instrumental noise in a single detector?''

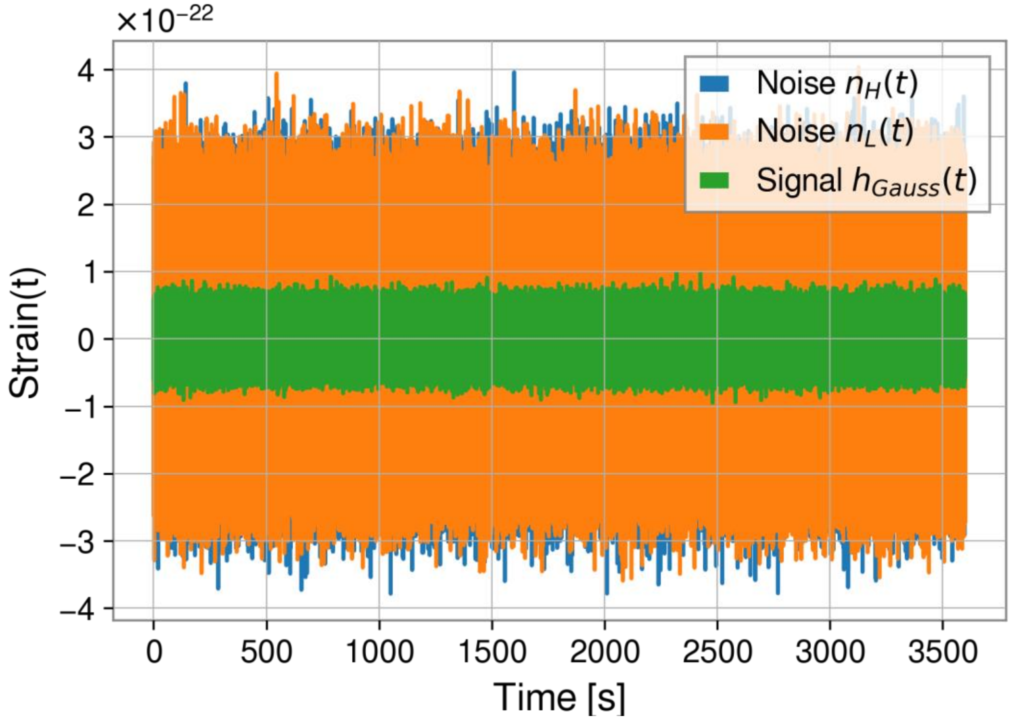

Basic idea of the cross-correlation search

Answer to the question:
''How to deal with the fact that SGWB is indistinguishable from unidentified instrumental noise in a single detector?''

Cross-correlation statistic

Cross-correlated

2 different detectors data $d_1 = h + n_1, \qquad d_2 = h + n_2$

$$\langle \hat{C}_{12} \rangle = \langle d_1 d_2 \rangle = \langle h^2 \rangle + \underbrace{\cancel{\langle h n_2 \rangle}}_{0} + \underbrace{\cancel{\langle n_1 h \rangle}}_{0} + \langle n_1 n_2 \rangle = \langle h^2 \rangle + \langle n_1 n_2 \rangle$$

Non-zero, in general (e.g. Schumann resonances), yet distinguishable from SGWB

Basic idea of the cross-correlation search

Answer to the question:
''How to deal with the fact that SGWB is indistinguishable from unidentified instrumental noise in a single detector?''

Cross-correlation statistic

2 different detectors data $d_1 = h + n_1, \qquad d_2 = h + n_2$

Cross-correlated

$$\langle \hat{C}_{12} \rangle = \langle d_1 d_2 \rangle = \langle h^2 \rangle + \overset{0}{\cancel{\langle h n_2 \rangle}} + \overset{0}{\cancel{\langle n_1 h \rangle}} + \langle n_1 n_2 \rangle = \langle h^2 \rangle + \langle n_1 n_2 \rangle$$

Non-zero, in general (e.g. Schumann resonances), yet distinguishable from SGWB

Moreover, assuming uncorrelated noise $\langle n_1 n_2 \rangle = 0$

It simplifies to

$$\langle \hat{C}_{12} \rangle = \langle h^2 \rangle \equiv S_h$$

Cross-correlation as **estimator of the GW power spectral density**

Caveat: This is a very basic example (co-aligned, co-located, identical detectors); **things get much more complicated in practice** (detector geometry, discrete sampling, discrete frequency, multiple data samples, multiple detectors, different properties of the SGWB)!!!

Detector response and geometry

Detector acts like a **linear filter** on the GW signal, due to its weakness.

This translates in

Convolution in time domain

$$h(t) = (\boldsymbol{F} * \boldsymbol{h})(t, \vec{\boldsymbol{x}}) \equiv \int_{-\infty}^{\infty} d\tau \int d^3y\, F^{ab}(\tau, \vec{\boldsymbol{y}})\, h_{ab}(t-\tau, \vec{\boldsymbol{x}} - \vec{\boldsymbol{y}})$$

Detector impulse response

Detector response and geometry

Detector acts like a **linear filter** on the GW signal, due to its weakness.

This translates in

Convolution in time domain

$$h(t) = (\boldsymbol{F} * \boldsymbol{h})(t, \vec{\boldsymbol{x}}) \equiv \int_{-\infty}^{\infty} d\tau \int d^3y\, F^{ab}(\tau, \vec{\boldsymbol{y}})\, h_{ab}(t-\tau, \vec{\boldsymbol{x}} - \vec{\boldsymbol{y}})$$

Detector impulse response

Plane wave expansion + Fourier transform

Frequency domain

(polarization basis)

$$\tilde{h}(\mathrm{f}) = \int d^2\Omega_{\hat{\boldsymbol{n}}} F^{ab}(f, \hat{\boldsymbol{n}}) h_{ab}(f, \hat{\boldsymbol{n}}) = \int d^2\Omega_{\hat{\boldsymbol{n}}} \sum_A F^A(f, \hat{\boldsymbol{n}}) h_A(f, \hat{\boldsymbol{n}})$$

$$F^A(f, \hat{\boldsymbol{n}}) = F^{ab}(f, \hat{\boldsymbol{n}}) e^A_{ab}(\hat{\boldsymbol{n}})$$

$$F = \sqrt{|F^+(f, \hat{\boldsymbol{n}})|^2 + |F^\times(f, \hat{\boldsymbol{n}})|^2}$$

Antenna beam patterns

$\boldsymbol{F}^+$ $\quad$ $\boldsymbol{F}^\times$ $\quad$ $\boldsymbol{F}$

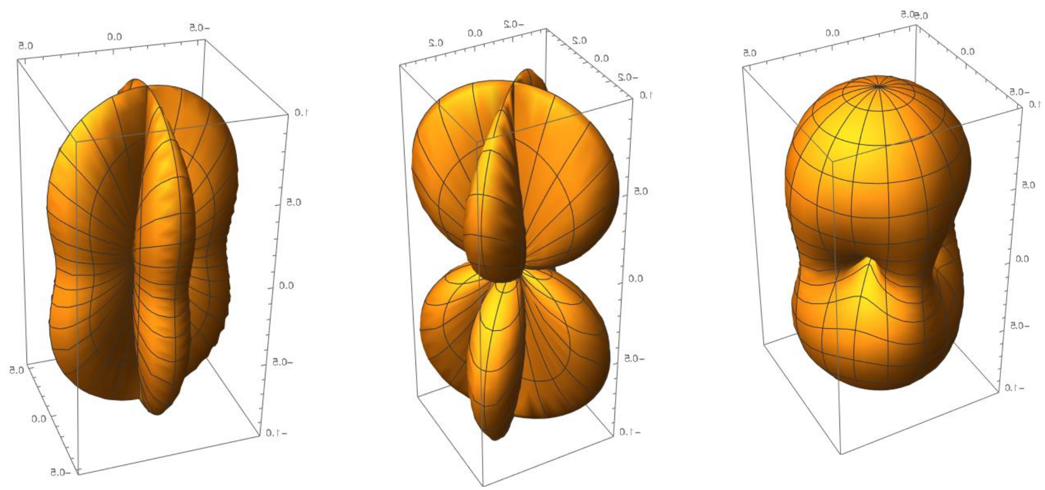

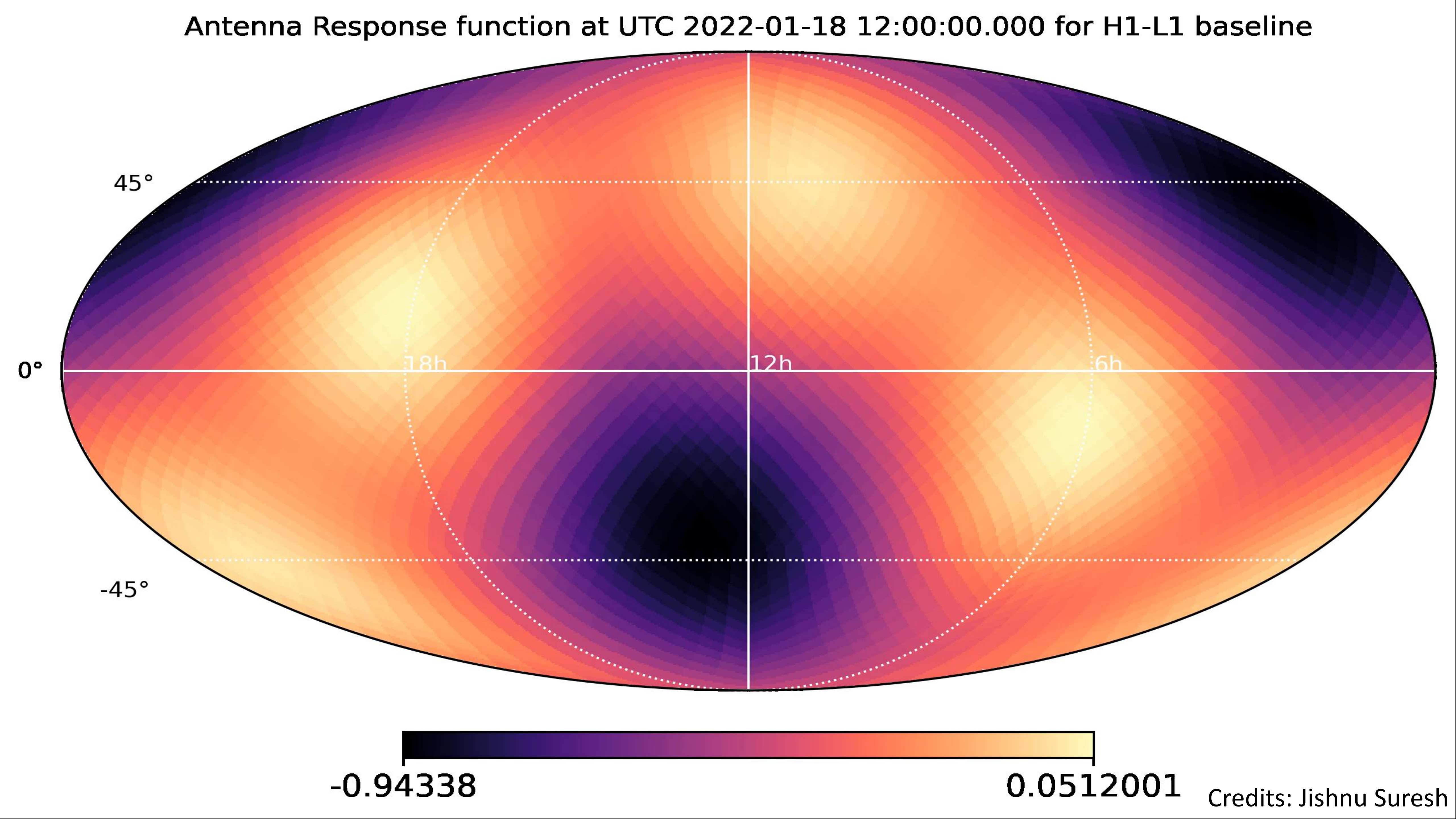
Antenna Response function at UTC 2022-01-18 12:00:00.000 for H1-L1 baseline
45°
0°
-45°
18h
12h
6h
-0.94338
0.0512001
Credits: Jishnu Suresh

Detector response and geometry

Detector acts like a **linear filter** on the GW signal, due to its weakness.

This translates in

$$h(t) = (\boldsymbol{F} * \boldsymbol{h})(t, \vec{\boldsymbol{x}}) \equiv \int_{-\infty}^{\infty} d\tau \int d^3y\, F^{ab}(\tau, \vec{\boldsymbol{y}})\, h_{ab}(t-\tau, \vec{\boldsymbol{x}} - \vec{\boldsymbol{y}})$$

Detector impulse response

Convolution in time domain

Plane wave expansion +
Fourier transform

Frequency domain

(polarization basis)

$$\tilde{h}(\mathrm{f}) = \int d^2\Omega_{\hat{\boldsymbol{n}}} F^{ab}(f, \hat{\boldsymbol{n}})\, h_{ab}(f, \hat{\boldsymbol{n}}) = \int d^2\Omega_{\hat{\boldsymbol{n}}} \sum_A F^A(f, \hat{\boldsymbol{n}})\, h_A(f, \hat{\boldsymbol{n}})$$

$$F^A(f, \hat{\boldsymbol{n}}) = F^{ab}(f, \hat{\boldsymbol{n}})\, e^A_{ab}(\hat{\boldsymbol{n}})$$

$$F = \sqrt{|F^+(f, \hat{\boldsymbol{n}})|^2 + |F^\times(f, \hat{\boldsymbol{n}})|^2}$$

Antenna beam patterns

$$\boxed{\langle \hat{C}_{12}(f) \rangle = \langle \tilde{d}_1(f)\tilde{d}_2^*(f') \rangle \approx \langle \tilde{h}_1(f)\tilde{h}_2^*(f') \rangle = \frac{1}{2}\delta(f-f')\Gamma_{12}(f) S_h(f)}$$

Overlap reduction function

The overlap reduction function: definitions

ORF: **Geometrical factor** that quantifies the **reduction in sensitivity** of the cross-correlation to a SGWB due to the **non-trivial response** of the two detectors and their **separation and orientation** relative to one another.

$$\Gamma_{IJ}(f) \equiv \frac{1}{8\pi}\int d^2\Omega_{\hat{\boldsymbol{n}}} \boxed{\sum_A F_I^A(f,\hat{\boldsymbol{n}})\, F_J^{A*}(f,\hat{\boldsymbol{n}})}$$

Antenna pattern = non-trivial response of single detectprs

Relative separation and orientation of the two detectors

The overlap reduction function: definitions

ORF: **Geometrical factor** that quantifies the **reduction in sensitivity** of the cross-correlation to a SGWB due to the **non-trivial response** of the two detectors and their **separation and orientation** relative to one another.

$$\Gamma_{IJ}(f) \equiv \frac{1}{8\pi} \int d^2\Omega_{\hat{\boldsymbol{n}}} \sum_A F_I^A(f, \hat{\boldsymbol{n}}) F_J^{A*}(f, \hat{\boldsymbol{n}})$$

Antenna pattern = non-trivial response of single detectprs

Relative separation and orientation of the two detectors

Suitable normalization

$$\gamma_{IJ}(f) = \frac{5}{\sin^2 \boxed{\beta}} \Gamma_{IJ}(f)$$

Opening angle between the two arms

Normalized ORF for two identical equal-arm Michelson interferometers

$$\gamma_{IJ}(0) = 1$$

Co-located, co-coaligned, identical detectors

The overlap reduction function: definitions

ORF: **Geometrical factor** that quantifies the **reduction in sensitivity** of the cross-correlation to a SGWB due to the **non-trivial response** of the two detectors and their **separation and orientation** relative to one another.

$$\Gamma_{IJ}(f) \equiv \frac{1}{8\pi}\int d^2\Omega_{\hat{\boldsymbol{n}}} \sum_A F_I^A(f,\hat{\boldsymbol{n}})\,F_J^{A*}(f,\hat{\boldsymbol{n}})$$

Antenna pattern = non-trivial response of single detectprs

Relative separation and orientation of the two detectors

Suitable normalization

$$\gamma_{IJ}(f) = \frac{5}{\sin^2\boxed{\beta}}\Gamma_{IJ}(f)$$

Opening angle between the two arms

$$\gamma_{IJ}(0) = 1$$

Co-located, co-coaligned, identical detectors

Normalized ORF for two identical equal-arm Michelson interferometers

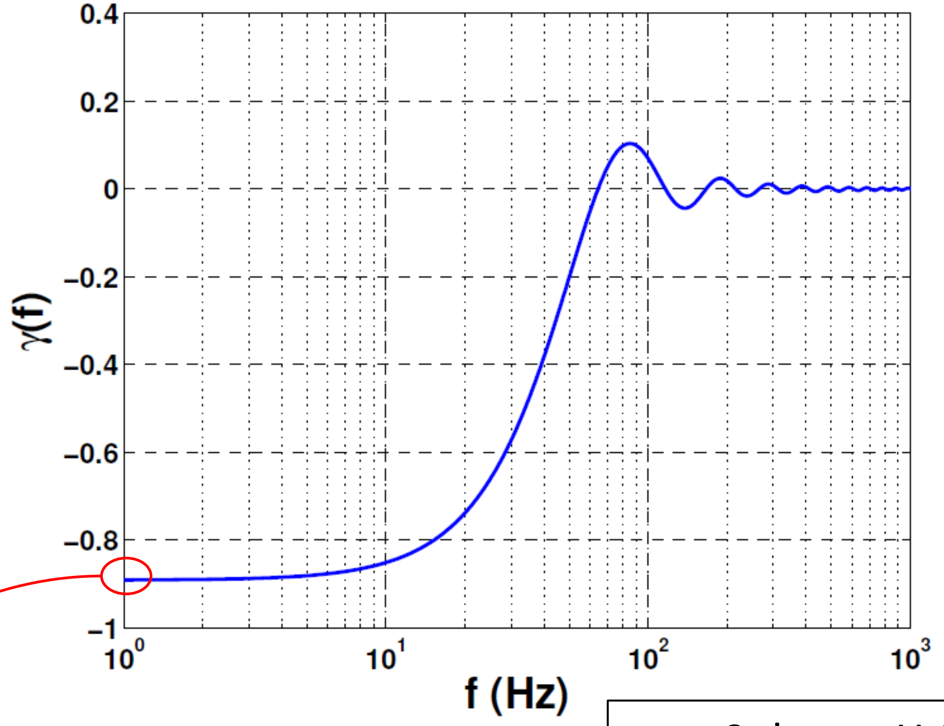

$\gamma_{HL}(0) = -0.89$

Why?

- < 0 due to H-L arms rotated 90° with respect to one another
- Less than unity: 27.2° between the detectors planes as seen from the Earth center
- First zero at 60 Hz, close to c/(2s) = 50 Hz, s = 3000 Km

The isotropic search: optimal filtering (1)

Searching for a power-law model

$$S_h(f) = \frac{3\,H_0^2}{2\pi^2}\frac{\Omega_\alpha}{f_{ref}^3}\left(\frac{f}{f_{ref}}\right)^{\alpha-3} \equiv \Omega_\alpha S_\alpha(f), \qquad S_\alpha(f) \equiv \frac{3H_0^2}{2\pi^2}\frac{1}{f_{ref}^3}\left(\frac{f}{f_{ref}}\right)^{\alpha-3}$$

The isotropic search: optimal filtering (1)

Searching for a power-law model

$$S_h(f) = \frac{3\,H_0^2}{2\pi^2}\frac{\Omega_\alpha}{f_{ref}^3}\left(\frac{f}{f_{ref}}\right)^{\alpha-3} \equiv \Omega_\alpha S_\alpha(f), \qquad S_\alpha(f) \equiv \frac{3H_0^2}{2\pi^2}\frac{1}{f_{ref}^3}\left(\frac{f}{f_{ref}}\right)^{\alpha-3}$$

Get an estimator for Ω_α through

Optimal filtering

$$\hat{C}_{12}(t) = \int_{-\infty}^{\infty} df\,\tilde{Q}(t;f)\tilde{d}_1(t;f)\tilde{d}_2^*(t;f)$$

Filter to be determined given a model

Starting from

Cross-correlation estimator

Total observation time (segment duration)

$$\langle\hat{C}_{12}(f)\rangle = \langle\tilde{d}_1(f)\tilde{d}_2^*(f)\rangle \approx \langle\tilde{h}_1(f)\tilde{h}_2^*(f)\rangle \underset{(*)}{=} \frac{T}{2}\Gamma_{12}(f)S_h(f)$$

$(*)\,\delta(f-f') \to T sinc[\pi(f-f')T]$

The isotropic search: optimal filtering (1)

Searching for a power-law model

$$S_h(f) = \frac{3\,H_0^2}{2\pi^2}\frac{\Omega_\alpha}{f_{ref}^3}\left(\frac{f}{f_{ref}}\right)^{\alpha-3} \equiv \Omega_\alpha S_\alpha(f), \qquad S_\alpha(f) \equiv \frac{3H_0^2}{2\pi^2}\frac{1}{f_{ref}^3}\left(\frac{f}{f_{ref}}\right)^{\alpha-3}$$

Get an estimator for Ω_α through

Optimal filtering

$$\hat{C}_{12}(t) = \int_{-\infty}^{\infty} df\, \tilde{Q}(t;f)\tilde{d}_1(t;f)\tilde{d}_2^*(t;f)$$

Filter to be determined given a model

Starting from

Cross-correlation estimator

Total observation time (segment duration)

$$\langle \hat{C}_{12}(f)\rangle = \langle \tilde{d}_1(f)\tilde{d}_2^*(f)\rangle \approx \langle \tilde{h}_1(f)\tilde{h}_2^*(f)\rangle \underset{(*)}{=} \frac{T}{2}\Gamma_{12}(f)S_h(f)$$

with

(Noise) correlation matrix

$$N_{ff'} \equiv \langle \hat{C}_{12}(f)\hat{C}_{12}^*(f')\rangle - \langle \hat{C}_{12}(f)\rangle\langle \hat{C}_{12}^*(f')\rangle \approx \langle n_1(f)n_1^*(f')\rangle\langle n_2(f)n_2^*(f')\rangle$$

Weak-signal limit

$$= \frac{T}{4}P_{n_1}(f)P_{n_2}(f)\delta(f-f') \qquad \langle n_I(f)n_I^*(f')\rangle = \frac{1}{2}P_{n_I}(f)\delta(f-f')$$

1-sided noise power spectral density

$(*)\delta(f-f') \to T sinc[\pi(f-f')T]$

The isotropic search: optimal filtering (2)

Optimal estimator

Energy ratio estimator

$$\boxed{\hat{\Omega}_\alpha = \mathcal{N} \int_{-\infty}^{\infty} \frac{\Gamma_{12}(f) S_\alpha(f)}{P_{n_1}(f) P_{n_2}(f)} \tilde{d}_1(f) \tilde{d}_2^*(f) df}$$

Estimator variance

$$\sigma_{\hat{\Omega}_\alpha}^2 = \left[T \int_{-\infty}^{\infty} \frac{\Gamma_{12}^2(f) S_\alpha^2(f)}{P_{n_1}(f) P_{n_2}(f)} df \right]^{-1}$$

$$\mathcal{N} \equiv \left[\frac{T}{2} \int_{-\infty}^{\infty} \frac{\Gamma_{12}^2(f) S_\alpha^2(f)}{P_{n_1}(f) P_{n_2}(f)} df \right]^{-1}$$

Model dependent, optimal filter,

$$\tilde{Q}(f) \equiv \mathcal{N} \frac{\Gamma_{12}(f) S_\alpha(f)}{P_{n_1}(f) P_{n_2}(f)}$$

$$\boxed{SNR = \sqrt{T \int_{-\infty}^{\infty} \frac{\Gamma_{12}^2(f) S_h^2(f)}{P_{n_1}(f) P_{n_2}(f)} df}}$$

Signal-to-noise ratio proportional to $\sqrt{T}$

The isotropic search: optimal filtering (2)

Optimal estimator

Energy ratio estimator

$$\boxed{\hat{\Omega}_\alpha = \mathcal{N}\int_{-\infty}^{\infty}\frac{\Gamma_{12}(f)S_\alpha(f)}{P_{n_1}(f)P_{n_2}(f)}\tilde{d}_1(f)\tilde{d}_2^*(f)df}$$

Estimator variance

$$\sigma^2_{\hat{\Omega}_\alpha} = \left[T\int_{-\infty}^{\infty}\frac{\Gamma_{12}^2(f)S_\alpha^2(f)}{P_{n_1}(f)P_{n_2}(f)}df\right]^{-1}$$

$$\mathcal{N} \equiv \left[\frac{T}{2}\int_{-\infty}^{\infty}\frac{\Gamma_{12}^2(f)S_\alpha^2(f)}{P_{n_1}(f)P_{n_2}(f)}df\right]^{-1}$$

Model dependent, optimal filter,

$$\tilde{Q}(f) \equiv \mathcal{N}\frac{\Gamma_{12}(f)S_\alpha(f)}{P_{n_1}(f)P_{n_2}(f)}$$

$$\boxed{SNR = \sqrt{T\int_{-\infty}^{\infty}\frac{\Gamma_{12}^2(f)S_h^2(f)}{P_{n_1}(f)P_{n_2}(f)}df}}$$

Signal-to-noise ratio proportional to $\sqrt{T}$

But in real world

Single frequency bins

$$\hat{\Omega}_\alpha(\mathrm{f}) \equiv \frac{2}{T}\frac{Re\left[\tilde{d}_1(f)\tilde{d}_2^*(f)\right]}{\Gamma_{12}(f)S_\alpha(f)} \qquad \sigma^2_{\hat{\Omega}_\alpha}(f) \approx \frac{1}{2T\Delta f}\frac{P_{n_1}(f)P_{n_2}(f)}{\Gamma_{12}^2(f)S_\alpha^2(f)}$$

"Narrow-band" estimator

$$\hat{\Omega}_\alpha = \frac{\sum_k \hat{\Omega}_\alpha(\mathrm{f}_k)\sigma^{-2}_{\hat{\Omega}_\alpha}(f_k)}{\sum_{k'}\sigma^{-2}_{\hat{\Omega}_\alpha}(f_{k'})} \qquad \sigma^2_{\hat{\Omega}_\alpha} = \frac{1}{\sum_{k'}\sigma^{-2}_{\hat{\Omega}_\alpha}(f_{k'})}$$

"Broad-band" estimator

Monthly Notices
of the
ROYAL ASTRONOMICAL SOCIETY

MNRAS **513**, 1105–1114 (2022) https://doi.org/10.1093/mnras/stac984
Advance Access publication 2022 April 9

Stochastic gravitational-wave background searches and constraints on neutron-star ellipticity

Federico De Lillo,★ Jishnu Suresh and Andrew L. Miller

Centre for Cosmology, Particle Physics and Phenomenology (CP3), Université catholique de Louvain, Louvain-la-Neuve B-1348, Belgium

Accepted 2022 April 5. Received 2022 April 4; in original form 2022 March 14

ABSTRACT

Rotating neutron stars (NSs) are promising sources of gravitational waves (GWs) in the frequency band of ground-based detectors. They are expected to emit quasi-monochromatic, long-duration GW signals, called continuous waves (CWs), due to their deviations from spherical symmetry. The degree of such deformations, and hence the information about the internal structure of an NS, is encoded in a dimension-less parameter ε called ellipticity. Searches for CW signals from isolated Galactic NSs have shown to be sensitive to ellipticities as low as $\varepsilon \sim \mathcal{O}(10^{-9})$. These searches are optimal for detecting and characterizing GWs from individual NSs, but they are not designed to measure the properties of NSs as population, such as the average ellipticity $\varepsilon_{\rm av}$. These ensemble properties can be determined by the measurement of the stochastic gravitational-wave background (SGWB) arising from the superposition of GW signals from individually undetectable NSs. In this work, we perform a cross-correlation search for such a SGWB using the data from the first three observation runs of Advanced LIGO and Virgo. Finding no evidence for an SGWB signal, we set upper limits on the dimension-less energy density parameter $\Omega_{\rm gw}(f)$. Using these results, we also constrain the average ellipticity of Galactic NSs and five NS 'hotspots', as a function of the number of NSs emitting GWs within the frequency band of the search $N_{\rm band}$. We find $\varepsilon_{\rm av} \lesssim 1.8 \times 10^{-8}$, with $N_{\rm band} = 1.6 \times 10^{7}$, for Galactic NSs, and $\varepsilon_{\rm av} \lesssim [3.5 - 11.8] \times 10^{-7}$, with $N_{\rm band} = 1.6 \times 10^{10}$, for NS hotspots.

Key words: gravitational waves.

Monthly Notices
of the
ROYAL ASTRONOMICAL SOCIETY

MNRAS **513,** 1105–1114 (2022) https://doi.org/10.1093/mnras/stac984
Advance Access publication 2022 April 9

Stochastic gravitational-wave background searches and constraints on neutron-star ellipticity

Federico De Lillo,★ Jishnu Suresh and Andrew L. Miller

Centre for Cosmology, Particle Physics and Phenomenology (CP3), Université catholique de Louvain, Louvain-la-Neuve B-1348, Belgium

Accepted 2022 April 5. Received 2022 April 4; in original form 2022 March 14

ABSTRACT

Rotating neutron stars (NSs) are promising sources of gravitational waves (GWs) in the frequency band of ground-based detectors. They are expected to emit quasi-monochromatic, long-duration GW signals, called continuous waves (CWs), due to their deviations from spherical symmetry. The degree of such deformations, and hence the information about the internal structure of an NS, is encoded in a dimension-less parameter ε called ellipticity. Searches for CW signals from isolated Galactic NSs have shown to be sensitive to ellipticities as low as $\varepsilon \sim \mathcal{O}(10^{-9})$. These searches are optimal for detecting and characterizing GWs from individual NSs, but they are not designed to measure the properties of NSs as population, such as the average ellipticity $\varepsilon_{\rm av}$. These ensemble properties can be determined by the measurement of the stochastic gravitational-wave background (SGWB) arising from the superposition of GW signals from individually undetectable NSs. In this work, we perform a cross-correlation search for such a SGWB using the data from the first three observation runs of Advanced LIGO and Virgo. Finding no evidence for an SGWB signal, we set upper limits on the dimension-less energy density parameter $\Omega_{\rm gw}(f)$. Using these results, we also constrain the average ellipticity of Galactic NSs and five NS 'hotspots', as a function of the number of NSs emitting GWs within the frequency band of the search $N_{\rm band}$. We find $\varepsilon_{\rm av} \lesssim 1.8 \times 10^{-8}$, with $N_{\rm band} = 1.6 \times 10^{7}$, for Galactic NSs, and $\varepsilon_{\rm av} \lesssim [3.5 - 11.8] \times 10^{-7}$, with $N_{\rm band} = 1.6 \times 10^{10}$, for NS hotspots.

Key words: gravitational waves.

Introduction and motivations

Isolated, rotating non-axisymmetric, neutron stars (NSs)

Expected to be

Gravitational wave (GW) sources

Single isolated NS

Expected to generate

Continuous waves (CWs)
(quasi-) monochromatic, persistent GW signals

CWs carry information about **individual properties**

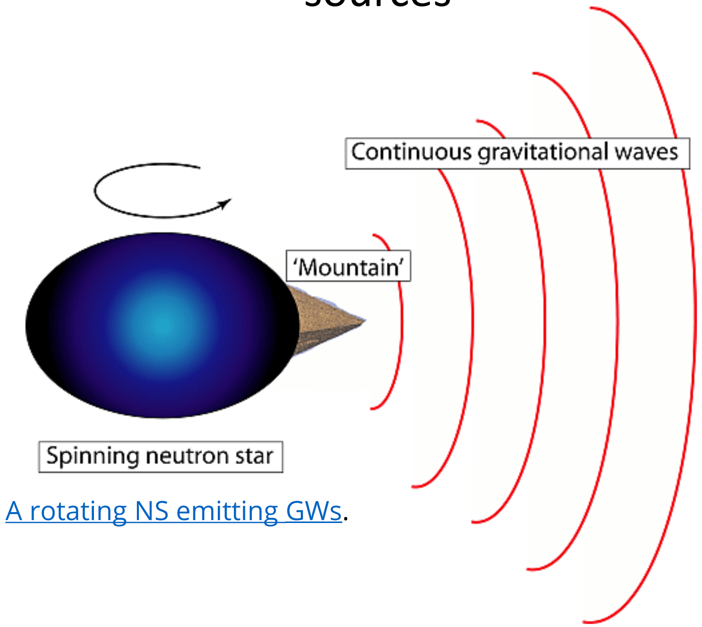

A rotating NS emitting GWs.

Introduction and motivations

Isolated, rotating non-axisymmetric, neutron stars (NSs)

Expected to be

Gravitational wave (GW) sources

Single isolated NS

Expected to generate

Continuous waves (CWs)
(quasi-) monochromatic, persistent GW signals

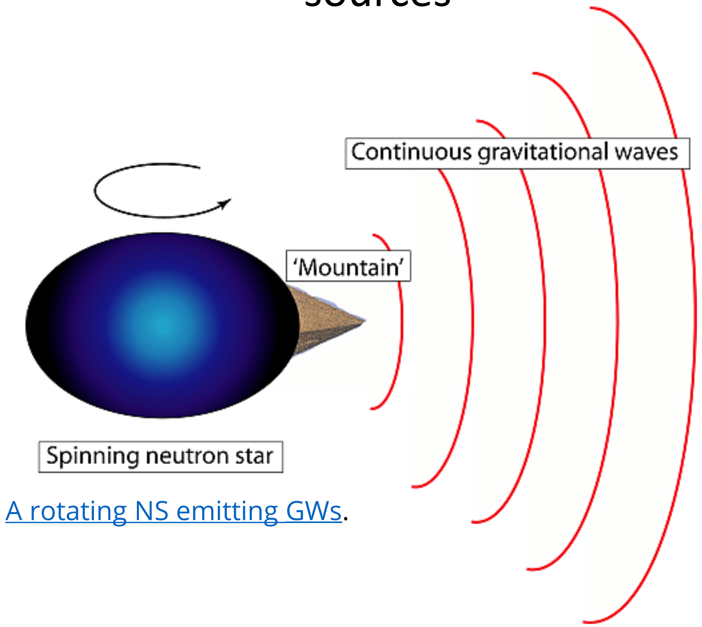

A rotating NS emitting GWs.

Galactic and Extra-Galactic **NS populations GWs**

Expected to generate

Stochastic gravitational-wave background from the overlap of weak signals from individually undetectable pulsars

CWs carry information about **individual properties**

SGWB carries information about **population properties**

Complementarity between the two searches!

Modelling the source – The signal

- GW strain amplitude from an isolated, rotating, non-axisymmetric neutron star, at a distance d from Earth, with a moment of inertia along z-axis I_{zz}, and an ellipticity $\varepsilon = \frac{I_{xx}-I_{yy}}{I_{zz}}$:

$$h_0(f) = \frac{4\pi^2 G\, \varepsilon\, I_{zz}}{c^4 d} f^2$$

Modelling the source – The signal

- GW strain amplitude from an isolated, rotating, non-axisymmetric neutron star, at a distance d from Earth, with a moment of inertia along z-axis I_{zz}, and an ellipticity $\varepsilon = \frac{I_{xx}-I_{yy}}{I_{zz}}$:

$$h_0(f) = \frac{4\pi^2 G\, \varepsilon\, I_{zz}}{c^4 d} f^2$$

- GW power spectral density from incoherent sum of the individual contributions:

$$\boxed{H(f) = 8\pi^4 \frac{32\pi^4 G^2 \langle \varepsilon^2 \rangle_{NS} \langle I_{zz}^2 \rangle_{NS}}{5c^8} \left\langle \frac{1}{d^2} \right\rangle_{NS} f^4 N(f),}$$

Modelling the source – The signal

- GW strain amplitude from an isolated, rotating, non-axisymmetric neutron star, at a distance d from Earth, with a moment of inertia along z-axis I_{zz}, and an ellipticity $\varepsilon = \frac{I_{xx}-I_{yy}}{I_{zz}}$:

$$h_0(f) = \frac{4\pi^2 G\, \varepsilon\, I_{zz}}{c^4 d} f^2$$

- GW power spectral density from incoherent sum of the individual contributions:

$$\boxed{H(f) = 8\pi^4 \frac{32\pi^4 G^2 \langle \varepsilon^2 \rangle_{NS} \langle I_{zz}^2 \rangle_{NS}}{5c^8} \left\langle \frac{1}{d^2} \right\rangle_{NS} f^4 N(f),}$$

with $\langle \ldots \rangle_{NS}$ the ensemble average over the NS population, and $N(f)$ the number of NSs emitting GWs between $[f, f+df]$, defined as

$$N(f) = N_0 \Phi(f), \qquad N_0 \int_0^\infty \Phi(f)\, df = N_0.$$

Modelling the source – The population

- $\langle I_{zz}^2 \rangle_{NS}{}^{1/2} = 10^{38} kg\ m^2$
- $\left\langle \frac{1}{d^2} \right\rangle_{NS}^{-1/2} = 6\ kpc$ for Galactic NSs

Modelling the source – The population

- ${\langle I_{zz}^2 \rangle_{NS}}^{1/2} = 10^{38} kg\ m^2$
- $\left\langle \frac{1}{d^2} \right\rangle_{NS}^{-1/2} = 6\ kpc$ for Galactic NSs
- $N_0 \sim 10^8$, assuming a Galactic supernovae rate to be $10^{-2} yr^{-1}$[Diel et al. 2006], and the age of the Milky Way to be $10^{10} yr$.

Modelling the source – The population

- $\langle I_{zz}^2 \rangle_{NS}^{1/2} = 10^{38} kg\, m^2$
- $\left\langle \frac{1}{d^2} \right\rangle_{NS}^{-1/2} = 6\ kpc$ for Galactic NSs
- $N_0 \sim 10^8$, assuming a Galactic supernovae rate to be $10^{-2} yr^{-1}$[Diel et al. 2006], and the age of the Milky Way to be $10^{10} yr$.
- $\Phi(f)$ from the ($\log_{10}$-) frequency distribution of the $\simeq 3000$ pulsars of the ATNF catalogue, by means of a Gaussian Kernel Density Estimator (KDE)

Modelling the source – The population

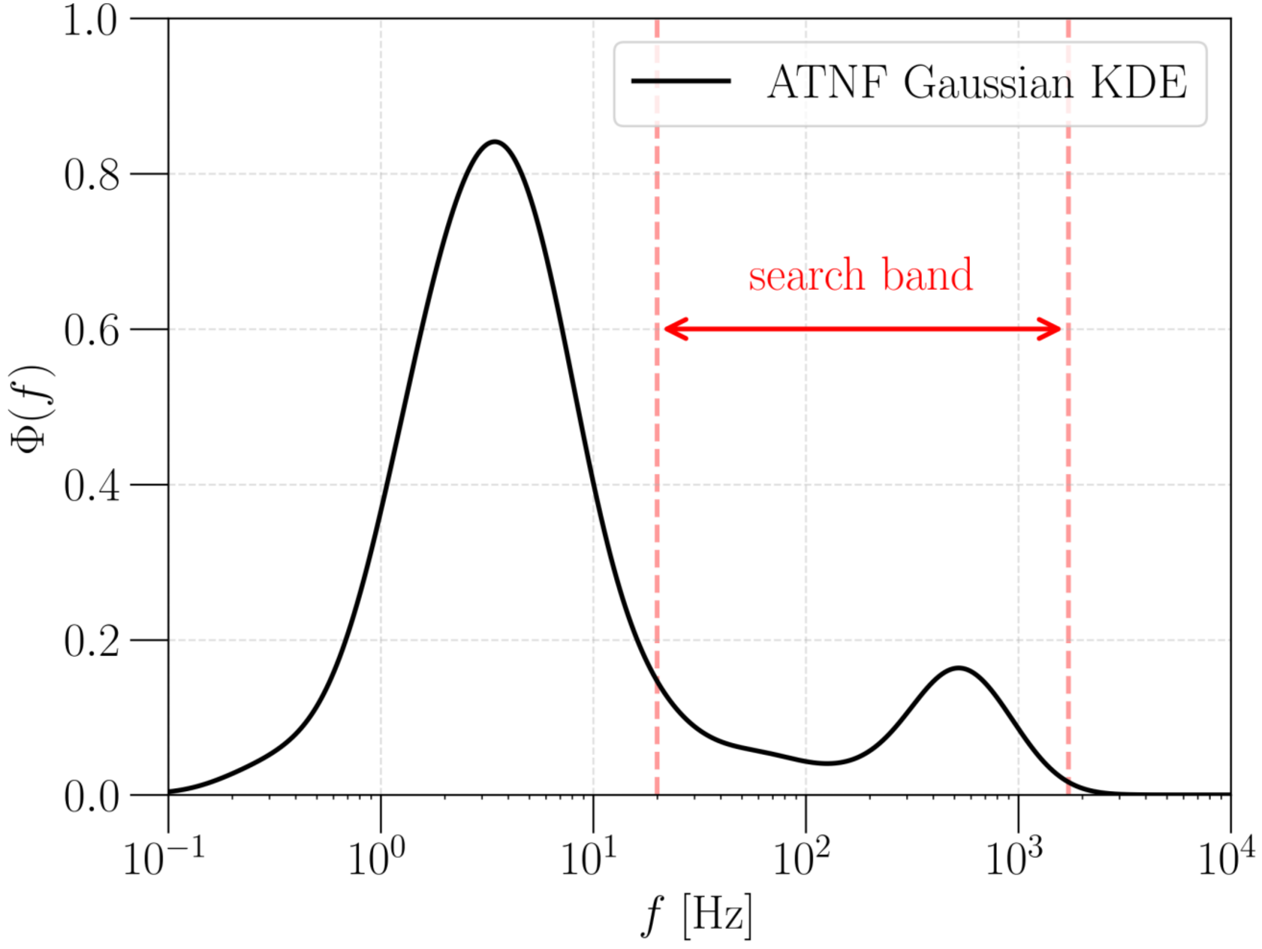

$\Phi(f)$ Gaussian KDE from ATNF catalogue . Secondary peak at 526 Hz, falling within the frequency band to which the ground-based gravitational-wave detectors are sensitive.

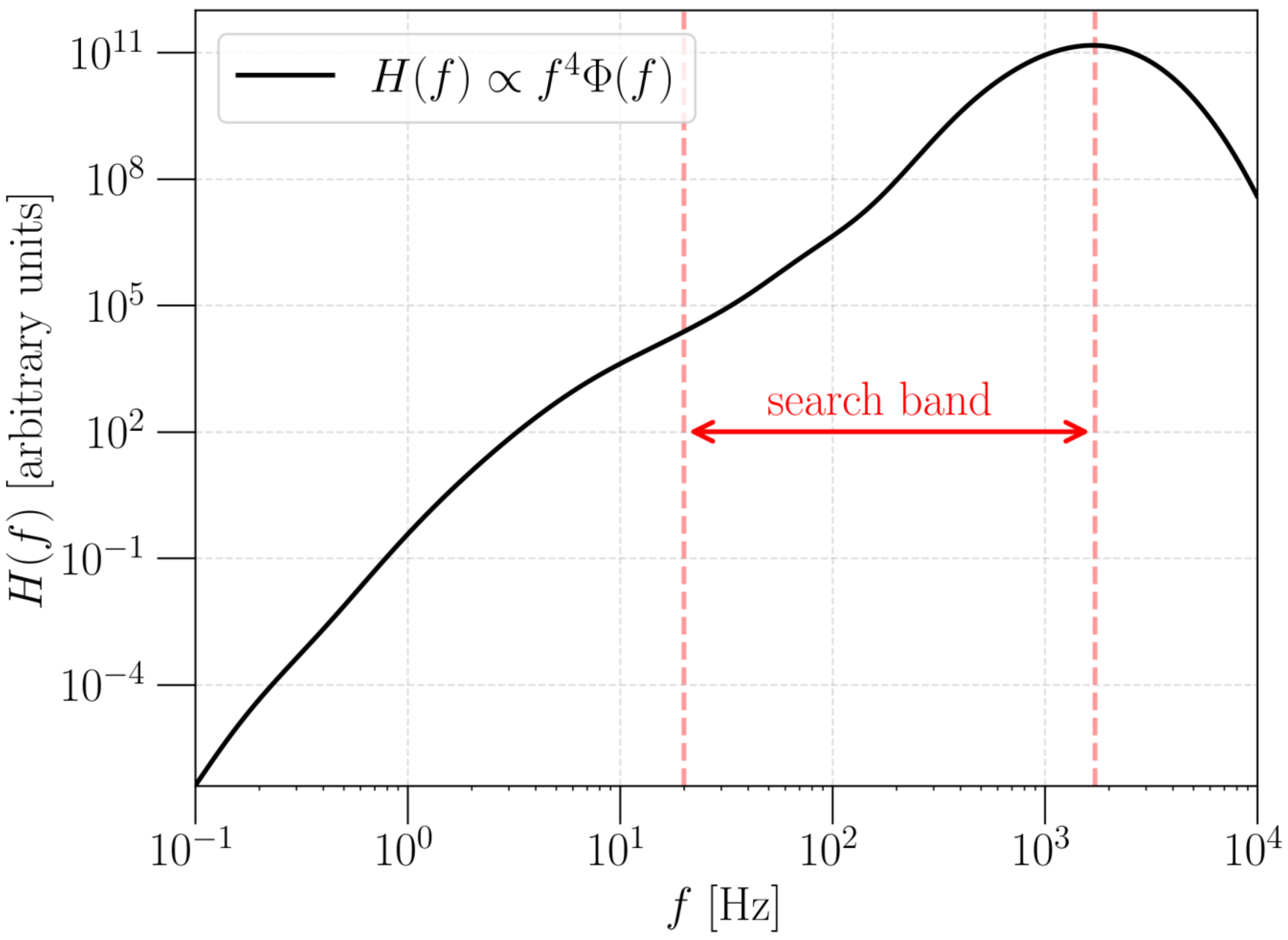

Unnormalised H(f): due to the dominant contribution of the f^4 term, the peak is shifted to a higher frequency , at 1688 Hz.

Modelling the source – The population

- $\langle I_{zz}^2 \rangle_{NS}^{1/2} = 10^{38} kg\ m^2$
- $\left\langle \frac{1}{d^2} \right\rangle_{NS}^{-1/2} = 6\ kpc$ for Galactic NSs

- $N_0 \sim 10^8$, assuming a Galactic supernovae rate to be $10^{-2} yr^{-1}$[Diel et al. 2006], and the age of the Milky Way to be $10^{10} yr$.
- $\Phi(f)$ from the ($\log_{10}$-) frequency distribution of the $\simeq$3000 pulsars of the ATNF catalogue, by means of a Gaussian Kernel Density Estimator (KDE)

- N_{band}, number of NSs emitting GWs in the frequency band of the search $[f_{min}, f_{max}] = [20, 1726]$ Hz:

$$\boxed{N_{band} = N_0 \int_{f_{min}}^{f_{max}} \Phi(f) df = N_0 \int_{20\ Hz}^{1726\ Hz} \Phi(f) df = 0.16\ N_0 \sim 1.6 \times 10^7}$$

Modelling the source – The population

- $\langle I_{zz}^2 \rangle_{NS}{}^{1/2} = 10^{38} kg\ m^2$
- $\left\langle \frac{1}{d^2} \right\rangle_{NS}^{-1/2} = 6\ kpc$ for Galactic NSs

- $N_0 \sim 10^8$, assuming a Galactic supernovae rate to be $10^{-2} yr^{-1}$[Diel et al. 2006], and the age of the Milky Way to be $10^{10} yr$.
- $\Phi(f)$ from the ($\log_{10}$-) frequency distribution of the $\simeq 3000$ pulsars of the ATNF catalogue, by means of a Gaussian Kernel Density Estimator (KDE)

- N_{band}, number of NSs emitting GWs in the frequency band of the search $[f_{min}, f_{max}] = [20, 1726]$ Hz:

$$N_{band} = N_0 \int_{f_{min}}^{f_{max}} \Phi(f) df = N_0 \int_{20\ Hz}^{1726\ Hz} \Phi(f) df = 0.16\ N_0 \sim 1.6 \times 10^7$$

Remark1: In this work, we have not considered the angular distribution of the Galactic NSs, and we have treated the corresponding stochastic gravitational-wave background as isotropic.

Remark2: Including the all the anisotropies would require to employ the matched-filtered ''λ-statistic'', proposed in Talukder et al., 2011, and produce a template bank, out of the scope of the present work. See the recent paper by Agarwal at al., 2022, where this method is implemented.

Isotropic analysis: recap about notation

Gaussian, stationary, unpolarized, homogeneus **isotropic background**, not simple power-law.

$$\langle \tilde{h}_A(f,\hat{n})\,\tilde{h}^*_{A'}(f',\hat{n}')\rangle = \frac{1}{16\pi} H(f)\delta(f-f')\delta_{AA'}\delta^2(\hat{n},\hat{n}')$$

$$H(f) = \frac{3H_0^2}{2\pi^2}\frac{\Omega_{gw}(f)}{f^3} \qquad \Omega_{gw}(f) = \Omega_{\alpha,ref}\left(\frac{f}{f_{ref}}\right)^7 \frac{\Phi(f)}{\Phi(f_{ref})}$$

Isotropic analysis: recap about notation

Gaussian, stationary, unpolarized, homogeneus **isotropic background**, not simple power-law.

$$\langle \tilde{h}_A(f,\hat{n})\,\tilde{h}^*_{A'}(f',\hat{n}') \rangle = \frac{1}{16\pi} H(f)\delta(f-f')\delta_{AA'}\delta^2(\hat{n},\hat{n}')$$

$$H(f) = \frac{3H_0^2}{2\pi^2}\frac{\Omega_{gw}(f)}{f^3} \qquad \Omega_{gw}(f) = \Omega_{\alpha,ref}\left(\frac{f}{f_{ref}}\right)^7 \frac{\Phi(f)}{\Phi(f_{ref})}$$

Cross-correlation spectra as **narrow-band estimator** (IJ = {H, L, V}) of $\Omega_{gw}(f)$.

$$\hat{C}^{IJ}(f) = \frac{2}{T}\frac{Re[\tilde{s}_1(f)\tilde{s}_2^*(f)]}{\gamma_{IJ}S_0(f)} \qquad \sigma_{IJ}^2(f) \approx \frac{1}{2T\Delta f}\frac{P_I(f)P_J(f)}{\gamma_{IJ}^2(f)S_0^2(f)}$$

$$S_0(f) = \frac{3H_0^2}{2\pi^2 f^3} \qquad \langle \hat{C}^{IJ}(f) \rangle = \Omega_{gw}(f)$$

Isotropic analysis: recap about notation

Gaussian, stationary, unpolarized, homogeneus **isotropic background**, not simple power-law.

$$\langle \tilde{h}_A(f,\hat{n})\,\tilde{h}^*_{A'}(f',\hat{n}')\rangle = \frac{1}{16\pi} H(f)\delta(f-f')\delta_{AA'}\delta^2(\hat{n},\hat{n}')$$

$$H(f) = \frac{3H_0^2}{2\pi^2}\frac{\Omega_{gw}(f)}{f^3} \qquad \Omega_{gw}(f) = \Omega_{\alpha,ref}\left(\frac{f}{f_{ref}}\right)^7 \frac{\Phi(f)}{\Phi(f_{ref})}$$

Cross-correlation spectra as **narrow-band estimator** (IJ = {H, L, V}) of $\Omega_{gw}(f)$.

$$\hat{C}^{IJ}(f) = \frac{2}{T}\frac{Re[\tilde{s}_1(f)\tilde{s}_2^*(f)]}{\gamma_{IJ}S_0(f)} \qquad \sigma^2_{IJ}(f) \approx \frac{1}{2T\Delta f}\frac{P_I(f)P_J(f)}{\gamma^2_{IJ}(f)S_0^2(f)}$$

$$S_0(f) = \frac{3H_0^2}{2\pi^2 f^3} \qquad \langle \hat{C}^{IJ}(f)\rangle = \Omega_{gw}(f)$$

Broad-band estimator, from weighted sum over frequencies and independent baselines

$$\hat{C}^{IJ} = \frac{\sum_k w(f_k)\ \hat{C}^{IJ}(f_k)/\sigma^2_{IJ}(f_k)}{\sum_k w^2(f_k)\,/\sigma^2_{IJ}(f_k)} \qquad \sigma^2_{IJ} = \frac{1}{\sum_k w^2(f_k)\,/\sigma^2_{IJ}(f_k)}$$

$$\hat{C} = \frac{\sum_{IJ}\hat{C}^{IJ}/\sigma^2_{IJ}}{\sum_{IJ}1/\sigma^2_{IJ}} \qquad \sigma^2 = \frac{1}{\sum_{IJ}1/\sigma^2_{IJ}}$$

Flexibility: $w(f) = \frac{\Omega_{gw}(f)}{\Omega_{gw}(f_{ref})}$

Getting the estimator for the ensemble ellipticity (1)

Final goal: use results of the previous analysis to build an estimator for the average ellipticity of the NS population

Getting the estimator for the ensemble ellipticity (1)

Final goal: use results of the previous analysis to build an estimator for the average ellipticity of the NS population

Starting point $$H(f) = \frac{3H_0^2}{2\pi^2}\frac{\Omega_{gw}(f)}{f^3}$$ $$H(f) = 8\pi^4 \frac{32\pi^4 G^2 \langle \varepsilon^2 \rangle_{NS} \langle I_{zz}^2 \rangle_{NS}}{5c^8} \left\langle \frac{1}{d^2} \right\rangle_{NS} f^4 \mathrm{N}_{band} \Phi(f)$$

Getting the estimator for the ensemble ellipticity (1)

Final goal: use results of the previous analysis to build an estimator for the average ellipticity of the NS population

Starting point

$$H(f) = \frac{3H_0^2}{2\pi^2}\frac{\Omega_{gw}(f)}{f^3} \qquad H(f) = 8\pi^4\frac{32\pi^4 G^2\langle\varepsilon^2\rangle_{NS}\langle I_{zz}^2\rangle_{NS}}{5c^8}\left\langle\frac{1}{d^2}\right\rangle_{NS} f^4 \mathrm{N}_{band}\Phi(f)$$

Combine

$$\Omega(\mathrm{f}) = \frac{64\,\pi^6 G^2}{3H_0^2}\frac{\langle\varepsilon^2\rangle_{NS}\langle I_{zz}^2\rangle_{NS}}{5c^8}\left\langle\frac{1}{d^2}\right\rangle_{NS} f^7 N_{band}\Phi(f)$$

and recast

$$\Omega(f) = \left(\frac{f}{f_{ref}}\right)^7\left(\frac{\Phi(f)}{\Phi(f_{ref})}\right)\xi(N_{band})\langle\varepsilon^2\rangle_{NS} = w(f)\xi\langle\varepsilon^2\rangle_{NS}$$

Getting the estimator for the ensemble ellipticity (1)

Final goal: use results of the previous analysis to build an estimator for the average ellipticity of the NS population

Starting point $H(f) = \frac{3H_0^2}{2\pi^2}\frac{\Omega_{gw}(f)}{f^3}$ $\qquad$ $H(f) = 8\pi^4 \frac{32\pi^4 G^2 \langle \varepsilon^2 \rangle_{NS} \langle I_{zz}^2 \rangle_{NS}}{5c^8} \left\langle \frac{1}{d^2} \right\rangle_{NS} f^4 \mathrm{N}_{band} \Phi(f)$

Combine

$$\Omega(\mathrm{f}) = \frac{64\,\pi^6 G^2}{3H_0^2} \frac{\langle \varepsilon^2 \rangle_{NS} \langle I_{zz}^2 \rangle_{NS}}{5c^8} \left\langle \frac{1}{d^2} \right\rangle_{NS} f^7 N_{band} \Phi(f)$$

and recast

$$\Omega(f) = \left(\frac{f}{f_{ref}}\right)^7 \left(\frac{\Phi(f)}{\Phi(f_{ref})}\right) \xi(N_{band}) \langle \varepsilon^2 \rangle_{NS} = w(f)\xi\langle \varepsilon^2 \rangle_{NS}$$

$\Omega_{GW}(f) = \Omega_{GW}(f_{ref})w(f)$

Estimator for $\boldsymbol{(\varepsilon^2)_{av} \equiv \langle \varepsilon^2 \rangle_{NS}}$

$$\boxed{\widehat{(\varepsilon^2)}_{av}(\mathrm{f_k}) \equiv \frac{\widehat{\Omega}_{ref}(f_k)}{\xi}}$$

Getting the estimator for the ensemble ellipticity (2)

Final goal: use results of the previous analysis to build an estimator for the average ellipticity of the NS population

Estimator for $\left(\boldsymbol{\varepsilon}^2\right)_{av} \equiv \left\langle\boldsymbol{\varepsilon}^2\right\rangle_{NS}$

$$\widehat{\left(\varepsilon^2\right)}_{av}(\mathrm{f_k}) \equiv \frac{\widehat{\Omega}_{ref}(f_k)}{\xi} \xrightarrow[\text{value}]{\text{With expectation}} \left\langle\widehat{\left(\varepsilon^2\right)}_{av}(f_k)\right\rangle = \langle\varepsilon^2\rangle_{NS} = \underbrace{\varepsilon^2_{av}(f_k)}_{\text{Squared mean value}} + \underbrace{\sigma^2_{\varepsilon}(f_k)}_{\text{Intrinsic variance}} \approx \varepsilon^2(f_k)$$

Getting the estimator for the ensemble ellipticity (2)

Final goal: use results of the previous analysis to build an estimator for the average ellipticity of the NS population

Estimator for $\boldsymbol{(\varepsilon^2)_{av} \equiv \langle \varepsilon^2 \rangle_{NS}}$

$$\widehat{(\varepsilon^2)}_{av}(\mathrm{f_k}) \equiv \frac{\widehat{\Omega}_{ref}(f_k)}{\xi} \xrightarrow[\text{value}]{\text{With expectation}} \left\langle \widehat{(\varepsilon^2)}_{av}(f_k) \right\rangle = \langle \varepsilon^2 \rangle_{NS} = \varepsilon^2_{av}(f_k) + \sigma^2_{\varepsilon}(f_k) \approx \varepsilon^2(f_k)$$

Squared mean value

Intrinsic variance

Estimator for $\boldsymbol{\varepsilon_{av} \equiv \langle \varepsilon \rangle_{NS}}$

$$\boxed{\hat{\varepsilon}_{av}(f_k) = \sqrt{\widehat{(\varepsilon^2)}_{av}\ (\mathrm{f_k})}} \longrightarrow$$

What is its likelihood function?

Getting the estimator for the ensemble ellipticity (2)

Final goal: use results of the previous analysis to build an estimator for the average ellipticity of the NS population

Estimator for $\boldsymbol{(\varepsilon^2)_{av} \equiv \langle \varepsilon^2 \rangle_{NS}}$

$$\widehat{(\varepsilon^2)}_{av}(\mathrm{f_k}) \equiv \frac{\widehat{\Omega}_{ref}(f_k)}{\xi} \xrightarrow{\text{With expectation value}} \left\langle \widehat{(\varepsilon^2)}_{av}(f_k) \right\rangle = \langle \varepsilon^2 \rangle_{NS} = \underbrace{\varepsilon_{av}^2(f_k)}_{\text{Squared mean value}} + \underbrace{\sigma_\varepsilon^2(f_k)}_{\text{Intrinsic variance}} \approx \varepsilon^2(f_k)$$

Estimator for $\boldsymbol{\varepsilon_{av} \equiv \langle \varepsilon \rangle_{NS}}$

$$\boxed{\hat{\varepsilon}_{av}(f_k) = \sqrt{\widehat{(\varepsilon^2)}_{av}\ (\mathrm{f_k})}} \longrightarrow$$

What is its likelihood function?

From the likelihood for the cross-correlation statistic

$$p\left(\hat{C}(f_k)\middle|\Omega(f_k)\right) = \frac{1}{\sqrt{2\pi}\sigma_\Omega(f_k)} e^{-\left(\hat{C}(f_k) - \Omega(f_k)\right)^2 / 2\sigma_\Omega^2(f_k)}$$

Getting the estimator for the ensemble ellipticity (2)

Final goal: use results of the previous analysis to build an estimator for the average ellipticity of the NS population

Estimator for $\boldsymbol{(\varepsilon^2)_{av} \equiv \langle \varepsilon^2 \rangle_{NS}}$

$$\widehat{(\varepsilon^2)}_{av}(\mathrm{f_k}) \equiv \frac{\widehat{\Omega}_{ref}(f_k)}{\xi} \xrightarrow[\text{value}]{\text{With expectation}} \left\langle \widehat{(\varepsilon^2)}_{av}(f_k) \right\rangle = \langle \varepsilon^2 \rangle_{NS} = \underbrace{\varepsilon^2_{av}(f_k)}_{\text{Squared mean value}} + \underbrace{\sigma^2_\varepsilon(f_k)}_{\text{Intrinsic variance}} \approx \varepsilon^2(f_k)$$

Estimator for $\boldsymbol{\varepsilon_{av} \equiv \langle \varepsilon \rangle_{NS}}$

$$\boxed{\hat{\varepsilon}_{av}(f_k) = \sqrt{\widehat{(\varepsilon^2)}_{av}\ (\mathrm{f_k})}} \longrightarrow$$

What is its likelihood function?

From the likelihood for the cross-correlation statistic

$$p\big(\hat{C}(f_k)\big|\Omega(f_k)\big) = \frac{1}{\sqrt{2\pi}\sigma_\Omega(f_k)} e^{-\left(\hat{C}(f_k) - \Omega(f_k)\right)^2 / 2\sigma^2_{\Omega}(f_k)}$$

Change of variable

No longer gaussian distributed!

$$\boxed{p_\varepsilon(\hat{\varepsilon}_{av}(f_k)|\varepsilon_{av}(f_k)) = \sqrt{\frac{8}{\pi}} \frac{\varepsilon_{av}(f_k)\xi}{\sigma_{\widehat{\Omega}}(f_k)} e^{-\left(\hat{\varepsilon}^2_{av}(f_k) - \varepsilon^2_{av}(f_k)\right)^2 \xi^2 / 2\sigma^2_{\widehat{\Omega}}(f_k)}}$$

Getting the estimator for the ensemble ellipticity (2)

Final goal: use results of the previous analysis to build an estimator for the average ellipticity of the NS population

Estimator for $\boldsymbol{\left(\varepsilon^2\right)_{av} \equiv \left\langle \varepsilon^2 \right\rangle_{NS}}$

$$\widehat{\left(\varepsilon^2\right)}_{av}(\mathrm{f_k}) \equiv \frac{\widehat{\Omega}_{ref}(f_k)}{\xi} \xrightarrow[\text{value}]{\text{With expectation}} \left\langle \widehat{\left(\varepsilon^2\right)}_{av}(f_k) \right\rangle = \langle \varepsilon^2 \rangle_{NS} = \varepsilon^2_{av}(f_k) + \sigma^2_{\varepsilon}(f_k) \approx \varepsilon^2(f_k)$$

Squared mean value

Intrinsic variance

Estimator for $\boldsymbol{\varepsilon_{av} \equiv \langle \varepsilon \rangle_{NS}}$

$$\boxed{\hat{\varepsilon}_{av}(f_k) = \sqrt{\widehat{\left(\varepsilon^2\right)}_{av}(\mathrm{f_k})}} \longrightarrow$$

What is its likelihood function?

From the likelihood for the cross-correlation statistic

$$p\left(\hat{C}(f_k) \middle| \Omega(f_k)\right) = \frac{1}{\sqrt{2\pi}\sigma_\Omega(f_k)} e^{-\left(\hat{C}(f_k) - \Omega(f_k)\right)^2 / 2\sigma^2_\Omega(f_k)}$$

Change of variable

No longer gaussian distributed!

$$\boxed{p_\varepsilon(\hat{\varepsilon}_{av}(f_k)|\varepsilon_{av}(f_k)) = \sqrt{\frac{8}{\pi}} \frac{\varepsilon_{av}(f_k)\xi}{\sigma_{\widehat{\Omega}}(f_k)} e^{-\left(\hat{\varepsilon}^2_{av}(f_k) - \varepsilon^2_{av}(f_k)\right)^2 \xi^2 / 2\sigma^2_{\widehat{\Omega}}(f_k)}}$$

Variance of $\boldsymbol{\hat{\varepsilon}_{av}(f_k)}$

$$\boxed{\sigma^2_{\hat{\varepsilon}}(f_k)\Big|_{\hat{\varepsilon}(f_k) \ll 1} \approx 0.12 \frac{\sigma_{\widehat{\Omega}}(f_k)}{\xi}}$$

Getting the estimator for the ensemble ellipticity (3)

Final goal: use results of the previous analysis to build an estimator for the average ellipticity of the NS population

Estimator for $\boldsymbol{\varepsilon_{av} \equiv \langle \varepsilon \rangle_{NS}}$

$$\hat{\varepsilon}_{av}(f_k) \equiv \sqrt{\left(\widehat{\varepsilon^2}\right)_{av}\ (\mathrm{f_k})}$$

$$\sigma^2_{\hat{\varepsilon}}(f_k)\Big|_{\hat{\varepsilon}(f_k) \ll 1} \approx 0.12\,\frac{\sigma_\Omega(f_k)}{\xi}$$

Variance of $\boldsymbol{\hat{\varepsilon}_{av}(f_k)}$

These are narrow-band estimators, and we need to combine them over the frequencies

Getting the estimator for the ensemble ellipticity (3)

Final goal: use results of the previous analysis to build an estimator for the average ellipticity of the NS population

Estimator for $\boldsymbol{\varepsilon_{av} \equiv \langle \varepsilon \rangle_{NS}}$

$$\hat{\varepsilon}_{av}(f_k) = \sqrt{\widehat{\left(\varepsilon^2\right)}_{av}\ (\mathrm{f_k})}$$

$$\sigma_{\hat{\varepsilon}}^2(f_k)\Big|_{\hat{\varepsilon}(f_k)\ll 1} \approx 0.12\,\frac{\sigma_\Omega(f_k)}{\xi}$$

Variance of $\boldsymbol{\hat{\varepsilon}_{av}(f_k)}$

These are narrow-band estimators, and we need to combine them over the frequencies

Optimal broadband estimator

$$\hat{\varepsilon}_{opt} = \frac{\sum_k \hat{\varepsilon}(f_k)/\sigma_\varepsilon^2(f_k)}{\sum_k 1/\sigma_\varepsilon^2(f_k)}$$

$$\hat{\sigma}^2{}_{opt} = \frac{1}{\sum_k 1/\sigma_\varepsilon^2(f_k)}$$

Why are we doing this?

Getting the estimator for the ensemble ellipticity (3)

Final goal: use results of the previous analysis to build an estimator for the average ellipticity of the NS population

Estimator for $\boldsymbol{\varepsilon_{av} \equiv \langle \varepsilon \rangle_{NS}}$

$$\hat{\varepsilon}_{av}(f_k) = \sqrt{\left(\widehat{\varepsilon^2}\right)_{av}\ (\mathrm{f_k})}$$

$$\sigma^2_{\hat{\varepsilon}}(f_k)\Big|_{\hat{\varepsilon}(f_k)\ll 1} \approx 0.12\,\frac{\sigma_\Omega(f_k)}{\xi}$$

Variance of $\boldsymbol{\hat{\varepsilon}_{av}(f_k)}$

These are narrow-band estimators, and we need to combine them over the frequencies

Optimal broadband estimator

$$\hat{\varepsilon}_{opt} = \frac{\sum_k \hat{\varepsilon}(f_k)/\sigma^2_{\varepsilon}(f_k)}{\sum_k 1/\sigma^2_{\varepsilon}(f_k)}$$

$$\hat{\sigma}^2{}_{opt} = \frac{1}{\sum_k 1/\sigma^2_{\varepsilon}(f_k)}$$

Why are we doing this?

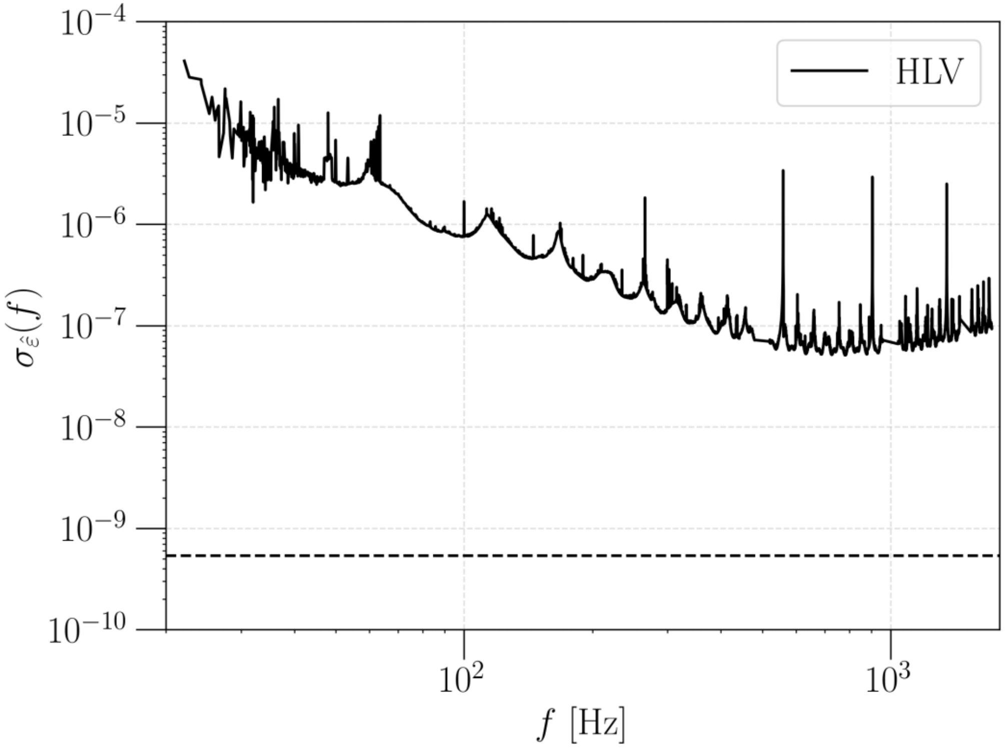

Figure 3. Plot of the 1σ sensitivity to the average ellipticity of Galactic NSs. The solid curve shows the uncertainty $\sigma_{\varepsilon}(f_k)$ associated to the narrowband estimators, while the dashed one is the broadband value of $\sigma_{\rm opt}$. The improvement of the search sensitivity by combining the narrowband estimators ranges between two and four orders of magnitude. The plot assumes $N_{\rm band} = 1.6 \times 10^7$, $\langle 1/d^2 \rangle_{\rm NS}^{-1/2} = 6$ kpc, and $\langle I_{zz}^2 \rangle_{\rm NS}^{1/2} = 10^{38}$ kg m^2.

Results

$\Omega(f)$	$\hat{C}^{\mathrm{O1+O2+O3}}/(10^{-14})$	$\Omega_{\mathrm{ref}}^{95\%,\ \mathrm{Uniform}}$	$\Omega_{\mathrm{ref}}^{95\%,\ \mathrm{Log-uniform}}$	$\Phi(f)$	N_{band}	$\hat{\varepsilon}_{\mathrm{opt}}^{\mathrm{O1+O2+O3}}/10^{-11}$	$\varepsilon_{\mathrm{Log-uniform}}^{95\%}$
$\propto (f)^7\,\Phi(f)$	0.9 ± 1.9	4.5×10^{-14}	2.0×10^{-14}	ATNF-KDE	1.6×10^7	2.5 ± 53.5	1.8×10^{-8}

Table 1. Results of the isotropic search for a SGWB from an ensemble of Galactic NSs using data from the first three LIGO-Virgo-KAGRA observing runs, and the subsequent constraints on the average ellipticity of the Galactic NS population. The first four columns are the results from our search, in which $\Omega(f)$, the cross-correlation statistics, and the upper limits on Ω_{ref}, using a uniform and log-uniform prior, are reported. The last four columns encode information about the Galactic NS population, such as $\Phi(f)$ and N_{band}, the average ellipticity optimal estimator, and the upper limit obtained by assuming a log-uniform prior on ε between $10^{-12} - 10^{-4}$.

Results

$\Omega(f)$	$\hat{C}^{\mathrm{O1+O2+O3}}/(10^{-14})$	$\Omega_{\mathrm{ref}}^{95\%,\ \mathrm{Uniform}}$	$\Omega_{\mathrm{ref}}^{95\%,\ \mathrm{Log-uniform}}$	$\Phi(f)$	N_{band}	$\hat{\varepsilon}_{\mathrm{opt}}^{\mathrm{O1+O2+O3}}/10^{-11}$	$\varepsilon_{\mathrm{Log-uniform}}^{95\%}$
$\propto (f)^7\,\Phi(f)$	0.9 ± 1.9	4.5×10^{-14}	2.0×10^{-14}	ATNF-KDE	1.6×10^7	2.5 ± 53.5	1.8×10^{-8}

Table 1. Results of the isotropic search for a SGWB from an ensemble of Galactic NSs using data from the first three LIGO-Virgo-KAGRA observing runs, and the subsequent constraints on the average ellipticity of the Galactic NS population. The first four columns are the results from our search, in which $\Omega(f)$, the cross-correlation statistics, and the upper limits on Ω_{ref}, using a uniform and log-uniform prior, are reported. The last four columns encode information about the Galactic NS population, such as $\Phi(f)$ and N_{band}, the average ellipticity optimal estimator, and the upper limit obtained by assuming a log-uniform prior on ε between $10^{-12} - 10^{-4}$.

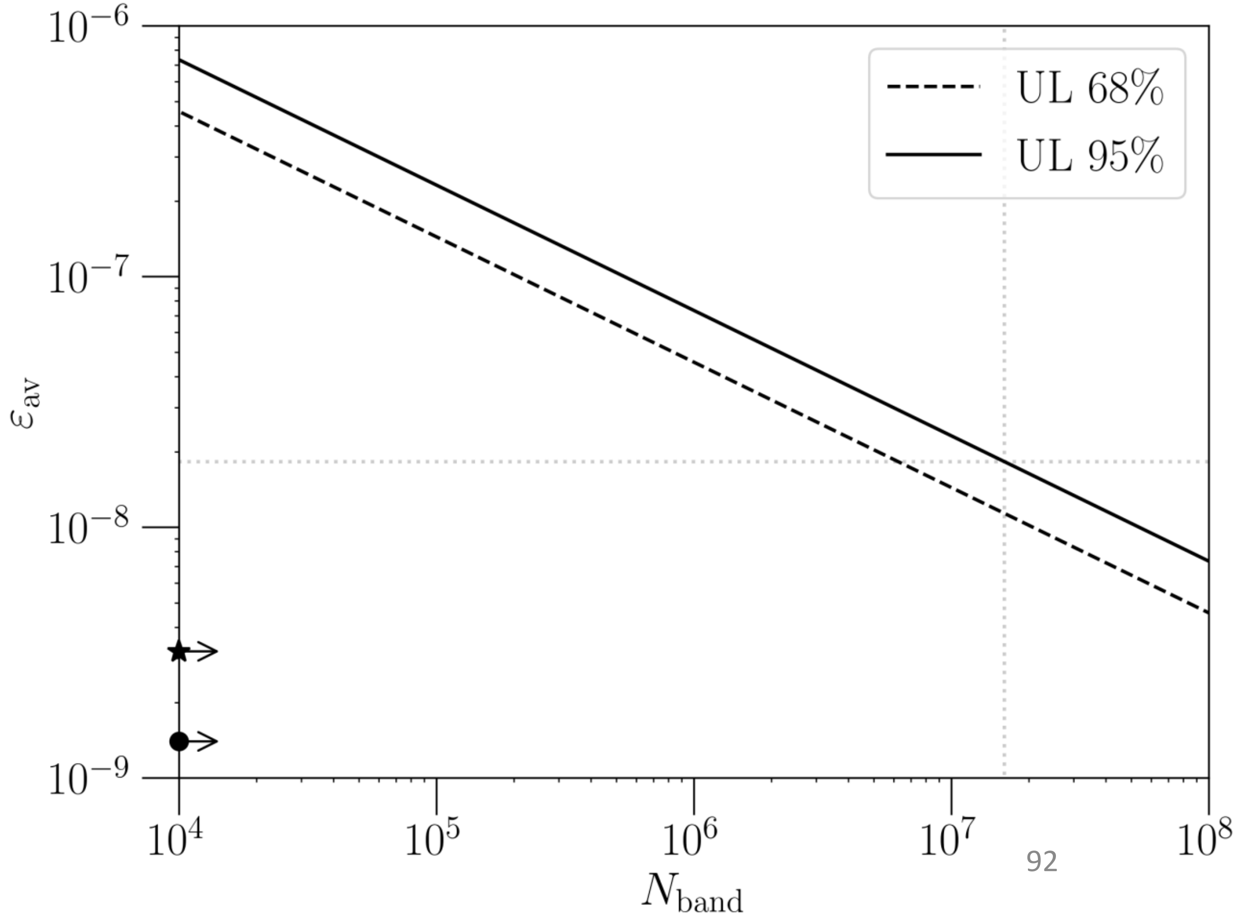

Figure 4. 68% (dashed) and 95% (solid) confidence-level Bayesian upper limits in the $N_{\mathrm{band}} - \varepsilon_{\mathrm{av}}$ plane, assuming a log-uniform prior on $\varepsilon_{\mathrm{av}}$. Here, we have set N_{band} to range from 10^4 and 10^8. The dotted grey lines identify the 95% upper limit on $\varepsilon_{\mathrm{av}}$ obtained with the pivot value of in-band NSs, $N_{\mathrm{band}} = 1.6 \times 10^7$. The star and the circle on the y-axis denote the most recent, lowest upper limits on a single NS ellipticity (*independent of* N_{band}), respectively $\varepsilon \lesssim 3.2 \times 10^{-9}$ from targeted (Abbott et al. 2021d) CW searches and $\varepsilon \lesssim 1.4 \times 10^{-9}$ (assuming 10 pc distance from Earth and a GW frequency of 2047.5 Hz) from all-sky (Abbott et al. 2022) ones.

Discussion and Conclusions

- In this work, we have derived constraints on the average ellipticity of a neutron-star population from the results of a cross-correlation-based search for a stochastic gravitational-wave background.

- In this talk, we have focussed on the Galactic neutron stars, and the search for isotropic background, using the the data from the first three observation runs of Advanced LIGO and Virgo. (See backup slides for the ‘‘hotspot’’ case.)

Discussion and Conclusions

- In this work, we have derived constraints on the average ellipticity of a neutron-star population from the results of a cross-correlation-based search for a stochastic gravitational-wave background.

- In this talk, we have focussed on the Galactic neutron stars, and the search for isotropic background, using the the data from the first three observation runs of Advanced LIGO and Virgo. (See backup slides for the ‘‘hotspot’’ case.)

- We have not found compelling evidence of a SGWB signal from any of the considered sources and hence have set upper limits on the intensity of the background by bounding the energy density parameter $\Omega_{gw}(f)$.

- These results have then been translated to constraints of the Galactic NS average ellipticity, obtained to be as low as $\varepsilon_{av} \leq 1.8 \times 10^{-8}$ with $N_{band} = 1.6 \times 10^{7}$NSs, and are the first of their kind.

Discussion and Conclusions

- In this work, we have derived constraints on the average ellipticity of a neutron-star population from the results of a cross-correlation-based search for a stochastic gravitational-wave background.

- In this talk, we have focussed on the Galactic neutron stars, and the search for isotropic background, using the the data from the first three observation runs of Advanced LIGO and Virgo. (See backup slides for the ‘‘hotspot’’ case.)

- We have not found compelling evidence of a SGWB signal from any of the considered sources and hence have set upper limits on the intensity of the background by bounding the energy density parameter $\Omega_{gw}(f)$.

- These results have then been translated to constraints of the Galactic NS average ellipticity, obtained to be as low as $\varepsilon_{av} \leq 1.8 \times 10^{-8}$ with $N_{band} = 1.6 \times 10^{7}$NSs, and are the first of their kind.

- These results are not directly comparable to the ones obtained from continuous wave searches, which are have a stronger constraining power ($\varepsilon \sim 10^{-9}$), but target one neutron star at a time, and are limited by their computational cost.

- Stochastic searches, on the other hand, have become computationally efficient and faster, and allow to instantaneously identifying the features of an ensemble of known or unknown NSs, which would otherwise require decades/centuries to be determined through individual NS discoveries.

- Possible synergies between the two searches, using the stochastic ones to perform a blind, rapid all-sky search for NS signals and transmit the coordinates of possible outliers as inputs of the continuous wave ones, for a more refined and sensitive search.

How to extend this work

- We could gain even more information about NS populations by treating the average squared moment of inertia and the average square inverse distance as free parameters.

- Additionally, we could estimate and set constraints on these quantities through a full Bayesian search, in which priors could be derived from population synthesis simulations.

How to extend this work

- We could gain even more information about NS populations by treating the average squared moment of inertia and the average square inverse distance as free parameters.

- Additionally, we could estimate and set constraints on these quantities through a full Bayesian search, in which priors could be derived from population synthesis simulations.

- These simulations could also be used to model the NS frequency and angular distributions, which could then be used as an alternative to those derived from the ATNF catalogue, especially in the case of extra-galactic NSs.

- The inclusion of angular distribution of the NSs would allow to perform a template-based matched-filtering search using the λ-statistics from Talukder et al. 2011, which may set less conservative upper limits. (This has actually already been implemented in Agarwal at al., 2022).

How to extend this work

- We could gain even more information about NS populations by treating the average squared moment of inertia and the average square inverse distance as free parameters.

- Additionally, we could estimate and set constraints on these quantities through a full Bayesian search, in which priors could be derived from population synthesis simulations.

- These simulations could also be used to model the NS frequency and angular distributions, which could then be used as an alternative to those derived from the ATNF catalogue, especially in the case of extra-galactic NSs.

- The inclusion of angular distribution of the NSs would allow to perform a template-based matched-filtering search using the λ-statistics from Talukder et al. 2011, which may set less conservative upper limits. (This has actually already been implemented in Agarwal at al., 2022).

- Finally, from the synthesised population, the corresponding SGWB signal could be simulated, and its prospects for detection and characterization could be examined within the networks of the future detector.

- Two ways of doing this would be to consider a network, where KAGRA and the future LIGO-India are included, or considering the next-generation interferometers, such as Einstein Telescope and Cosmic Explorer, and evaluate their impact on these kinds of searches.


Thank you for your attention!
Merci beaucoup de votre attention!

GRAVITATIONAL WAVE ORCHESTRA

SEPTEMBER 08-09, 2022

UNIVERSITÉ CATHOLIQUE DE LOUVAIN, BELGIUM

GWO

Current and Future
Stochastic Gravitational-Wave Background Probes in Multiple Frequency Bands

- Review on stochastic gravitational-wave background searches
- Theoretical developments in stochastic background modelling
- Most updated results from:
  LIGO-Virgo-KAGRA collaboration and Pulsar Timing Arrays
- Future probes and strategies using:
  Einstein Telescope, Cosmic Explorer, and LISA

INVITED SPEAKERS:

Joseph Romano (TTU, Lubbock)
Tania Regimbau (LAPP, Annecy)
Vuk Mandic (UMN, Minneapolis)
Irina Dvorkin (IAP, Paris)
Sanjit Mitra (IUCAA, Pune)
Carlo Contaldi (Imperial College)
Giulia Cusin (U. Geneva & IAP, Paris)
Stephen Taylor (Vanderbilt U., Nashville)
Chiara Caprini (APC, Paris)
Josquin Errard (APC, Paris)
Aditya Parthasarathy (MPIfR, Bonn)
Boris Goncharov (GSSI, L'Aquila)
Guillaume Boileau (U. Antwerpen)
Alex Jenkins (UCL, London)
Kamiel Janssens (U. Antwerpen)
Sébastien Clesse (ULB, Brussels)

Registration and Abstract Submission Deadline*: AUGUST 05, 2022

https://agenda.irmp.ucl.ac.be/e/gwo2022

Place croix du Sud, SUD-19,
Université catholique de Louvain,
Louvain-la-Neuve, B-1348.

ORGANIZING COMMITTEE

Jishnu Suresh, Federico De Lillo,
Antoine Depasse, Giacomo Bruno.

*You are strongly encouraged to submit abstracts on stochastic gravitational-wave background-related research for a poster presentation. Details can be found on the workshop website.

UCLouvain IRMP fnrs

ORGANIZING SECRETARY
Carinne Mertens
carinne.mertens@uclouvain.be


I guess you have some questions for me…

O3-iso: main results summary

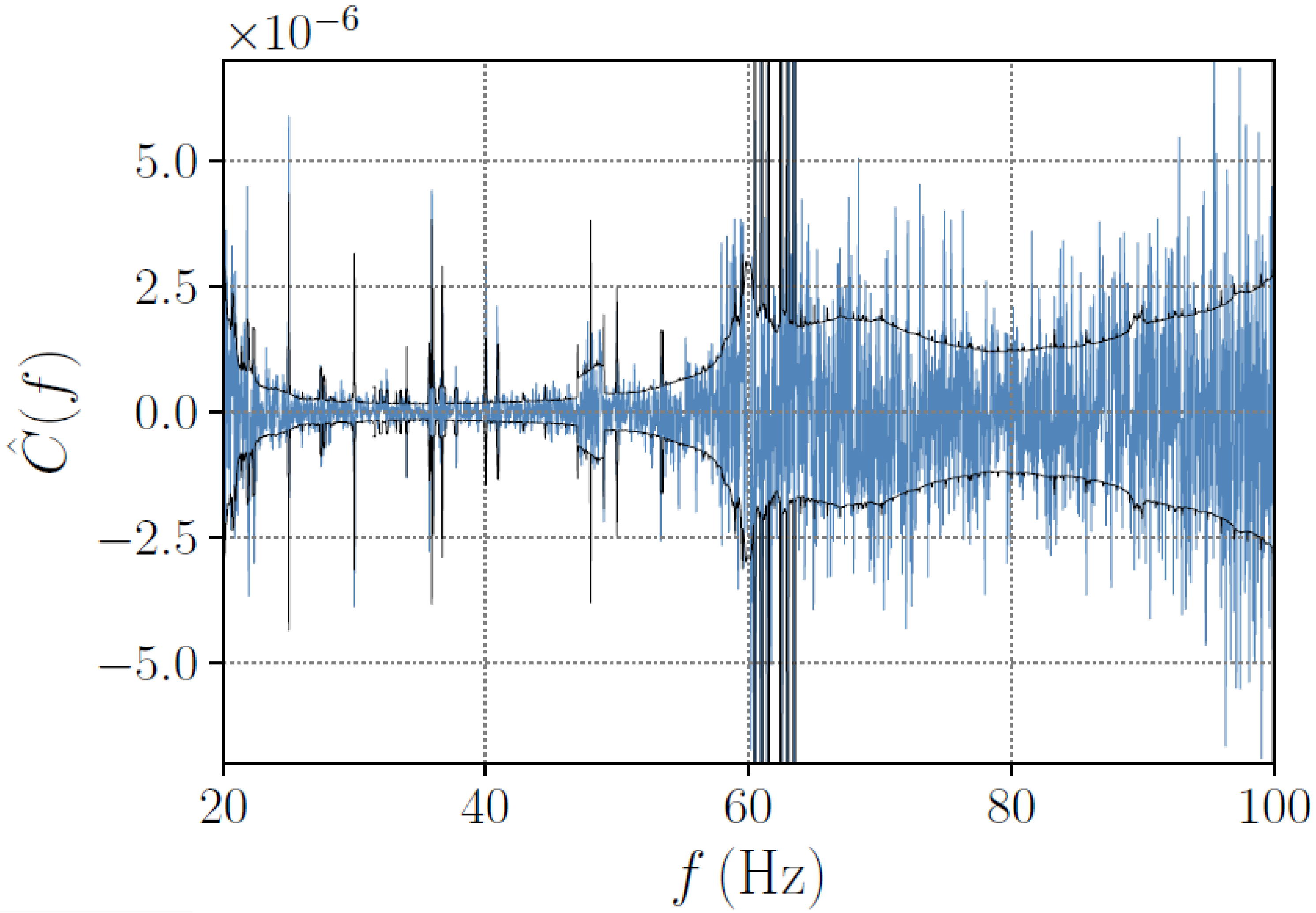

FIG. 3. Cross-correlation spectra combining data from all three baselines in O3, as well as the HL baseline in O1 and O2. As described in the main text, the spectrum is consistent with expectations from uncorrelated, Gaussian noise.

[Phys. Rev. D 104, 022004 (2021)]

Power law	$f_{99\%}^{HL}$ [Hz]	$\hat{C}^{HL}/10^{-9}$	$f_{99\%}^{HV}$ [Hz]	$\hat{C}^{HV}/10^{-9}$	$f_{99\%}^{LV}$ [Hz]	$\hat{C}^{LV}/10^{-9}$	$f_{99\%}^{\mathrm{O1+O2+O3}}$ [Hz]	$\hat{C}^{\mathrm{O1+O2+O3}}/10^{-9}$
0	76.1	-2.1 ± 8.2	97.7	229 ± 98	88.0	-134 ± 63	76.6	1.1 ± 7.5
2/3	90.2	-3.4 ± 6.1	117.8	145 ± 60	107.3	-82 ± 40	90.6	-0.2 ± 5.6
3	282.8	-1.3 ± 0.9	375.8	9.1 ± 4.1	388.0	-4.9 ± 3.1	291.6	-0.6 ± 0.8

TABLE I. Search results for an isotropic GWB, using the optimal filter method for power law GWBs with $\alpha = \{0, 2/3, 3\}$. For each of the three baselines IJ, we show the point estimate and 1σ uncertainty for the cross-correlation estimate C_{IJ}, along with the frequency band from 20 Hz to $f_{99\%}^{IJ}$ containing 99% of the sensitivity. We see that the HL baseline is the most sensitive, and the HV and LV baselines are more sensitive at higher frequencies, and for larger spectral indices, due to the longer baseline. In the last two columns, we also present the search result combining all three baselines from O3, as well as the O1 and O2 data. As noted in the main text, the point estimates for the HV and LV are approximately 2σ away from zero, however this is not consistent with a GWB given the result of the much more sensitive HL baseline.

	Uniform prior			Log-uniform prior		
α	O3	O2 [43]	Improvement	O3	O2 [43]	Improvement
0	1.7×10^{-8}	6.0×10^{-8}	3.6	5.8×10^{-9}	3.5×10^{-8}	6.0
2/3	1.2×10^{-8}	4.8×10^{-8}	4.0	3.4×10^{-9}	3.0×10^{-8}	8.8
3	1.3×10^{-9}	7.9×10^{-9}	5.9	3.9×10^{-10}	5.1×10^{-9}	13.1
Marg.	2.7×10^{-8}	1.1×10^{-7}	4.1	6.6×10^{-9}	3.4×10^{-8}	5.1

TABLE II. Upper limits at the 95% credible level on Ω_{ref} under the power law model for the GWB. We show upper limits conditioned on different fixed power law indices α, as well as a marginalized limit obtained by integration over α, using a Gaussian prior with zero mean and a standard deviation of 3.5. We show the results using a prior that is uniform in Ω_{ref}, as well as uniform in $\log \Omega_{\mathrm{ref}}$. As described in the main text, the uniform upper limits are more conservative, while the log uniform priors are more sensitive to weak signals. We also compare with the upper limits from [43], and give the improvement factor we achieve using O3 data.

Phys. Rev. D 104, 022004 (2021)

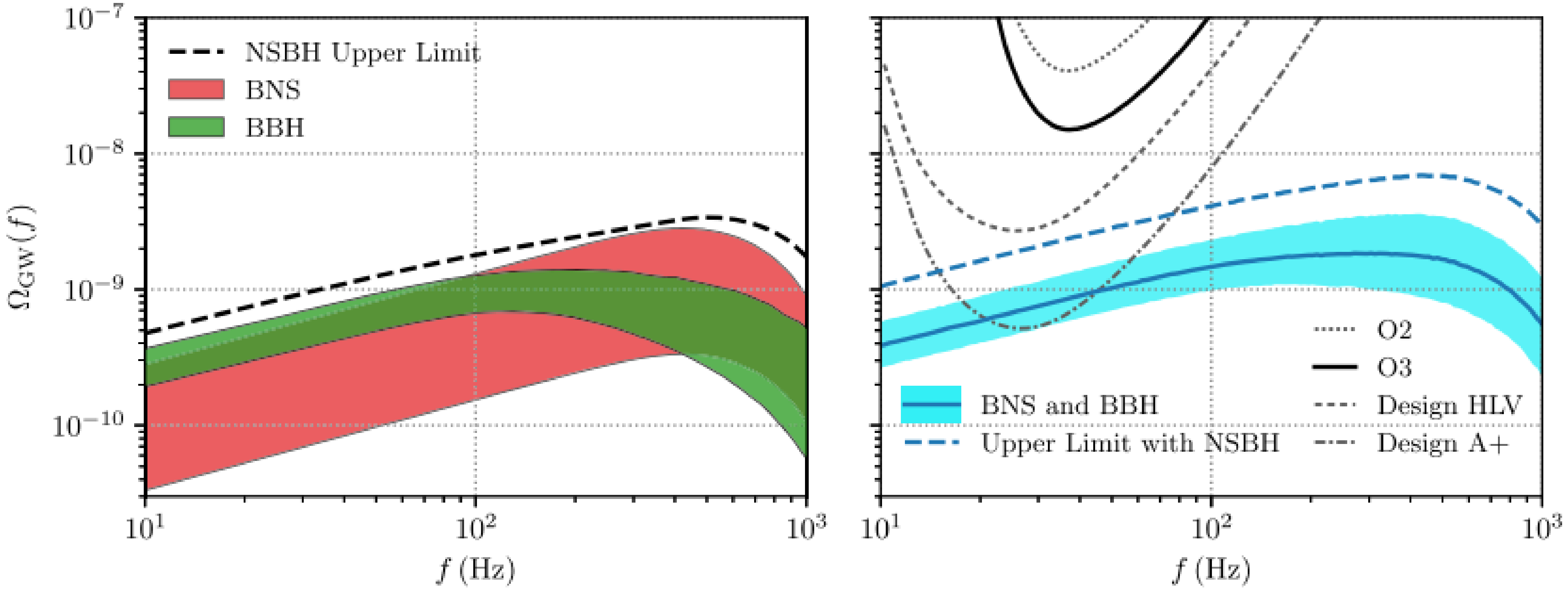

FIG. 5. Fiducial model predictions for the GWB from BBHs, BNSs, and NSBHs, along with current and projected sensitivity curves. In the left panel we show 90% credible bands for the GWB contributions from BNS and BBH mergers. Whereas the BNS uncertainty band illustrates purely the statistical uncertainties in the BNS merger rate, the BBH uncertainty band additionally includes systematic uncertainties in the binary mass distribution, as described in the main text. As no unambiguous NSBH detections have been made, we only show an upper limit on the possible contribution from such systems. The right panel compares the combined BBH and BNS energy density spectra, and 2σ power-law integrated (PI) curves for O2, O3, and projections for the HLV network at design sensitivity, and the A + detectors. The solid blue line shows the median estimate of $\Omega_{\rm BBH+BNS}(f)$ as a function of frequency, while the shaded blue band illustrates 90% credible uncertainties. The dashed line, meanwhile, marks our projected upper limit on the total GWB, including our upper limit on the contribution from NSBH mergers.

Phys. Rev. D 104, 022004 (2021)

Anisotropic analysis

Spacial distribution of GW power on the sky at frequency f

Gaussian, stationary, unpolarized, anisotropic background

$$\boxed{\langle h_A(f,\hat{\boldsymbol{n}})h^*_{A'}(f',\hat{\boldsymbol{n}}')\rangle = \frac{1}{4}\boldsymbol{\mathcal{P}}(f,\hat{\boldsymbol{n}})\delta(f-f')\delta_{AA'}\delta^2(\widehat{\hat{\boldsymbol{n}},\boldsymbol{n}'})}$$

Back to isotropic case by defining

$$S_h(f) = \int d^2\Omega_{\hat{\boldsymbol{n}}}\boldsymbol{\mathcal{P}}(f,\hat{\boldsymbol{n}})$$

Ansatz

The only unknown quantity

$$\boxed{\boldsymbol{\mathcal{P}}(f,\hat{\boldsymbol{n}}) = \bar{H}(f)\mathcal{P}(\hat{\boldsymbol{n}}) \qquad \bar{H}(f) = \left(\frac{f}{f_{ref}}\right)^{\beta-3}}$$

From theory

Anisotropic analysis

Spacial distribution of GW power
on the sky at frequency f

Gaussian, stationary, unpolarized, anisotropic background

$$\langle h_A(f,\hat{\boldsymbol{n}})h^*_{A'}(f',\hat{\boldsymbol{n}}')\rangle = \frac{1}{4}\boldsymbol{\mathcal{P}}(f,\hat{\boldsymbol{n}})\delta(f-f')\delta_{AA'}\delta^2(\widehat{\hat{\boldsymbol{n}},\boldsymbol{n}'})$$

Back to isotropic case by defining

$$S_h(f) = \int d^2\Omega_{\hat{\boldsymbol{n}}}\boldsymbol{\mathcal{P}}(f,\hat{\boldsymbol{n}})$$

Ansatz

The only unknown quantity

$$\boldsymbol{\mathcal{P}}(f,\hat{\boldsymbol{n}}) = \bar{H}(f)\mathcal{P}(\hat{\boldsymbol{n}}) \qquad \bar{H}(f) = \left(\frac{f}{f_{ref}}\right)^{\beta-3}$$

From theory

2-sphere basis

Spherical Harmonics Decomposision (SHD)

$$\mathcal{P}(\hat{\boldsymbol{n}}) = \sum_{l=}^{l_{max}}\sum_{m=-l}^{l}\mathcal{P}_{lm}Y_{lm}(\hat{\boldsymbol{n}}) \xrightarrow{\text{Optimal for}} \textbf{Extended sources}$$

Embeds the isotropic case

$$\mathcal{P}_{00} = S_h(f_{ref})/\sqrt{4\pi}$$

Anisotropic analysis

Spacial distribution of GW power on the sky at frequency f

Gaussian, stationary, unpolarized, anisotropic background

$$\langle h_A(f,\hat{\boldsymbol{n}})h^*_{A'}(f',\hat{\boldsymbol{n}}')\rangle = \frac{1}{4}\boldsymbol{\mathcal{P}}(f,\hat{\boldsymbol{n}})\delta(f-f')\delta_{AA'}\delta^2(\widehat{\hat{\boldsymbol{n}},\boldsymbol{n}'})$$

Back to isotropic case by defining

$$S_h(f) = \int d^2\Omega_{\hat{\boldsymbol{n}}}\boldsymbol{\mathcal{P}}(f,\hat{\boldsymbol{n}})$$

Ansatz

The only unknown quantity

$$\boldsymbol{\mathcal{P}}(f,\hat{\boldsymbol{n}}) = \bar{H}(f)\mathcal{P}(\hat{\boldsymbol{n}}) \qquad \bar{H}(f) = \left(\frac{f}{f_{ref}}\right)^{\beta-3}$$

From theory

2-sphere basis

Spherical Harmonics Decomposision (SHD)

$$\mathcal{P}(\hat{\boldsymbol{n}}) = \sum_{l=}^{l_{max}}\sum_{m=-l}^{l}\mathcal{P}_{lm}Y_{lm}(\hat{\boldsymbol{n}}) \xrightarrow{\text{Optimal for}} \textbf{Extended sources}$$

Embeds the isotropic case

$$\mathcal{P}_{00} = S_h(f_{ref})/\sqrt{4\pi}$$

Radiometer search: Pixel basis

Optimal for → **Point-like sources** → **Broadband analysis** / **Narrowband analysis**

$$\mathcal{P}(\hat{\boldsymbol{n}}) = \mathcal{P}_{\hat{\boldsymbol{n}}_0}\delta^2(\hat{\boldsymbol{n}},\hat{\boldsymbol{n}}_0)$$

Maximum likelihood approach

Cross-correlation

$$\hat{C}_{IJ}(\boxed{t;}f) = \frac{2}{\tau}\tilde{d}_I(t;f)\tilde{d}_J^*(t;f) \qquad \langle \hat{C}_{IJ}(t;f) \rangle = \bar{H}(f)\int d^2\Omega_{\hat{\boldsymbol{n}}}\gamma_{IJ}(t;f,\hat{\boldsymbol{n}})\mathcal{P}(\hat{\boldsymbol{n}})$$

Segment label

τ: much larger than light travel time between detectors but small enough to prevent significant variation of the detector response function

Maximum likelihood approach

Cross-correlation

$$\hat{C}_{IJ}(\boxed{t;}f) = \frac{2}{\tau}\tilde{d}_I(t;f)\tilde{d}_J^*(t;f) \qquad \langle \hat{C}_{IJ}(t;f)\rangle = \bar{H}(f)\int d^2\Omega_{\hat{\boldsymbol{n}}}\gamma_{IJ}(t;f,\hat{\boldsymbol{n}})\mathcal{P}(\hat{\boldsymbol{n}})$$

Segment label

τ: much larger than light travel time between detectors but small enough to prevent significant variation of the detector response function

Short Fourier transform

$$\tilde{d}_I(t;f) = \int_{t-\frac{\tau}{2}}^{t+\frac{\tau}{2}} dt'\, d_I(t')e^{-2\pi i f t'}$$

Geometrical factor

$$\gamma_{IJ}(t;f,\hat{\boldsymbol{n}}) \equiv \frac{1}{2}\sum_A F_I^A(f,\hat{\boldsymbol{n}})\ F_J^{A*}(f,\hat{\boldsymbol{n}})$$

Maximum likelihood approach

Cross-correlation

$$\hat{C}_{IJ}(\boxed{t};f) = \frac{2}{\tau}\tilde{d}_I(t;f)\tilde{d}_J^*(t;f) \qquad \langle \hat{C}_{IJ}(t;f)\rangle = \bar{H}(f)\int d^2\Omega_{\hat{\boldsymbol{n}}}\gamma_{IJ}(t;f,\hat{\boldsymbol{n}})\mathcal{P}(\hat{\boldsymbol{n}})$$

Segment label

τ: much larger than light travel time between detectors but small enough to prevent significant variation of the detector response function

Short Fourier transform

$$\tilde{d}_I(t;f) = \int_{t-\frac{\tau}{2}}^{t+\frac{\tau}{2}} dt'\, d_I(t')e^{-2\pi i f t\prime}$$

Geometrical factor

$$\gamma_{IJ}(t;f,\hat{\boldsymbol{n}}) \equiv \frac{1}{2}\sum_A F_I^A(f,\hat{\boldsymbol{n}})\ F_J^{A*}(f,\hat{\boldsymbol{n}})$$

Recasting to

Matrix formalism

$$\langle \hat{C}_{IJ}(t;f)\rangle = \bar{H}(f)\int d^2\Omega_{\hat{\boldsymbol{n}}}\gamma_{IJ}(t;f,\hat{\boldsymbol{n}})\mathcal{P}(\hat{\boldsymbol{n}}) \equiv M_{IJ}\mathcal{P} \qquad N_{tf,t'f'} \approx \delta_{tt'}\delta_{\mathrm{ff}'}P_{n_1}(t;f)P_{n_2}(t;f)$$

and assuming

Gaussian-stationary noise

$$p(\hat{C}|\mathcal{P}) \propto exp\left[-\frac{1}{2}(\hat{C}-M\mathcal{P})N^{-1}(\hat{C}-M\mathcal{P})\right]$$

Maximum likelihood estimator

ML estimator

Dirty map	**Fisher matrix**	**Clean map**
$X \equiv M^\dagger N^{-1}\hat{C}$	$F \equiv M^\dagger N^{-1}M$	$\hat{\mathcal{P}} = F^{-1}X$

$$\langle X \rangle = M^\dagger N^{-1} M \mathcal{P} = F\mathcal{P}$$

$$\mathcal{P}(\hat{\boldsymbol{n}}) = \delta^2(\hat{\boldsymbol{n}}, \hat{\boldsymbol{n}}_{\boldsymbol{0}})$$

$$\langle X(\hat{\boldsymbol{n}}) \rangle \to F(\hat{\boldsymbol{n}}, \hat{\boldsymbol{n}}_{\boldsymbol{0}})$$

Point spread function

Point-spread function

Phys. Rev. D 98, 024001

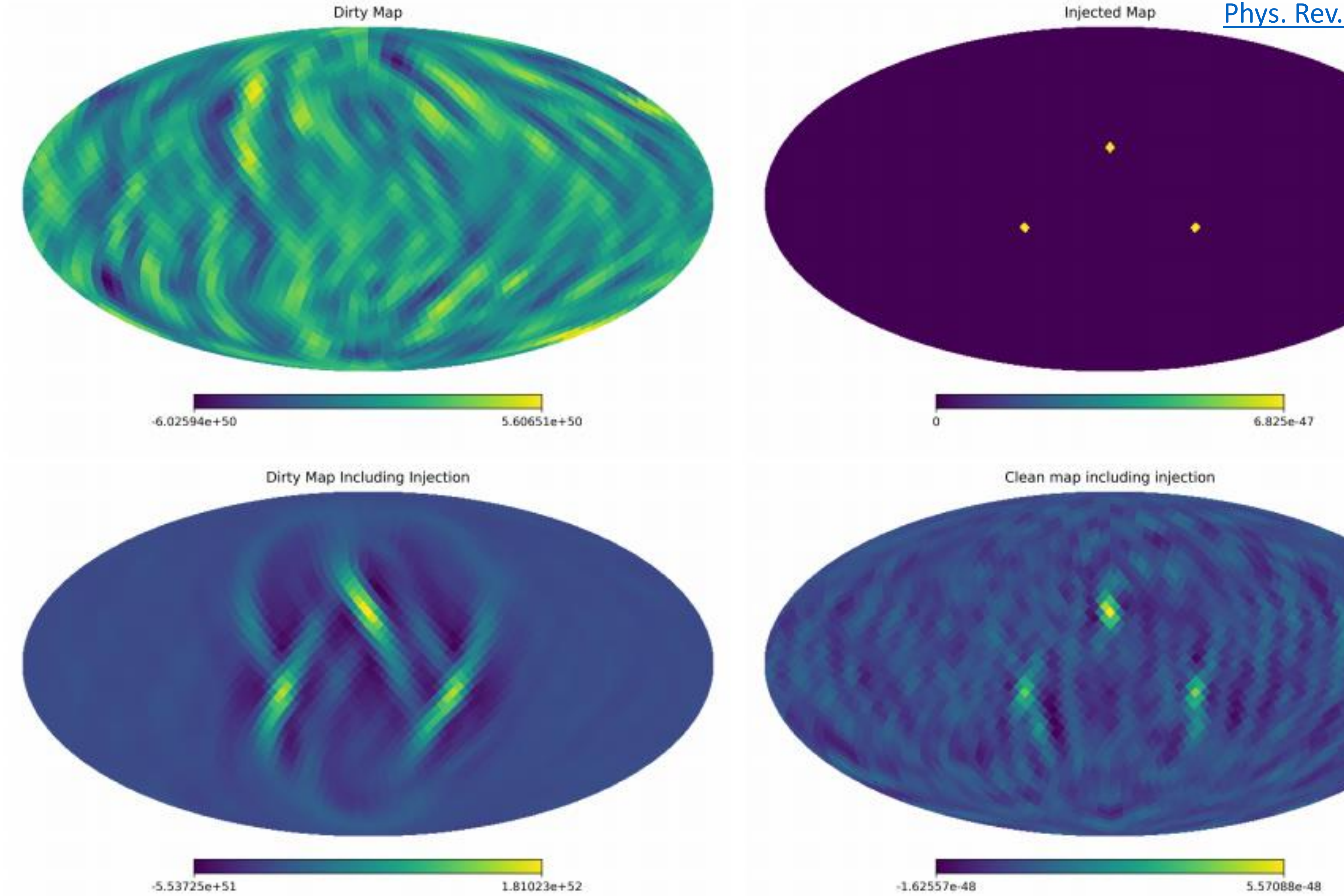

Maximum likelihood estimator

ML estimator

Dirty map	Fisher matrix	Clean map
$X \equiv M^{\dagger} N^{-1} \hat{C}$	$F \equiv M^{\dagger} N^{-1} M$	$\hat{\mathcal{P}} = F^{-1} X$

$$\langle X \rangle = M^{\dagger} N^{-1} M \mathcal{P} = F \mathcal{P}$$

$$\mathcal{P}(\hat{\boldsymbol{n}}) = \delta^2(\hat{\boldsymbol{n}}, \hat{\boldsymbol{n}}_0)$$
$$\langle X(\hat{\boldsymbol{n}}) \rangle \rightarrow F(\hat{\boldsymbol{n}}, \hat{\boldsymbol{n}}_0)$$

Point spread function

Extension to detectors network

$$X \equiv X_{\hat{\boldsymbol{n}}} = \sum_{I} \sum_{J>I} \sum_{t} \sum_{f} \gamma_{IJ}^{*}(t; f, \hat{\boldsymbol{n}}) \frac{\bar{H}(f)}{P_{n_1}(t; f) P_{n_2}(t; f)} \hat{C}_{IJ}(t; f)$$

$$F \equiv F_{\hat{\boldsymbol{n}}\hat{\boldsymbol{n}}'} = \sum_{I} \sum_{J>I} \sum_{t} \sum_{f} \gamma_{IJ}^{*}(t; f, \hat{\boldsymbol{n}}) \frac{\bar{H}^2(f)}{P_{n_1}(t; f) P_{n_2}(t; f)} \gamma_{IJ}(t; f, \widehat{\boldsymbol{n}'})$$

Upper limits

SHD GW energy flux per solid angle

$$\hat{\Omega}_{\hat{\boldsymbol{n}}} = \frac{2\pi^2}{3H_0^2} \mathrm{f}_{\mathrm{ref}}^{3} \hat{\mathcal{P}}_{\hat{\boldsymbol{n}}} \qquad \hat{\mathcal{F}}_{\hat{\boldsymbol{n}}} = \frac{c^3 \pi}{4G} \mathrm{f}_{\mathrm{ref}}^{2} \hat{\mathcal{P}}_{\hat{\boldsymbol{n}}}$$

GW energy density ratio per solid angle **BBR**

O3-directional: BBR results

All-sky BBR Results

α	Ω_{GW}	$H(f)$	Max SNR (% p-value) HL(O3)	HV(O3)	LV(O3)	O1+O2+O3 (HLV)	Upper limit ranges (10^{-8}) O1+O2+O3 (HLV)	O1 + O2 (HL)
0	constant	$\propto f^{-3}$	2.3 (66)	3.4 (24)	3.1 (51)	2.6 (23)	1.7 – 7.6	4.5 – 21
2/3	$\propto f^{2/3}$	$\propto f^{-7/3}$	2.5 (59)	3.7 (14)	3.1 (62)	2.7 (24)	0.85 – 4.1	2.3 – 12
3	$\propto f^{3}$	constant	3.7 (32)	3.6 (47)	4.1 (12)	3.6 (20)	0.013 – 0.11	0.047 – 0.32

TABLE I. The maximum SNR across all sky positions, its estimated p-value, and the range of the 95% upper limits on gravitational-wave energy flux $F_{\alpha,\Theta}$ [erg cm^{-2} s^{-1} Hz^{-1}] set by the BBR search for each baseline and for the three baselines combined using data from LIGO three observing runs and Virgo O3. The median improvement across the sky compared to limits from O2 analysis is a factor of 3.5 - 3.8, depending on α. O1+O2 upper limits reported in the last column differ from the upper limits reported in [55] for the reasons explained in the main text.

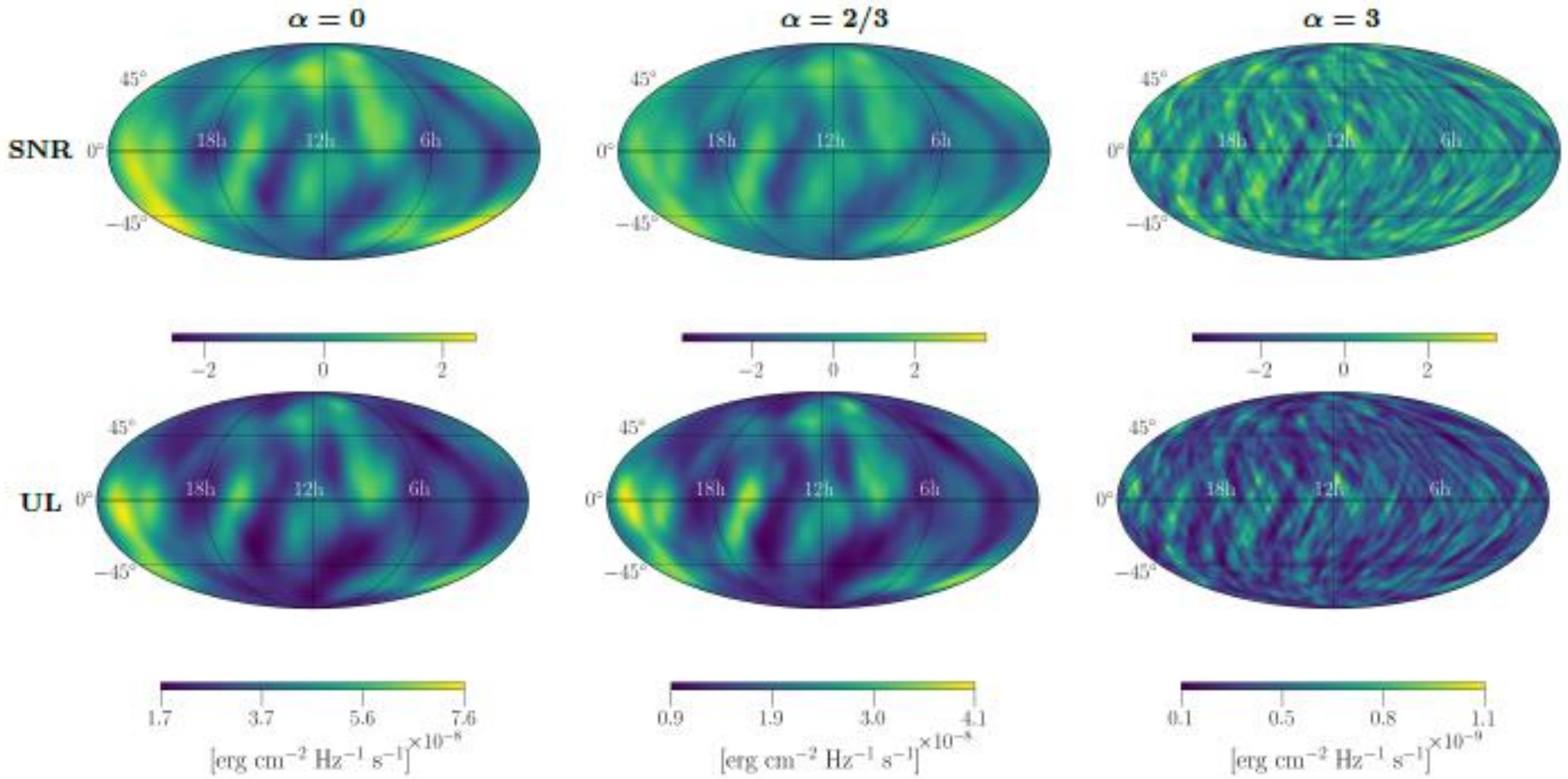

FIG. 2. Top row: SNR maps from a BBR search for point-like sources. Bottom row: upper limit (UL) sky maps of the gravitational-wave energy flux. Both sets of maps, presented in equatorial coordinate system, are derived by combining all three LIGO observing runs and the Virgo O3 data. $\alpha = 0$, 2/3, and 3 are represented from left to right.

[Phys.Rev.D 104 (2021) 2, 022005](https://doi.org/10.1103/PhysRevD.104.022005)

O3-directional: SHD results

SHD Results

α	Ω_{GW}	$H(f)$	Max SNR (% p-value) HL(O3)	HV(O3)	LV(O3)	O1+O2+O3 (HLV)	Upper limit range (10^{-9}) O1+O2+O3 (HLV)	O1 + O2 (HL)
0	constant	$\propto f^{-3}$	1.6 (78)	2.1 (40)	1.5 (83)	2.2 (43)	3.2–9.3	7.8–29
2/3	$\propto f^{2/3}$	$\propto f^{-7/3}$	3.0 (13)	3.9 (0.98)	1.9 (82)	3.7 (1.7)	1.9–9.7	6.5–25
3	$\propto f^{3}$	constant	3.9 (12)	4.0 (10)	3.9 (11)	3.2 (60)	0.56–3.4	1.9–11

TABLE II. We present the maximum SNR across all sky positions with its estimated p-value for the three separate baselines in the O3 observing as well as all three observing runs combined. We also present the range of the 95% upper limits on the normalized gravitational-wave energy density $\Omega_\alpha(\Theta)[\mathrm{sr}^{-1}]$ after combining data from LIGO-Virgo's three observing runs. Note that for both the p-values and the upper limits, Virgo-related baselines are incorporated only for O3. The median improvement across the sky compared to limits set by the O1+O2 analysis is 2.8 – 3.2 for the SHD search, depending on α.

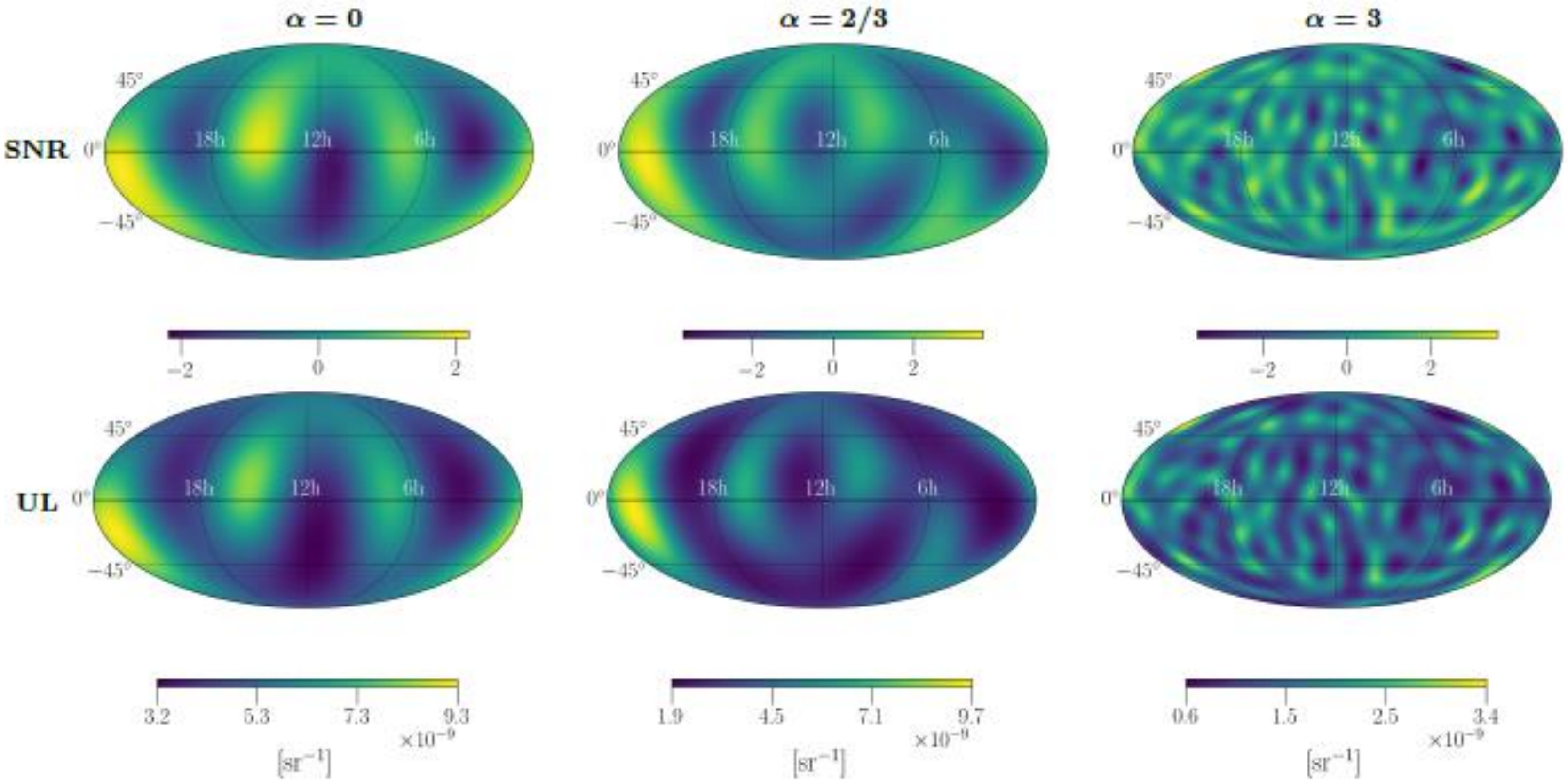

FIG. 3. Top row: SNR maps from the SHD search for extended sources. Bottom row: sky maps representing 95% upper limit on the normalized gravitational-wave energy density $\Omega_\alpha(\Theta)[\mathrm{sr}^{-1}]$. Both sets of maps, presented in equatorial coordinate system, are derived by combining all three observing runs of LIGO-Virgo data (Virgo was incorporated only for O3). $\alpha = 0$, 2/3, and 3 are represented from left to right.

Phys.Rev.D 104 (2021) 2, 022005

$$\Omega_{\rm gw}(f,\hat{n}) = \frac{f}{\rho_c}\frac{d^3\rho_{\rm gw}(f,\hat{n})}{df\,d^2\hat{n}} = \frac{2\pi^2}{3H_0^2}\,f^3\,\mathcal{P}(f,\hat{n}),$$

with $\mathcal{P}(f,\hat{n})$ being the GW strain power.

$$\mathcal{P}(f,\hat{n}) = \bar{H}(f)\mathcal{P}(\hat{n}), \tag{C7}$$

where $\bar{H}(f)$ is defined in such a way that $\bar{H}(f_{\rm ref}) = 1$, $\mathcal{P}(\hat{n})$ is the angular distribution of gravitational-wave power to be estimated by the search. For the signal model presented in section 3, $\bar{H}(f)$ turns out to be

$$\bar{H}(f) = \left(\frac{f}{f_{\rm ref}}\right)^4 \frac{\Phi(f)}{\Phi(f_{\rm ref})}\,. \tag{C8}$$

$$\hat{\mathcal{P}}^{\rm patch}_{\rm ref} = \frac{\sum_{k,j}\hat{\mathcal{P}}(f_{\rm k},\hat{n}_{\rm j})\,\sigma^{-2}(f_{\rm k},\hat{n}_{\rm j})\,\bar{H}(f)}{\sum_{k,j}\sigma^{-2}(f_{\rm k},\hat{n}_{\rm j})\,\bar{H}(f)^2}\,,$$

$$\sigma^{\rm patch}_{\rm ref} = \left(\sum_{k,j}\sigma^{-2}(f_{\rm k},\hat{n}_{\rm j})\,\bar{H}(f)^2\right)^{-1/2}.$$

To measure the anisotropies, the radiometer search introduces a maximum-likelihood (ML) estimator (Mitra et al. 2008; Thrane et al. 2009), as statistic, at each frequency and each direction (Abbott et al. 2021c) $\hat{\mathcal{P}}(f,\hat{n})$ with cross-correlation matrix $\sigma_{\hat{n},\hat{n}'}(f)$:

$$\hat{\mathcal{P}}(f,\hat{n}) = \sum_{\hat{n}'} [\Gamma_{\hat{n}\hat{n}'}(f)]^{-1} X_{\hat{n}'}(f), \tag{C2}$$

$$\sigma_{\hat{n},\hat{n}'}(f) = [\Gamma_{\hat{n}\hat{n}'}(f)]^{-1/2}, \tag{C3}$$

where $X_{\hat{n}'}(f)$ is called "dirty map" and $\Gamma_{\hat{n}\hat{n}'}$ is the Fisher information matrix in the small-signal limit. The summation over $\hat{n}'$ implies integration over the solid angle. The dirty map represents the sky seen through the response of a set of independent baselines IJ, defined as

$$X_{\hat{n}}(f) = \tau \Delta f\, \Re \sum_{IJ,t} \frac{[\gamma_{IJ}(t;f)]^*_{\hat{n}}\, \hat{C}_{IJ}(t;f)}{P_I(t;f)\, P_J(t;f)}, \tag{C4}$$

where $\hat{C}_{IJ}(t;f) \equiv (2/\tau)\, \tilde{s}^*_I(t;f)\, \tilde{s}_J(t;f)$ is the cross-correlation spectral density, while $\gamma_{IJ}(t;f,\hat{n})$ is the directional overlap reduction function, which is proportional to the isotropic one in equation (8) when integrated over the sky. The Fisher information matrix encodes the uncertainty in the measurement of the dirty map, and is defined as

$$\Gamma_{\hat{n},\hat{n}'}(f) = \tau \Delta f\, \Re \sum_{IJ,t} \frac{[\gamma_{IJ}(t;f)]^*_{\hat{n}}\, [\gamma_{IJ}(t;f)]_{\hat{n}'}}{P_I(t;f)\, P_J(t;f)}. \tag{C5}$$

The ML estimator $\hat{\mathcal{P}}(f,\hat{n})$ in equation (C2), involves the inversion of $\Gamma_{\hat{n},\hat{n}'}(f)$, which can be singular in general and must be regularised. However, for point-like sources considered here, we can work by employing the pixel basis

$$\mathcal{P}(f,\hat{n}) \equiv \mathcal{P}(f,\hat{n}')\, \delta^2(\hat{n},\hat{n}'), \tag{C6}$$

and ignore the correlation among neighbourhood directions in the sky (Abbott 2021b; Abbott et al. 2021c), and the Fisher information matrix is no longer singular and becomes diagonal. With this caveat, the estimator can be used to set upper limits on $\Omega_{\rm gw}(f,\hat{n})$ and related quantities.

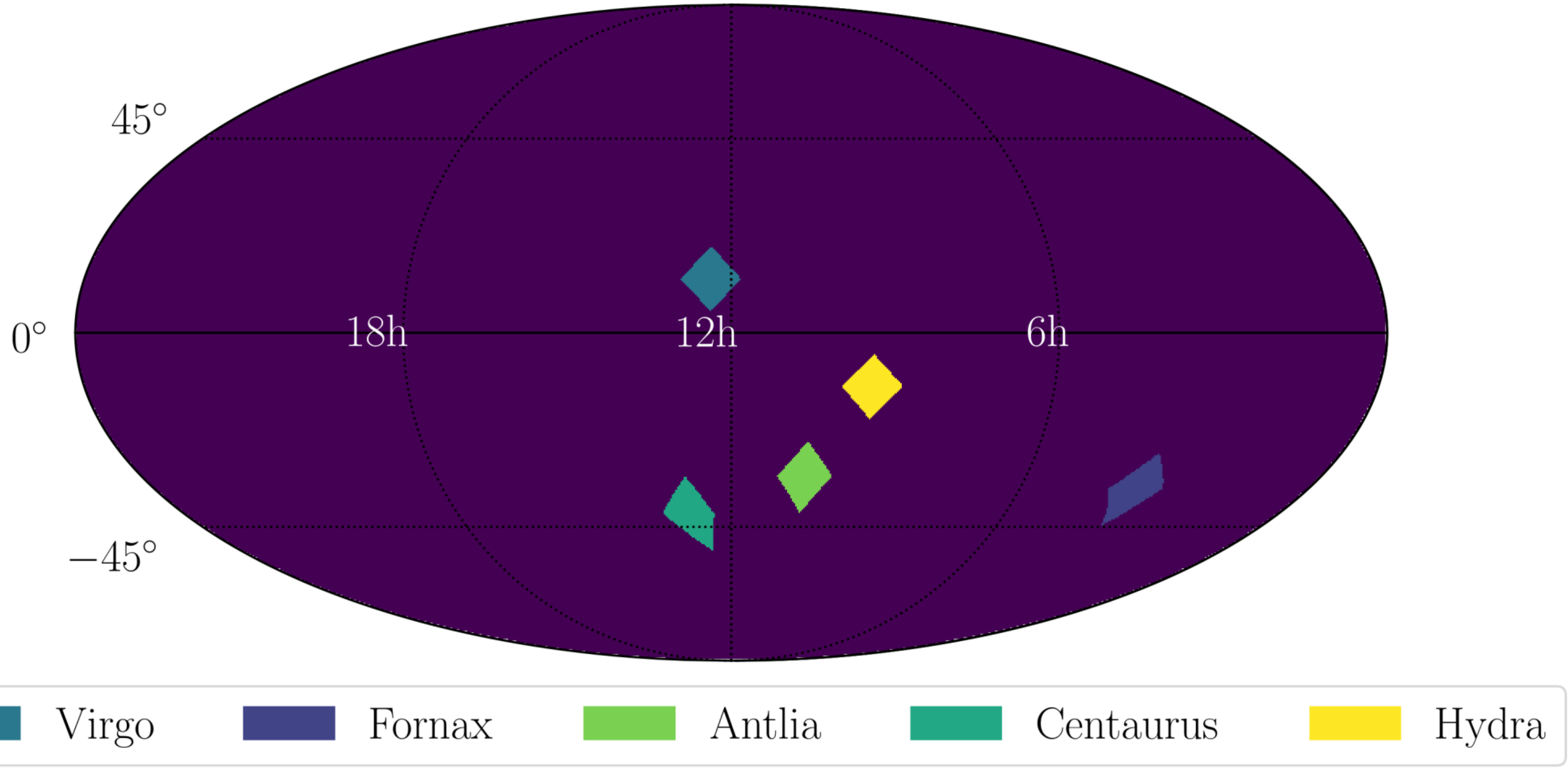

Figure 5. The sky-patches associated with the five NS hotspots: Virgo, Fornax, Antlia, Centaurus, and Hydra clusters. Each patch consists of 9 pixels with $N_{\mathrm{side}} = 16$: the central one being the one associated with the galaxy cluster, and the eight closest neighbours. The sky map is represented as a Mollweide projection of the sky in ecliptic coordinates.

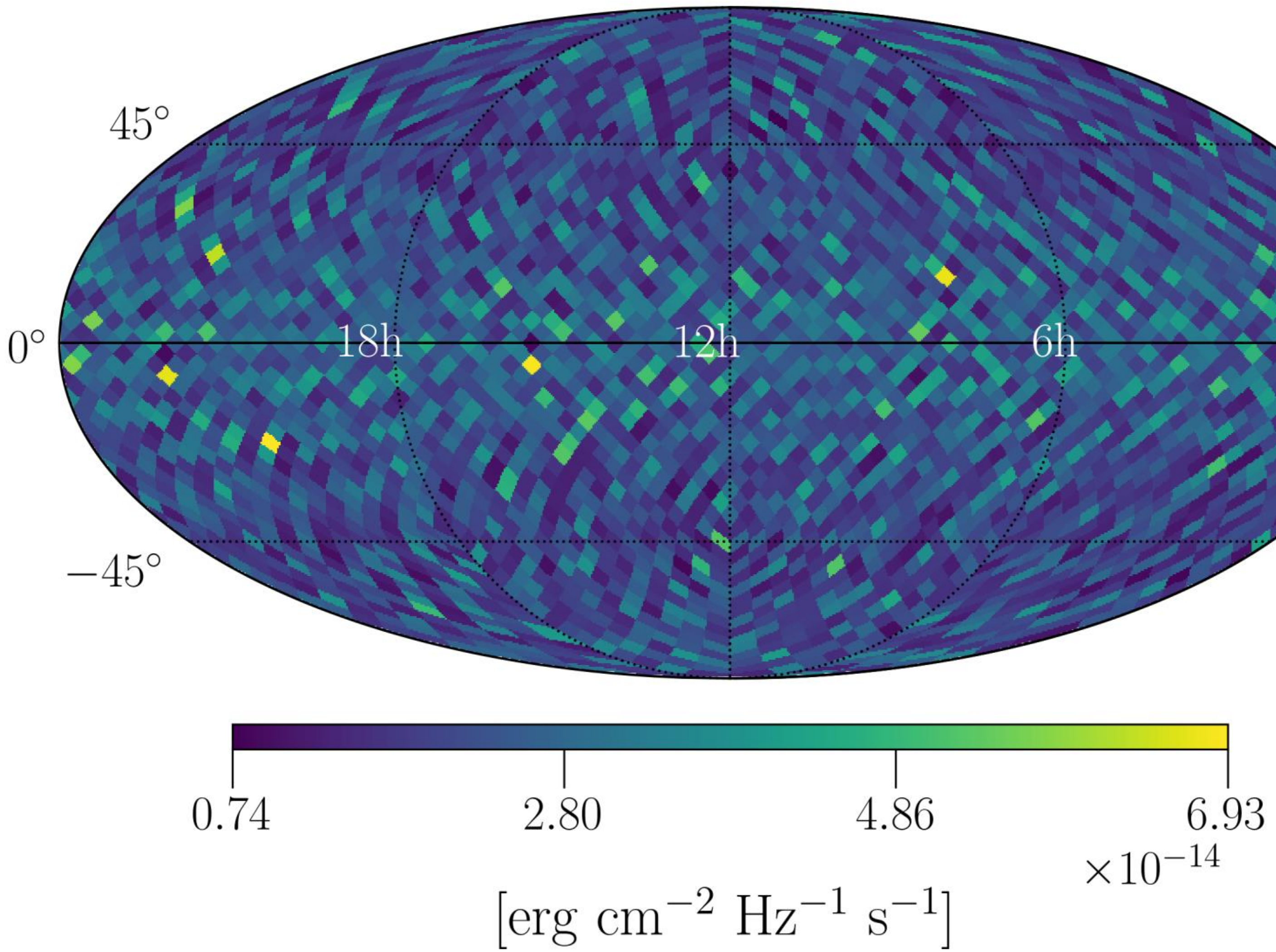

Figure C1. Upper limit sky maps on GW energy flux from the broadband-radiometer analysis for the model $\bar{H}(f)$ in equation (C8). Here the NSs frequency distribution $\Phi(f)$ is the one built from the ATNF catalogue as described in section 2. The sky map is represented as a color bar plot on a Mollweide projection of the sky in ecliptic coordinates with $N_{\text{side}} = 16$.

Hotspot	$\langle 1/d^2 \rangle_{\rm NS}^{-1/2}$ (Mpc)	$\hat{\varepsilon}_{\rm opt}^{\rm O1+O2+O3}/10^{-9}$	$\varepsilon^{95\%}_{\rm Log-uniform}/10^{-7}$
Virgo	18	0.6 ± 10.6	3.6
Fornax	19	0.5 ± 10.1	3.5
Antlia	40.7	1.5 ± 22.1	7.6
Centaurus	52.4	1.4 ± 27.9	9.6
Hydra	58.3	3.8 ± 34.2	11.8

Table 2. Relevant parameters and results of searches for NSs in hotspots. For each cluster of galaxies, a fiducial value of $\langle 1/d^2 \rangle_{\rm NS}^{-1/2}$ (second column), the broadband estimator $\hat{\varepsilon}_{\rm opt}$ (third column), and the 95% confidence level Bayesian upper limits on the average ellipticity of the population (fourth column) are reported. The upper limits have been obtained by assuming a log-uniform prior between $10^{-12} - 10^{-4}$ over the ellipticities.

Astrophysical GWB: nature

Duty cycle:

- ratio between the duration of the events and the time interval between successive events
  - average number of events present at the detector at a given observation time

$$\boxed{\Delta(z) = \int_0^z \bar{\tau}(1+z')\frac{\mathrm{d}R}{\mathrm{d}z'}(z')\mathrm{d}z'}$$

Continuous ($\Delta(z) >> 1$)

- time interval between events small compared to the duration of a single event
- waveforms overlap: Gaussian statistic
- completely determined by their spectral properties

Popcorn ($\Delta(z) \sim 1$)

- interval between events of the same order of the duration of a single event
- waveforms may overlap but no Gaussian statistic
- unpredictable amplitude on the detector at a given time

Shot noise ($\Delta(z) << 1$)

- time interval between events long compared to the duration of a single event
- waveforms are separated by long stretches of silence

Shot noise

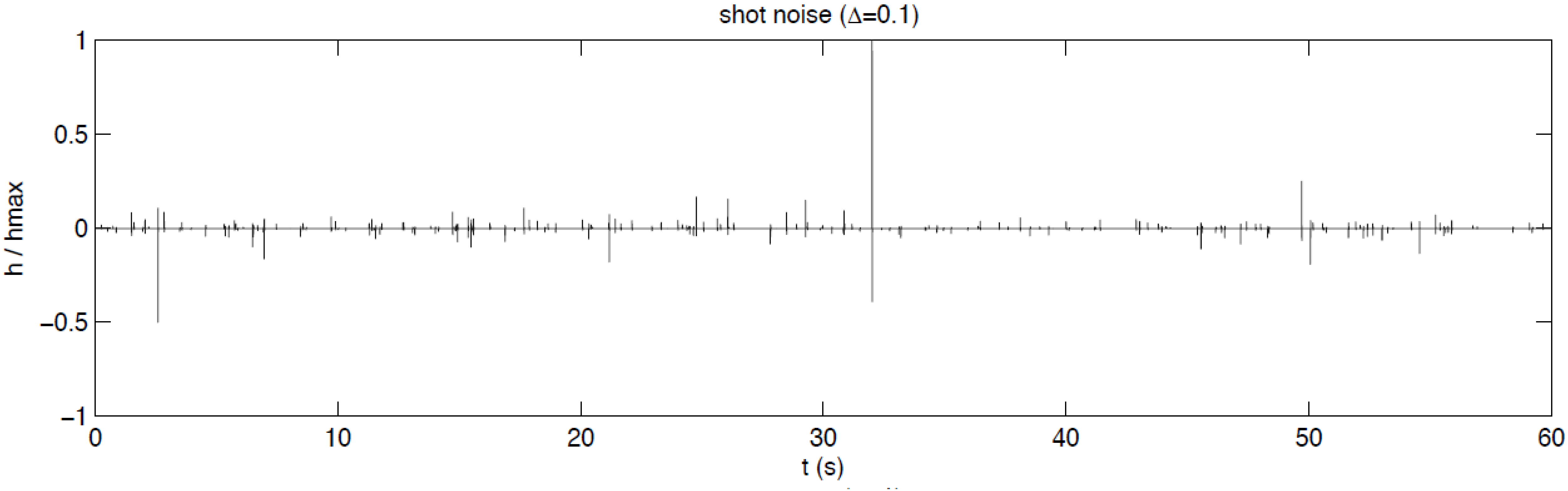

Popcorn

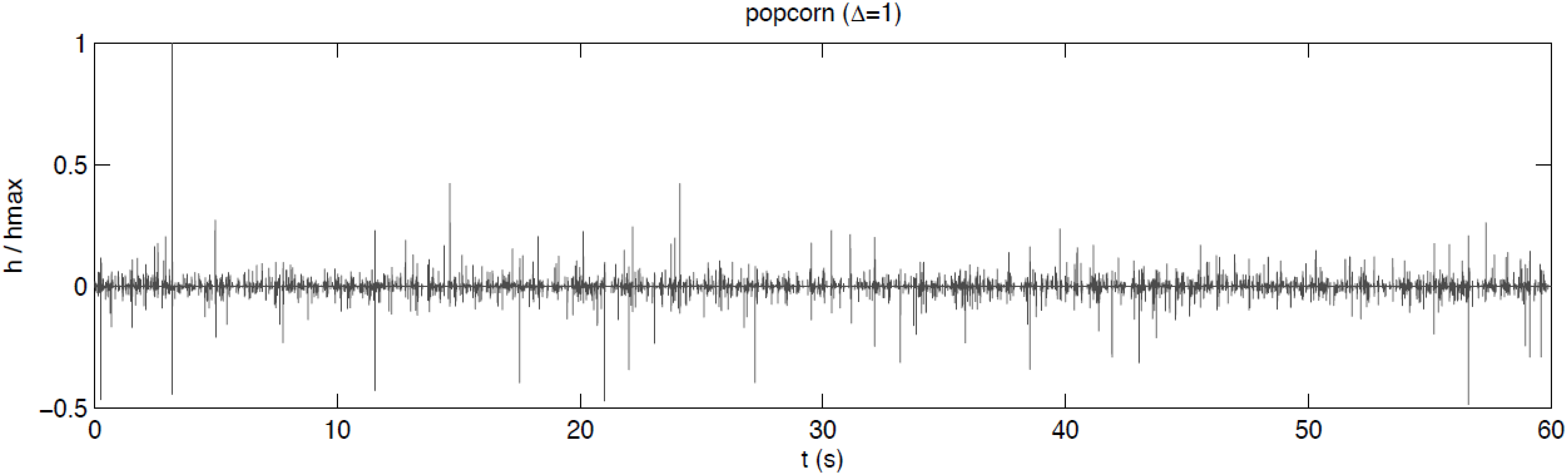

Continuous

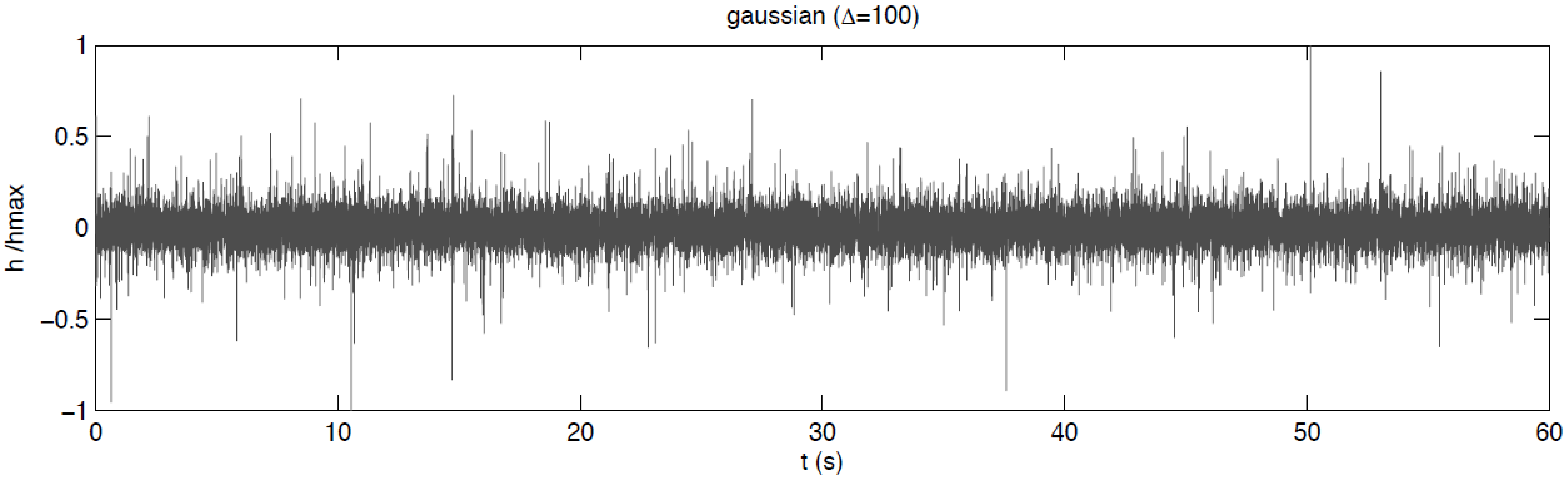

Cosmological GWB

Gravitational counterpart of the CMB

Expectation: a gaussian, stationary, unpolarized, **isotropic** background (first approximation)

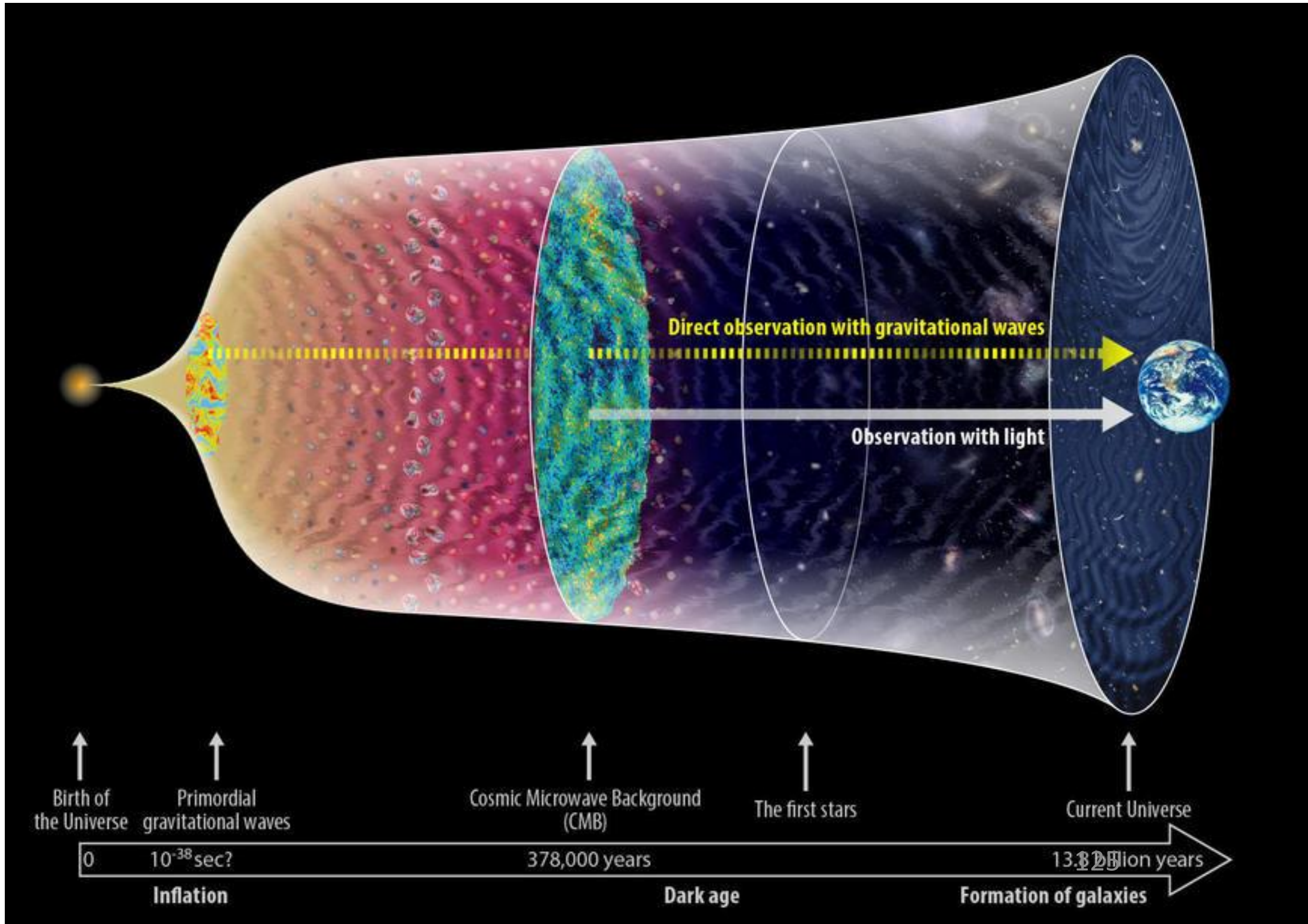

Cosmological GWB

Gravitational counterpart of the CMB

Expectation: a gaussian, stationary, unpolarized, **isotropic** background (first approximation)

A **Holy Grail** for **Cosmology**?!

$$\frac{\Gamma(T)}{H(T)} \sim \frac{G^2 T^5}{T^2/M_{Pl}} = \left(\frac{T}{M_{Pl}}\right)^3$$

<1: Expansion wins and GWs decouple

$T_* \sim M_{Pl} \leftrightarrow t_* \sim t_{Pl} \simeq 10^{-43} s$

Window to new Physics!

Beyond the Standard Model

Beyond General Relativityy